MODULATION OF SIGNAL TRANSDUCTION AND TRANSFORMATION BY KAPOSI'S SARCOMA-ASSOCIATED HERPESVIRUS

Penny M. Anders

A dissertation submitted to the faculty of the University of North Carolina at Chapel Hill in partial fulfillment of the requirements for the degree of Doctor of Philosophy in the Department of Microbiology and Immunology in the School of Medicine

Chapel Hill
2016

Approved by:

Nancy Raab-Traub

Blosssom Damania

Dirk Dittmer

Gary Johnson

Nathaniel Moorman

ABSTRACT

Penny M. Anders: Modulation of Signal Transduction and Transformation by Kaposi's Sarcoma-Associated Herpesvirus
(Under the direction of Blossom Damania)

Kaposi's sarcoma associated-herpesvirus (KSHV) is a double-strand DNA gamma herpesvirus that establishes lifelong latent infection in the human host. KSHV infection is associated with several cancers including the endothelial cell cancer, Kaposi's sarcoma (KS); and two B-cell lymphomas, primary effusion lymphoma (PEL) and multicentric Castleman's disease. This dissertation focuses on the importance of cellular signal transduction pathways in KSHV-associated cancers and focuses on two KSHV viral proteins, K1 and vPK, that modulate these signaling pathways.

KSHV encodes over 100 genes including many proteins that alter signaling pathways to create a cellular milieu that promotes survival of the virally infected cell. The PI3K and MAPK signaling pathways are aberrantly active in PEL and other non-Hodgkin lymphomas (NHL), and are important for PEL survival. Because there is always a need for new effective therapies to treat NHL, which includes KSHV-infected PEL, we sought to evaluate the effectiveness of dual inhibition of the PI3K and MAPK signaling pathways in killing NHL cells. We concluded that dual inhibition

of both pathways was no more effective at reducing cell viability and tumor burden *in vivo* than inhibition of the PI3K pathway alone.

Some viral proteins modulate host cellular proteins and thereby promote KSHV pathology. The KSHV K1 viral protein is thought to be a major contributor to KSHV-induced oncogenesis since the expression of K1 has been shown to lead to transformation *in vitro* and to tumor development *in vivo*.

We identified AMPKγ1 as a K1-associating protein, and the K1 N-terminus is important for association with AMPKγ1. AMPK is a metabolic regulator that responds to many types of cellular stress by regulating pathways to maintain energy homeostasis. We found that K1 expression gives cells a survival advantage when cells are stressed by serum starvation or when AMPK is inhibited, and that this survival advantage is dependent on K1's association with AMPK. AMPK activity is also increased in K1-expressing cells following exposure to metabolic stress.

Unlike K1, which is unique to KSHV, vPK (ORF36) is a viral serine/threonine kinase that is conserved among herpesviruses, underscoring the importance of this kinase in herpesvirus infection and KSHV biology. Our lab has found that vPK expression facilitates cellular transformation *in vitro* and that vPK phosphorylates ribosomal protein S6, a protein that is typically phosphorylated by S6 kinase and involved in protein synthesis. Thus far, our understanding of vPK function and its impact on the host has been based on data obtained from *in vitro* culture models. We sought to add novel insight into the function of vPK by evaluating the phenotype

of vPK *in vivo*. We found that naïve vPK transgenic mice have an activated immune system that is similar to immunized wild-type mice. Moreover, aged-vPK mice are more prone to lymphoma development than wild-type mice.

I dedicate this dissertation to my mother, Minnie Lee Vanhoy Anders, who quietly listened to me and supported me throughout all of my adventures.

ACKNOWLEDGEMENTS

I thank my advisor Blossom Damania for investing her resources and time in my development. I acknowledge the members of the Damania and Dittmer laboratories past and present for their support and conversation. I am also appreciative for my thesis committee including Drs. Dirk Dittmer, Gary Johnson, Nathaniel Moorman and Nancy Raab-Traub for taking their time to evaluate my research. Finally, I thank my brother, David Anders and sister, Cindy Anders for listening to me throughout my graduate career. I give special thanks to Dixie Flannery for answering my questions and for keeping me on track during my graduate studies.

TABLE OF CONTENTS

LIST OF TABLES

LIST OF FIGURES

LIST OF ABBREVIATIONS

4E-BP1	eukaryotic translation initiation factor 4E-binding protein 1
AICAR	5-Aminoimidazole-4-carboxamide ribonucleotide
AIDS	acquired immune deficiency syndrome
AMP	adenosine monophosphate
AMPK	5' adenosine monophosphate-activated protein kinase
ANOVA	analysis of variance
AP-1	activator protein-1
APC	allophycocyanin
ATCC	American Type Culture Collection
ATP	adenosine triphosphate
BAC16	bacterial artificial chromosome 16
BCA	bicinchoninic acid assay
BCR	B-cell receptor
BL	Burkitt lymphoma
CaMKKβ	calcium/ calmodulin dependent protein kinase kinase–beta
CD	cluster of differentiation
CDK6	cyclin-dependent kinase 6
CHOP	cyclophosphamide, hydroxydaunorubicin, oncovin, prednisone
CO_2	carbon dioxide
CSR	class switch recombination
CTLA-4	cytotoxic T-lymphocyte-associated protein 4
DLBCL	diffuse large B-cell lymphoma
DMEM	Dulbecco's Modified Eagle Medium
DMSO	dimethyl sulfoxide

DNA	deoxyribonucleic acid
EBM	Endothelial Basal Medium
EBV	Epstein–Barr virus
EDTA	ethylenediaminetetraacetic acid
EGM	Endothelial Growth Medium
eIF4B	eukaryotic translation initiation factor 4B
eIF4E	eukaryotic translation initiation factor 4E
ER	endoplasmic reticulum
ERK	extracellular signal–regulated kinases
FACS	fluorescence-activated cell sorting
FAK	focal adhesion kinase
FITC	fluorescein isothiocyanate
FL	follicular lymphoma
FOXO	forkhead box O
GPCR	G-protein-coupled receptors
Grab 2	growth factor receptor-bound protein 2
GSK-3β	glycogen synthase kinase 3 beta
GTP	guanosine-5'-triphosphate
H&E	hematoxylin and eosin
HCMV	human cytomegalovirus
HDAC	histone deacetylases
HEK	human embryonic kidney
HHV-6	human herpesvirus 6
HI-FBS	heat inactivated fetal bovine serum
HIV	human immunodeficiency virus
HSP90	heat shock protein 90

HSV	herpes simplex virus
hTERT	human telomerase reverse transcriptase
HUVEC	human umbilical vein endothelial cells
IgH	immunoglobulin heavy locus
IL-2	interleukin-2
IL-6	interleukin -6
IP3Rs	inositol 1,4,5-trisphosphate receptors
ITAM	immunoreceptor tyrosine-based activation motif
JAK3	janus kinase 3
JNK	c-Jun N-terminal kinase
KS	Kaposi's Sarcoma
KSHV	Kaposi's Sarcoma Associated Herpesvirus
LANA	latency-associated nuclear antigen
LBK1	liver kinase B1
LPS	lipopolysaccharides
MALDI	Matrix Assisted Laser Desorption/Ionization/
TOF	Time of Flight Mass Spectrometry
MAPK	mitogen-activated protein kinase
MAPKK	mitogen-activated protein kinase kinase
MAPKKK	mitogen-activated protein kinase kinase kinase
MEF	mouse embryonic fibroblasts
MKK4	mitogen-activated protein kinase kinase 4
MKK7	mitogen-activated protein kinase kinase 7
mTOR	mammalian target of rapamycin
NaCL	Sodium chloride
NF-kB	nuclear factor kappa-light-chain-enhancer of activated B cells

NFAT	nuclear factor of activated T-cells
NHL	Non-Hodgkin lymphoma
NP-KLH	keyhole limpet hemocyanin
NP-40	nonyl phenoxypolyethoxylethanol.
PBS	phosphate buffered saline
PCR	polymerase chain reaction
PDK1	3-phosphoinositide dependent protein kinase-1
PE	R-Phycoerythrin
PEL	Primary Effusion Lymphoma
PI3K	phosphoinositide 3-kinase
PIP2	phosphatidylinositol 4,5-bisphosphate
PIP3	phosphatidylinositol (3,4,5)-trisphosphate
PKCθ	protein kinase C theta
PLCγ2	phospholipase C, gamma 2
Ras GAP	Ras GTPase-activating protein
Rb	retinoblastoma protein
REV	revertant
RTA	replication and transcription activator
S6KB1	S6 kinase B1
SDS-PAGE	sodium dodecyl sulfate polyacrylamide gel electrophoresis
SERCA	sarco/endoplasmic reticulum
SH2	Src homology 2
SYK	spleen tyrosine kinase
TAK1	transforming growth factor beta-activated kinase 1
TLR	Toll-like receptors
TPA	12-O-Tetradecanoylphorbol-13-acetate

TSC2	tuberous sclerosis complex 2
v-FLIP	viral fas-associated death domain-like interleukin-1β-converting enzyme-inhibitory protein
v-IRF3	viral-interferon regulatory factor 3
Vpk	viral protein kianse
VZV	varicella zoster virus
WT	wild-type

.

CHAPTER 1. INTRODUCTION

OVERVIEW

Kaposi's sarcoma-associated herpesvirus (KSHV) or human herpesvirus-8 (HHV-8) is the causative agent of the endothelial cancer Kaposi's sarcoma (KS) and two B cell lymphomas, primary effusion lymphoma (PEL) and multicentric Castleman's disease (MCD) [1-3]. These KSHV-associated diseases mainly occur in immune-suppressed individuals such as those who are HIV positive or who are organ transplant recipients although they can also occur in seemingly immune competent individuals. KS is one of the most common cancers among sub-Saharan African men, and the most prevalent cancer in several countries in sub-Saharan Africa [4, 5].

Treatment options for individuals with KS include antiretroviral therapy for HIV-positive individuals, therapies that boost the immune system, and/or excision of the KS lesion. Individuals with PEL typically are treated with CHOP (cyclophosphamide, doxorubicin, vincristine, and prednisone) chemotherapies. PEL is often resistant to chemotherapies and median survival following diagnosis is approximately 6 months [6]. Thus, effective therapies for KSHV malignancies are warranted and understanding the mechanisms that lead to KSHV-associated cancers may provide insight into the development of therapies to treat other cancers as well.

INTRODUCTION

KSHV-ASSOCIATED CANCERS

Kaposi's sarcoma (KS) is a cancer that is believed to be of endothelial cell origin. During the 1980s, cases of Kaposi's sarcoma started appearing in immune-compromised individuals who were HIV positive. Although the KS lesion is typically viewed as a red patch that impacts the dermis on extremities, KS can also impact the mucosa and internal organs [7-9]. The KS lesion is composed of KSHV-infected spindle cells and a profusion of neovascular spaces [10]. The newly developed neovascular spaces are weak and allow leakage of fluids into the extravascular spaces, forming the characteristic KS red patch [9]. The KS lesions can progress from a patch, to a plaque, and then into a nodule. Although the KS lesion is composed of spindle cells, it is also filled with inflammatory cells including T, B and monocytic cells [11, 12].

Inflammation has been found to play an integral part in the development and progression of KS. In the early stages of KS, there's extensive inflammatory infiltrate including an influx of CD8+ and CD4+ -interferon-γ-producing T cells and the production of Th1-inflammatory cytokines [13]. Inflammatory cytokines re-activate KSHV from latency and stimulate endothelial cells to produce angiogenic factors thereby promoting KS progression [14]. *In vivo*, KS has also been found to localize to surgical sites or areas of skin trauma, further emphasizing the importance of inflammation to KS development [15, 16].

The various forms of KS include classic KS, post-transplant KS, African KS and AIDS-KS. Classic KS, an indolent form, impacts elderly men of Mediterranean and

Eastern European origin. Post-transplant KS impacts some transplant recipients and often resolves with the reduction or withdrawal of immunosuppressants although patients are then at risk for graft rejection [17]. African-KS, a more aggressive form that can impact the organs is found in children and young adults. AIDS-KS is the most aggressive form, causing lesions and impacting organs in HIV positive individuals. Anti-retroviral therapy has reduced the incidence of AIDS-KS [18].

Primary effusion lymphoma (PEL) is a monoclonal B cell lymphoma that is under the diagnostic umbrella of non-Hodgkin lymphoma [19]. It is a B cell-rich fluid localized to the body cavities. PEL occurs predominantly in HIV positive individuals. All PEL cells are latently infected with KSHV and can be cultured *ex vivo* [20, 21]

Multicentric Castleman's disease (MCD) is another B lymphoproliferative disease although it differs from PEL in that it is polyclonal and found as solid tumor affecting the lymphatic organs [22, 23]. MCD can occur in HIV positive and negative individuals, but when it is associated with KSHV infection, it usually occurs in individuals who are HIV positive [3].

KAPOSI'S SARCOMA-ASSOCIATED HERPESVIRUS, HHV-8

Chang et al. first isolated KSHV from KS lesions in 1994 [1]. KSHV is a double-strand DNA gamma herpesvirus that has a genome of approximately 165 to 170 kb long that code for over 85 open reading frames and 12 micro RNAs [24-30]. The KSHV genome contains multiple open reading frames that are conserved among other herpesviruses, and genes K1-K15 that are unique to KSHV [7]. Similar to other gammaherpesviruses, KSHV can vacillate between latent and lytic programs although latency is the default program following primary infection.

KSHV can infect a variety of cell types *in vitro* and *in vivo*. *In vivo*, KSHV has been found in monocytes, B cells, endothelial/spindle cells, and epithelial cells [10, 31-33]. Upon infection, KSHV typically establishes latency by forming an episome. The latency-associated nuclear antigen (LANA), binds the viral terminal repeats and tethers the viral genome to the host chromosome [7]. In this way, the viral genome is copied by host replication machinery and passed on to daughter cells during cell division.

During latency, a subset of viral genes is expressed including LANA, v-FLIP, v-Cyclin, kaposins A, B and C, v-IRF-3 as well as the twelve pre-microRNAs [34]. Although predominantly expressed during the lytic cycle, recent studies indicate that the proteins viral interleukin-6 (vIL-6) and K1 are expressed at low levels during latency as well [24, 35]. Upon reactivation, which can be induced *in vitro* with various compounds such as 12-O-tetradecanoylphorbol-13-acetate (TPA), histone deacetylase (HDAC) inhibitors, and TLR 7/8 ligands, KSHV enters the viral lytic cycle resulting in the production of infectious virions [24, 36].

Although KSHV is predominantly latent in KS spindle cells, PEL cells, and in MCD plasmablastic B cells [10], both latent and lytic phases appear to be important for KSHV pathology. Expression of latent genes generally promotes the survival of the infected cell and persistence of infection during cell division, and lytic gene expression results in the production of inflammatory cytokines, pro-angiogenic factors and viral proteins that subvert the host immune system and promote virion production.

KSHV LATENCY PROTEINS THAT PROMOTE TUMORIGENESIS

The KSHV viral proteins and microRNAs expressed during latency are implicated in making major contributions to KSHV-induced cancers. Expression of the latency locus in B cells, which contains the genes for LANA, K13 (v-FLIP), a cellular cyclin D2 homolog (v-Cyclin), K12 (kaposin), and all viral microRNAs, in transgenic mice results in chronic mature B cell activation and B cell hyperplasia [37]. B cells are hyper-responsive to T-dependent antigen as well as lipopolysaccharide (LPS), resulting in increased germinal center responses and an increase in the number of plasma cells. B cells expressing the latency locus are poised and responsive to unrelated pathogen, making these cells susceptible to expansion; and yet only a fraction of the latency locus transgenic mice go on to develop lymphomas [37].

Thus, the latency locus most likely contributes to, but is not the sole driver, of KSHV-induced oncogenesis. When transgenic mice expressing the latency locus are combined with mice containing a weak IgH Cα Myc allele, the latency locus/Myc mice develop lymphoma at a higher rate than the single transgenic mice expressing either the latency locus or Myc [38]. Again these data support the idea that the KSHV latency locus cooperates with host factors such as myc to promote oncogenesis.

Several of the latency locus genes have oncogenic properties when expressed individually in mice. LANA transgenic mice have germinal center formation and splenic follicular hyperplasia [39] . A subset of the LANA transgenic mice actually develop various types of lymphoma [39] . Mechanistically, LANA may promote

tumorigenesis by altering cell cycle and/or survival. LANA binds to p53, and p53 expressing cells have reduced sensitivity to p53-dependent apoptosis [24]. LANA interacts with the retinoblastoma protein (Rb) and increases E2F activity, suggesting that LANA inhibits Rb, promotes E2F activity and as a consequence promotes cell cycle progression [7].

Another latency protein that appears to have a major impact on promoting cellular transformation is Fas-associated death domain-like IL-1 converting enzyme inhibitor protein (v-FLIP). *In vitro*, v-FLIP inhibits caspase-8 and facilitates activation of NF-κB [40]. Viral-FLIP expression has also been shown to transform rodent fibroblasts, and the transforming potential of v-FLIP is dependent on NF-κB activation [40]. The expression of v-FLIP under the major histocompatibility $H2k^b$ promoter leads to constitutive NF-κB activation in various lymphoid organs and an increased incidence of lymphoma of various subsets compared to controls [41]. Viral-FLIP expressing mice do not have impaired Fas-induced apoptosis [41].

Expression of v-FLIP during different stages of B cell differentiation results in the development of B-cell lymphomas that have characteristics similar to PEL. These v-FLIP expressing mice also exhibit immune dysfunction in that they lack germinal center formation compared to controls following immunization [42]. Tumors from v-FLIP expressing mice contain cells exhibiting both B and macrophage/DC phenotypes as determined by markers specific for these cell types and flow cytometry, suggesting some sort of B cell plasticity in tumors from v-FLIP positive mice [42].

Kaposin (K12), another latent gene, may have oncogenic potential. The kaposin gene results in the generation of kaposins A, B and C due to translation of kaposin mRNA from different sites of initiation [43]. Kaposin A expression can transform rodent fibroblasts and nude mice injected with Kaposin A expressing cell lines develop tumors [44].

In this brief summary describing the oncogenic potential of some KSHV latent proteins, we can observe that KSHV latent proteins play a role in promoting cell survival by regulating cell cycle or by inhibiting apoptosis. Based on the *in vivo* models, we can also see that expression of some of these proteins alone or in concert with a cellular oncogene such as myc can result in tumor formation. Recent studies suggest that the expression of some latent and lytic proteins may not be assigned exclusively to either the latent or lytic program. The KSHV K1 protein was presumed to be expressed during the lytic cycle, but more recently has been found to be expressed during latency albeit at lower levels than during the lytic cycle [24, 35, 45].

K1 PROTEIN PROMOTES CELL SURVIVAL AND TUMORIGENESIS

K1 is a 46-kDa transmembrane glycoprotein that is primarily expressed in the endoplasmic reticulum as well as the plasma membrane [46]. K1 contains and immunoglobulin-like ectodomain, a transmembrane region and a cytoplasmic tail that contains an immunoreceptor-like tyrosine-based activation motif (ITAM), which is similar to the signaling molecules in the B cell receptor signaling complex [47, 48]. It is thought that K1 is maintained in an activated state by oligomerization of the K1 ectodomain and subsequent phosphorylation of the ITAM tyrosines by Src family

kinases [49]. K1 can interact with various SH2 (Src-Homology 2) containing signaling molecules, including Lyn, Syk, p85, PLCγ2, RasGAP, Vav, Grab 2 and SH2-containing tyrosine phosphatases 1/2 via the phosphorylated tyrosines in its ITAM [50]. Activation of K1 results in a signaling cascade leading to calcium mobilization, upregulation of the transcription factors NFAT and AP-1, and the production of inflammatory cytokines [50]. Expression of K1 induces the activation of phosphoinositide 3-kinase (PI3K) by phosphorylation of the p85 subunit of PI3K. Activation of PI3K leads to activation of downstream kinases including Akt and mammalian target of rapamycin (mTOR), which leads to the inhibition of forkhead transcription factor family and reduced cellular apoptosis [51]. K1 has also been shown to inhibit Fas-induced apoptosis [52, 53]. K1 may promote tumorigenesis by modulating signaling pathways that are important for cell survival and proliferation.

K1 is located in the KSHV genome at a position equivalent to the saimiri transforming protein (STP) of herpesvirus saimiri (HVS), a member of the rhadinovirus subgroup of gamma herpesvirues [54]. Replacement of oncogenic STP with K1 in HVS results in IL2-independent immortalization of T cells and the development of lymphoma in marmosets following infection with the K1 containing-recombinant HVS [54]. K1 expression also transforms rodent fibroblasts and immortalizes primary endothelial cells [54, 55]. K1 transgenic mice develop lymphomas and sarcomas at low incidence [56].

VIRAL PROTEIN KINASE (ORF36)

KSHV encodes the serine threonine kinase ORF36 also known as viral protein kinase (vPK) that can be found in the nucleus and cytoplasm when expressed

ectopically in cells [57]. ORF36 shares limited homology with the protein kinases expressed by the other herpesviruses including UL13 (HSV), ORF47 (VZV), BGLF4 (EBV), UL97 (HCMV), and U69 (HHV-6) [58]. However, there are also some differences. Viral PK appears to have diverse functions. Viral PK phosphorylates and activates the cellular targets, c-Jun N-terminal kinase (JNK), MKK4 and MKK7 as well as, the viral target K-bZIP, a transcription regulator that represses the latent/lytic switch protein, RTA (replication and transcription activator) protein [59, 60]. Kuny et al. also showed that vPK exhibits cellular cyclin dependent kinase-like activity, in that it can phosphorylate Rb thereby inactivating it and promoting cell cycle progression [57]. By binding to the activated form of interferon regulatory factor 3 (IRF-3), vPK also inhibits the anti-viral type I interferons [61].

Our lab has recently shown that vPK resembles and mimics the activity of the cellular protein S6 kinase (S6KB1) [62]. S6KB1 is downstream in the PI3K/mTOR pathway and is phosphorylated by mTOR. Activated S6KB1 phosphorylates multiple targets some of which are involved in protein synthesis such as ribosomal S6 protein, a protein that is part of the 40S ribosome; and eIF4B, a protein that is part of the translation pre-initiation complex [63]. Expression of vPK results in increased de novo protein synthesis, tubule formation and anchorage independent growth, compared to control cells, suggesting that vPK may be possess oncogenic properties [62].

KSHV is predominantly latent in both PEL and KS although there may be periodic episodes of reactivation in a small percentage of infected cells. It is generally thought that latent proteins drive tumorigenesis; whereas, lytic proteins

promote the production of chemokines and cytokines that support angiogenesis, and survival and growth of KSHV infected latent cells. Additionally, it is also possible that lytic proteins can be expressed in the absence of complete viral lytic replication. For example, vPK/ORF36 contains hypoxia responsive elements in its promoter, which may cause it to be expressed in isolation and in the absence of full-blown lytic replication [64, 65]. Thus, lytic proteins such as vPK, in addition to latent proteins, may be contributors to oncogenesis particularly in a changing cellular milieu.

CELLULAR SIGNAL TRANSDUCTION PATHWAYS

MAPK SIGNALING PATHWAY

There are 4 major cascades of the mitogen-activated protein kinase (MAPK) pathway. Each cascade is comprised of multiple nodes that are activated sequentially, MAPKKK-MAPKK-MAPK [66]. In response to various stimuli such as growth factors, stress or cytokines; there is engagement of the cell surface receptor and this event initiates the activation of kinases that subsequently activate one or more cascades of the MAPK pathway. We will be focusing on the RAF (MAPKKK)-MEK1/2 (MAPKK)-ERK1/2 (MAPK) cascade of the MAPK pathway, which is stimulated by growth factors, and involved in regulating cell survival and proliferation [66].

PI3K SIGNALING PATHWAY

The phosphoinositide 3-kinase (PI3K) pathway is constitutively active in many cancers and is involved in several major cellular processes including cell survival, proliferation, and metabolism [67]. PI3K is activated by engagement of receptor

tyrosine kinases and G-coupled protein receptors (GPCRs) and by small GTPases. The Class IA PI3Ks are composed of a p85-like regulatory subunit (p85α, p85β, and p55γ) and a p110 catalytic subunit (p110α, p110β, p110γ and p110δ) [67].

When inactive, the p85 subunit prevents activation of the p110 subunit. Upon activation, the p85 subunit localizes to the plasma membrane thereby relieving p110 so that it can phosphorylate PtdIns 4, 5-bisphosphate (PIP_2) generating PtdIns (3, 4, 5) P_3 (PIP_3). The serine threonine kinase, Akt, binds PIP_3 via its pleckstrin homology (PH) domain resulting in translocation of Akt to the membrane. Akt is phosphorylated at Thr308 by phosphoinositide-dependent kinase-1 (PDK1); and for full activation, Akt is also phosphorylated at S473 on its C-terminus by mTOR complex 2 (mTORC2) [68]. Akt phosphorylates many substrates including the proapoptotic factors Bad, GSK-3β, and the FOXO transcription family members resulting in the inhibition of these factors, thereby promoting cell survival and proliferation [69].

Activation of Akt also leads to the direct phosphorylation of tuberous sclerosis 2 (TSC2), which releases its inhibitory effect on the serine/threonine kinase, mammalian target of rapamycin (mTOR) [70-73]. mTOR is part of two distinct complexes, mTORC1 and mTORC2. While both complexes contain mTOR, each complex responds to different upstream signals and initiates different downstream outputs. Mammalian TORC2 can phosphorylate and activate Akt thereby promoting cell survival, proliferation and metabolism [74]. Mammalian TORC1 responds to a multitude of cues including: growth factors, stress, amino acids, oxygen and energy status [74]. During favorable conditions, mTORC1 promotes anabolic processes such as protein and lipid synthesis and inhibits catabolic processes such as

autophagy [74]. Mammalian TORC1 directly phosphorylates eukaryotic translation factor 4E (eIF4E)-binding protein 1 (4E-BP1) and S6 kinase 1 (S6K1), and promote protein synthesis [74]. Unlike mTORC2, mTORC1 is rapapmycin-sensitive [75].

KSHV AND ACTIVATION OF THE PI3K AND MAPK PATHWAYS

The PI3K and MAPK pathways are activated early and appear important for KSHV infectivity. Binding of KSHV virions to integrins on the cell surface, facilitates phosphorylation of focal adhesion kinase (FAK) [76]. Activation of FAK stimulates the activation of Src family tyrosine kinases, which results in the activation of PI3K and Rho GTPases [76, 77]. Activation of PI3K and Rho GTPases following KSHV infection facilitates cytoskeletal rearrangements and actin polymerization [76]. Inhibition of PI3K reduces KSHV infectivity [76, 78, 79], suggesting that activation of PI3K is important for KSHV infection. The MAPK pathway is also activated upon receptor-ligand binding and viral entry [79]. Although activation of the MAPK pathway is not necessary for viral DNA entry or nuclear delivery, it does promote the expression of various viral latent and lytic genes, including LANA and RTA respectively, as well as host genes thereby promoting an intracellular environment that is permissive to infection [79].

The PI3K and MAPK signaling pathways are constitutively active in latent KSHV-infected PEL [80-82]. When PEL cells are treated with either a dual PI3K pathway inhibitor that targets the two nodes, PI3K and mTOR or with rapamycin an inhibitor that targets mTORC1, there is reduced PEL survival and tumor size in PEL xenograft tumor models [80, 81]. Inhibiting mTORC1 also inhibits tumor growth in a

KSHV-endothelial xenograft model in which the virus is latent [83]. These data suggest that the PI3K pathway is important for latent KSHV cell survival.

Activation of the MAPK pathway is also important in facilitating KSHV reactivation from latency [82, 84]. Inhibition of ERK, JNK, and p38 MAPK pathways during TPA-mediated KSHV reactivation results in reduced expression of viral lytic genes and production of infectious virions [82]. Because both the PI3K and MAPK pathways support KSHV infection throughout its life cycle, we sought to evaluate inhibition of both pathways in non-Hodgkin lymphoma, which includes PEL.

AMPK, A CELLULAR KINASE

AMPK is a serine-threonine kinase composed of an alpha catalytic sub-unit and two regulatory units, beta and gamma [85]. AMPK is a major metabolic regulator that maintains energy homeostasis by responding to stress conditions that increase the AMP: ATP ratio such as during nutrient deprivation, oxidative stress or hypoxia [86, 87]. Activated AMPK leads to the activation of catabolic pathways that generate ATP and inhibition of anabolic pathways that consume ATP. Binding of AMP to the gamma subunit allosterically activates AMPK and promotes phosphorylation of AMPKα at Thr172 by the upstream kinase liver kinase B1 (LKB1) [88-90]. Bound AMP or ADP at higher concentrations prevents dephosphorylation of Thr172 [88, 91]. AMPK can also be phosphorylated by Ca^{2+}/calmodulin-dependent protein kinase kinase-β (CaMKKβ) and TAK1 [92-95]. Furthermore, AMPK may be activated by leptin, adiponectin, catecholamines and interleukin-6 [96-101].

The role of AMPK as a tumor promoter is actively being explored [102, 103]. Some studies suggest that AMPK promotes tumor cell survival *in vitro* and *in vivo*. Inhibition of AMPK results in reduced pancreatic cell survival and apoptosis under normal and stressed conditions [104, 105]. AMPK also promotes survival in multiple myeloma, colorectal and glioma cancer cell lines [106-109]. *In vivo*, AMPK signaling is elevated in developing tumors in a glioblastoma rat model [110]. Moreover, mouse embryonic fibroblasts (MEFs) that are null for LBK1, a kinase that phosphorylates and activates AMPK, have a reduced ability to undergo oncogene-induced transformation; and xenografts that have been prepared from AMPKα1/α2-null MEFs exhibit reduced tumor growth in comparison to wild-type (WT) [111, 112]. Thus, there is accumulating evidence suggesting that AMPK promotes cancer cell survival by facilitating the metabolic adaptation to the tumor environment.

CHAPTER 2. DUAL INHIBITION OF THE PI3K/MTOR AND MAPK PATHWAYS IN NON-HODGKIN LYMPHOMA[1]

OVERVIEW

NHL subtypes are classified based on clinical and histologic characteristics, as well as lymphocyte developmental stage. NHL sub-types include diffuse large B-cell lymphoma (DLBCL), follicular lymphoma (FL), mantle cell lymphoma (MCL), Burkitt lymphoma (BL), primary effusion lymphoma (PEL) to name just a few. Many lymphomas such as DLBCL, MCL, and AIDS-associated lymphomas are very aggressive and rapidly fatal if unresponsive to therapy. Indolent lymphomas, such as FL are also many times not curable with conventional chemotherapy. Clearly, novel treatment paradigms are needed to improve clinical outcomes of patients with NHL.

INTRODUCTION

We had previously shown that the phosphatidylinositol 3-kinase (PI3K) and mammalian target of rapamycin (mTOR) pathway was important for NHL survival and that single and dual inhibitors of this pathway effectively inhibited NHL

[1] Anders P, Bhende PM, Foote M, Dittmer DP, Park SI, Damania B., Accepted manuscript of an article published by Taylor & Francis in Leuk Lymphoma on 2015 Jan;56(1):263-6, available online: http://wwww.tandfonline.com/DOI 10.3109/10428194.2014.917639.

proliferation in vitro and in mouse xenograft models of NHL including FL and PEL [80, 113].

Another pathway that is linked to tumorigenesis is the mitogen activated protein kinase (MAPK), and many sub-types of NHL display an activated MAPK pathway [114-116].

Although conventional chemotherapeutic drugs are useful in some cases, a significant number of NHL patients will eventually relapse and develop resistance to chemotherapy, which necessitates determining additional therapeutics. Since both PI3K and MAPK pathways are activated in NHL, we decided to investigate combination therapy involving inhibition of both pathways. It has been demonstrated that such therapy is effective against certain solid tumors [117, 118].

RESULTS

In this study we used a combination of NVP-BEZ234 and AZD6244. NVP-BEZ235 is an imidazo[4,5-c]quinoline derivative compound, shown to inhibit PI3K and mTOR kinase activity both in vitro and in vivo including PEL and FL [119, 120]. AZD6244 is an inhibitor of MEK1 and MEK2 that does not compete with ATP binding. It is a potent and selective MEK1/2 inhibitor that demonstrates high activity in solid tumor models in vitro and in vivo [121].

Representative types of NHL cells, including SUDHL4 (DLBCL), FL-18 (FL), Raji (BL), Ramos (BL), and BC-1 (PEL), were treated with 0.1 nM, 1 nM, 10 nM, 100 nM, 1000 nM (1 μM), and 10,000 nM (10 μM) of the MEK inhibitor, AZD6244, either alone or in combination with 10 nM of the PI3K/mTOR inhibitor, NVP-BEZ235 for 72 hours (Figure 2.1a). The cells were also treated with 10 nM NVP-BEZ235 alone. An

MTS assay was performed similar to what we previously described [80, 113]. Each experiment was done in triplicate and standard deviation was calculated. The amount of NVP-BEZ235 was kept constant at 10 nM, and increasing doses of AZD6244 was tested in combination with NVP-BEZ235. In each case, we observed that AZD6244 by itself did not have any discernable effect on cell viability in cell culture, even at the highest dose of 10 μM AZD6244 (Figure 2.1a). Moreover, the combination of different amounts of AZD6244 with 10 nM NVP-BEZ235 did not affect cell viability when compared to 10 nM NVP-BEZ235 alone in each case (Figure 2.1a). A slight decrease in cell viability was only seen at the highest dose of AZD6244 (10 μM) with 10 nM NVP-BEZ235. This demonstrates that the combined inhibition of the PI3K and MAPK pathways was neither additive nor synergistic.

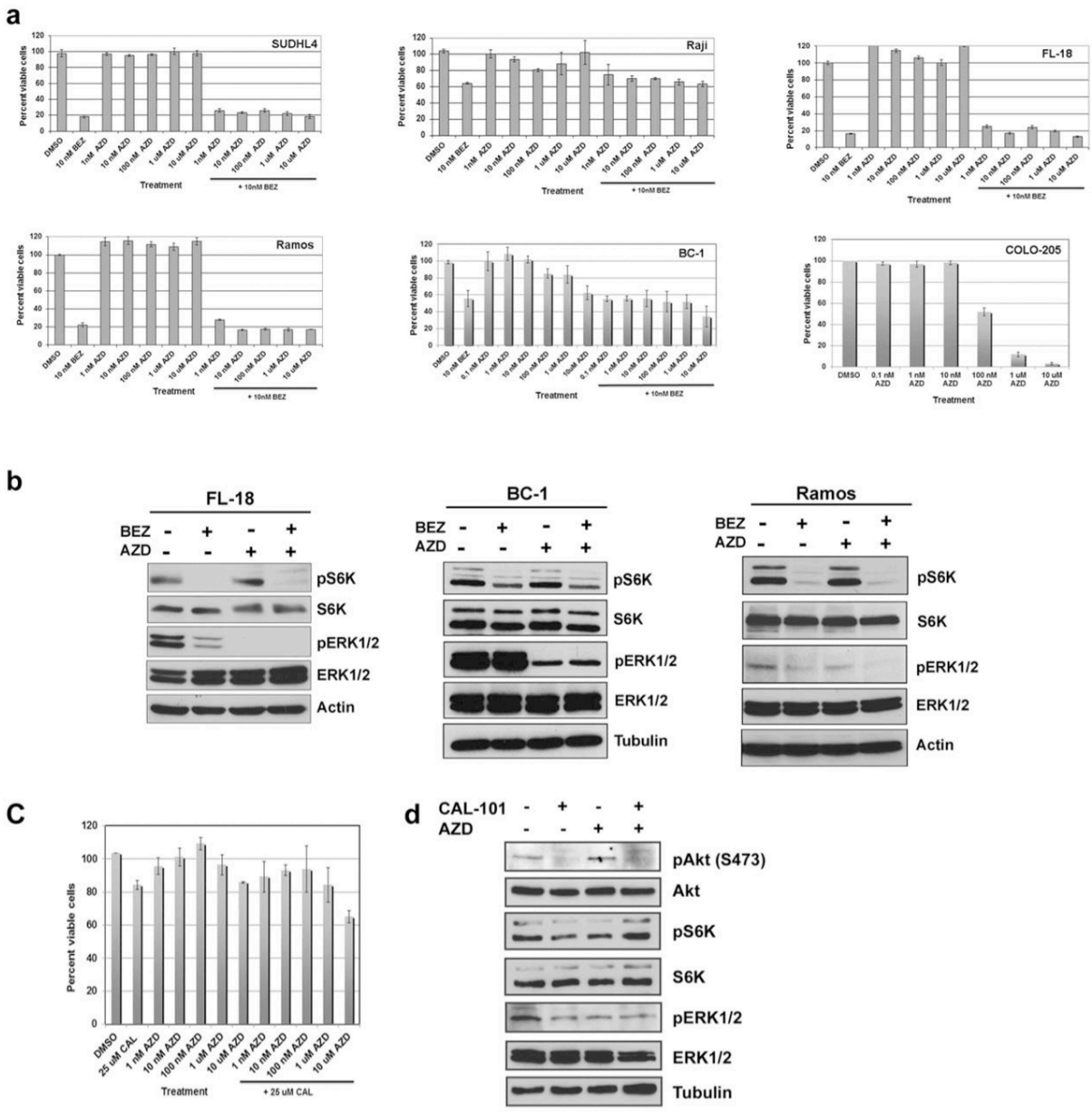

Figure 2.1. Simultaneous inhibition of the PI3K/mTOR and MEK/ERK pathways fails to synergistically reduce NHL cell proliferation in vitro. (a) Proliferation of NHL cell lines treated with drug(s) or vehicle were evaluated by MTS Assay using the Cell Titer 96 Aqueous One Solution Cell Proliferation Assay (Promega) according to the manufacturer's instructions. Cells ($1X10^5$/mL) were incubated with drug(s) or vehicle for 72 hours in a 12-well plate. Twenty microliters of MTS reagent was added to 100µL of cell suspension in a 96-well plate and incubated at 37°C for 1 hour. Percent of viable cells after 72 hours treatment is shown

on the y-axis. The percent of viable cells for untreated cells was set as 100% for each sample. Elevated absorbance values are indicative of metabolically active cells. The COLO-205 cells (5X103 cells/100µL) were added to each well of a 96-well plate. Increasing concentrations of drug(s) or vehicle were added the following day. The MTS reagent was added after 72 hours following the addition of the drug(s) or vehicle, and incubated with the cells for 4 hours at 37°C. Absorbance was measured at 490nm using a FLUOstar OPTIMA spectrophotometer. Percent viable cells after 72 hours treatment is shown on the y-axis. The percent of viable cells for vehicle treated was set as 100% for each sample. Elevated absorbance values are indicative of metabolically active cells. (b) Phosphorylation of ERK 1/2 and S6 kinase were determined by Western blot of NHL cell lines treated with AZD6244 (1µM) and/or NVP-BEZ235 (30nM) for 24 hours. Equal volume of DMSO (0.1%) was added for vehicle control. (c) Proliferation of cells with 25 µM CAL-101 and increasing concentrations of AZD6244 was determined by MTS assay after 48 hours following the addition of the drug(s) or vehicle as described in panel a. (d) Phosphorylation of Akt, ERK 1/2 and S6 kinase were determined by Western blot of NHL cell lines treated with AZD6244 (1µM) and/or CAL-101 (25µM) for 24 hours.

To confirm that the drug AZD6244 used in our experiments had similar activity to that recorded in previous reports [122], we evaluated the effect of AZD6244 on the COLO-205 colorectal cancer cell line by culturing these cells in increasing concentrations of AZD6244 or vehicle for 72 hours. We determined an IC50 of 107.18 ± 2.47 nM in COLO-205 (Figure 2.1a). Similar results were seen with another non-small cell lung cancer cell line Calu-6, that was previously shown to be inhibited by AZD6244 [122] (data not shown). We also evaluated NHL cell viability in the

presence of increasing concentrations of the chemically unrelated MEK inhibitor, PD184352 [123]. We found that PD184352 was ineffective at reducing cell viability in various NHL cell lines except at the highest dose of 10 μM (data not shown). This data supports our observations made with the MEK inhibitor, AZD6244, and suggests that NHL cells are not addicted to the MEK/ERK pathway for survival.

To verify that each of the drugs was inhibiting their respective targets, we performed Western blot analysis on the NHL cells that were treated with the above therapies for 24 hours (Figure 2.1b). We used phosphorylated S6K as a downstream marker for active PI3K/mTOR as we previously described [80, 113], and we used phosphorylated ERK1/2 as a downstream marker for MAPK activation [121]. We found that NVP-BEZ235 inhibited PI3K signaling as measured by reduced phosphorylated S6K levels, and that AZD6244 inhibited MAPK signaling as measured by reduced ERK1/2 phosphorylation (Figure 2.1b).

To determine whether a PI3K inhibitor only would be synergistic with AZD6244, we evaluated the combination of 25 μM CAL-101 (a PI3Kδ inhibitor) with increasing doses of AZD6244 on NHL cell viability. CAL-101 (5-fluoro-3-phenyl-2-[(S)-1-(9H-purin-6-ylamino)-propyl]-3H-quinazolin-4-one) is a small molecule inhibitor of the class I PI3K p110δ isoform[124]. CAL-101 has been found to have anti-tumor activity in patients with indolent NHL and hence we sought to investigate whether inhibiting PI3K p110δ and MAPK may be synergistic against NHL[125]. Figure 1c depicts a representative NHL cell line (Ramos) that was tested with CAL-101 and AZD6244. We did not observe a synergistic or additive effect when different amounts of AZD6244 was combined with 25 μM CAL-101 compared to 25 μM CAL-101 alone

(Figure 2.1c), although each drug appeared to be effective in inhibiting downstream effectors of the pathway. Treatment with CAL-101 inhibited phosphorylation of Akt and S6K, and AZD6244 inhibited phosphorylation of ERK1/2 (Figure 2.1d). We found similar results for FL-18 and Raji cells (data not shown). Thus, neither a dual inhibitor of the PI3K/mTOR pathway (NVP-BEZ235) nor a single inhibitor of PI3K (CAL-101) appears to synergize with AZD6244 in our system.

We next investigated the combination of NVP-BEZ235 and AZD6244 in a mouse xenograft model [113]. Four-to-five-week-old athymic nude-Foxn1^nu female mice were injected intraperitoneally with anti-asialo GM1 antibody (Wako). The following day, $1x10^6$ FL-18 lymphoma cells were subcutaneously injected with growth-factor reduced matrigel as we previously described [113]. Upon development of palpable tumors, the animals were split into four groups and treated by oral gavage 6 days a week with either vehicle, 45 mg/kg NVP-BEZ235, 45 mg/kg AZD6244, or 25mg/kg each of NVP-BEZ235 and AZD6244. While tumors grew in the mice treated with vehicle, mice treated with NVP-BEZ235 showed a significant inhibition of tumor growth as we previously reported [121]. Interestingly, in the xenograft model, mice treated with AZD6244 alone did show a modest inhibition of tumor growth compared to vehicle treated mice. However, the combination of NVP-BEZ235 and AZD6244 did not have a synergistic or additive effect on tumor growth compared to NVP-BEZ235 or AZD6244 alone (Figure 2.2a).

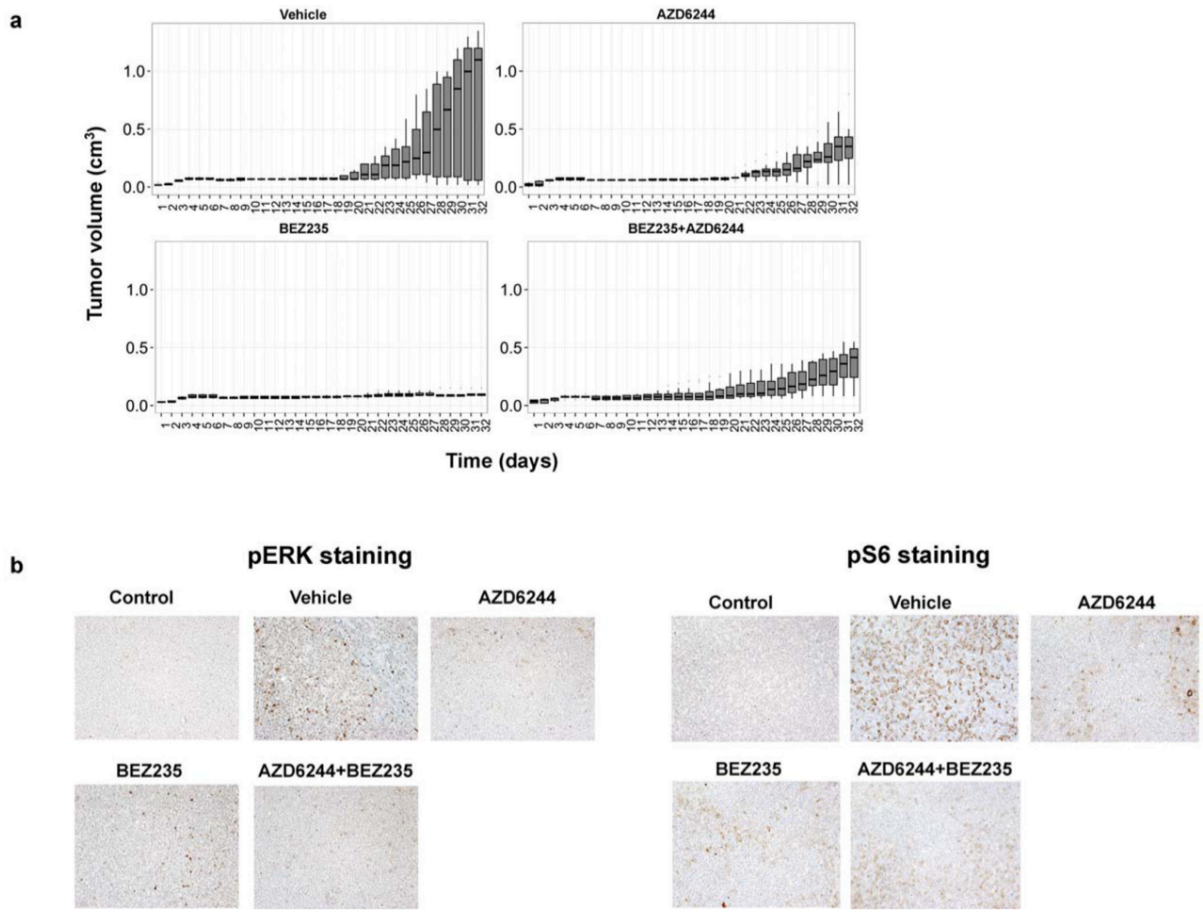

Figure 2.2. Combined inhibition of the MEK/ERK and PI3K/mTOR pathways is no more effective at reducing tumor burden than single blockade of the PI3K/mTOR pathway in vivo. (a) Athymic nude-Foxn1^nu 4-5-week-old female mice were injected subcutaneously into the right flank with 200 µL (1X106) of FL-18 cells. Five mice per group were treated with equal volume of vehicle, 45 mg/kg NVP-BEZ235, 45 mg/kg AZD6244, or 25 mg/kg each of NVP-BEZ235 and AZD6244 (combination therapy). Treatment involved oral gavage 6 times per week. Tumor volume was determined daily (L x W x D) and plotted over time. Shown for each time point is a box and whisker plot of the results per group. The horizontal bar indicates the median, the box indicates 25% and 75% of the data and the whiskers represent 1.5 x the interquartile range, which encompasses 50% of the data. (b) Phosphorylation of ERK 1/2 or S6 protein from each treatment group was evaluated on paraffin-embedded tumors by immunohistochemical staining. Sections were counterstained

with hematoxylin, and visualized at magnifications of 200X using a Leica DMLS microscope. Images were acquired using the Leica DFC480 camera and associated Leica Firecam software. Stored TIFF images were evaluated using Adobe Photoshop CS5.1.

The mice were sacrificed when maximal tumor size was reached. Tumors were excised, sectioned, and subjected to immunohistochemical analysis as we previously described [80]. S6 was consistently phosphorylated in almost all cells in the vehicle control group, however we found reduced phosphorylated levels of S6, a downstream effector of the PI3K pathway in the NVP-BEZ235 treated grafts, and reduced phosphorylated ERK1/2, an effector of the MAPK pathway in the AZD6244 treated grafts (Figure 2.2b). Both markers were reduced in animals treated with both drugs. This suggests that both drugs were delivered to the tumors and inhibited their respective targets in the tumor cells in vivo. Overall, our data demonstrate that the combined inhibition of the PI3K and MAPK pathways was not synergistic or additive in preventing tumor growth of NHL cells in vitro or in vivo.

DISCUSSION

Currently, there are a number of clinical trials testing MEK and PI3K or mTOR inhibitors in patients. Our data suggest that combining inhibitors specific for these two pathways may not be an effective treatment option for NHL since there was no preclinical evidence showing any significant enhancement of cell death in vitro or inhibition of tumor growth in vivo when these inhibitors were combined. This is in direct contrast to reports in solid tumors such as melanoma and breast cancer in which the combination of these inhibitors showed a synergy in curtailing tumor

growth in similar pre-clinical models [117, 118]. Davies et al. found that tumors with activating Ras mutations are more sensitive to AZD6244 than tumors with WT Ras [122]. Since activating mutations in Ras are infrequent in NHL [126], inhibition of the MEK/ERK pathway may not be as effective for NHL as for solid tumors despite the fact that ERK was highly phosphorylated in the cell lines tested.

Even though MEK/ERK and PI3K/mTOR pathways are active in NHL [80, 115, 116], our data suggests that NHL are more reliant on the PI3K/mTOR pathway than the MEK/ERK pathway for cell survival. Normal B-lymphocyte survival is also dependent on the PI3K pathway [127] and studies have shown that B-lymphocytes lacking BCR signaling do not survive while these cells can be rescued from apoptosis by being engineered to have constitutively active PI3K [127].

Although the MEK/ERK pathway may be important in NHL pathology, we found that targeting this pathway alone is not sufficient to reduce NHL cell survival in vitro or in vivo. There are multiple arms of the MAPK pathway [66] and to see additional benefit in NHL, we may need to modulate a different and/or multiple arms of this pathway along with PI3K/mTOR inhibition to see an enhancement in the reduction of NHL cell viability. Based on these results, we propose that further preclinical studies should be performed before a combination of MEK 1/2 and PI3K inhibitors is evaluated in a clinical trial setting for patients with NHL.

CHAPTER 3. THE KSHV K1 PROTEIN MODULATES AMPK FUNCTION TO ENHANCE CELL SURVIVAL[2]

OVERVIEW

Kaposi's sarcoma-associated herpesvirus (KSHV) is the etiologic agent of Kaposi's sarcoma (KS) as well as two lymphoproliferative diseases, primary effusion lymphoma and multicentric Castleman's disease. KSHV encodes viral proteins, such as K1, that alter signaling pathways involved in cell survival. Expression of K1 has been reported to transform rodent fibroblasts, and K1 transgenic mice develop multiple tumors, suggesting that K1 has an important role in KSHV pathogenesis. We found that cells infected with a KSHV virus containing a WT K1 gene had a survival advantage under conditions of nutrient deprivation compared to cells infected with KSHV K1 mutant viruses. 5' adenosine monophosphate-activated protein kinase (AMPK) responds to nutrient deprivation by maintaining energy homeostasis, and AMPK signaling has been shown to promote cell survival in various types of cancers. Under conditions of AMPK inhibition, we also observed that cells infected with KSHV containing a WT K1 gene had a survival advantage compared to KSHV K1 mutant virus infected cells. To explore the underpinnings of this phenotype, we identified K1-associated cellular proteins by tandem affinity

[2] Anders P, Zhang Z, Bhende PM, Giffin L, Damania B., Manuscript accepted in *PLOS Pathogens*.

purification and mass spectrometry. We found that the KSHV K1 protein associates with the gamma subunit of AMPK (AMPKγ1). We corroborated this finding by independently confirming that K1 co-immunoprecipitates with AMPKγ1. Co-immunoprecipitations of wild-type K1 ($K1_{WT}$) or K1 domain mutants and AMPKγ1, revealed that the K1 N-terminus is important for the association between K1 and AMPKγ1. We propose that the KSHV K1 protein promotes cell survival via its association with AMPKγ1 following exposure to stress.

INTRODUCTION

Kaposi's sarcoma-associated herpesvirus (KSHV) is the causative agent of the endothelial cancer, Kaposi's sarcoma (KS), and two B-cell lymphomas including primary effusion lymphoma (PEL) and multicentric Castleman's disease (MCD) [1-3]. KSHV-related malignancies primarily arise in immune-suppressed individuals including HIV-positive individuals and organ transplant recipients, although these cancers can also occur in the absence of immunosuppression. KS is a common cancer in some sub-Saharan African countries [4, 128].

KSHV is a double-strand DNA gammaherpesvirus that is 165 to 170 kb long [129]. The KSHV genome contains multiple open reading frames that are conserved among other herpesviruses, and genes K1-K15 that are unique to KSHV [7]. Similar to other herpesviruses, KSHV has latent and lytic phases. Upon entering the host cell, KSHV typically establishes latency and expresses a limited number of viral proteins. Upon reactivation, which can be induced in vitro with various compounds such as 12-O-tetradecanoylphorbol-13-acetate (TPA), histone deacetylase (HDAC)

inhibitors, and TLR 7/8 ligands, KSHV enters the viral lytic cycle resulting in the production of infectious virions [7, 36].

Both latent and lytic phases appear to be important for KSHV pathology. Expression of latent genes generally promotes the survival of the infected cell and persistence of infection during cell division. Lytic gene expression results in the production of inflammatory cytokines, pro-angiogenic factors and viral proteins that subvert the host immune system and promote virion production. KSHV K1 is primarily expressed during the lytic phase although recent studies indicate that K1 is also expressed at low levels during latency [24, 35, 45].

K1 is a 46-kDa transmembrane glycoprotein that contains a C-terminal immunoreceptor tyrosine-based activation motif (ITAM) analogous to the signaling molecules in the B-cell receptor (BCR) signaling complex [47]. The K1 ITAM has been found to interact with various SH2 containing signaling molecules, including among others, the p85 regulatory unit of phosphoinositide-3-kinase (PI3K) [50]. K1 has been shown to initiate a signaling cascade leading to intracellular calcium mobilization, upregulation of NFAT and AP-1 transcription factors, and production of inflammatory cytokines [47, 50]. It is thought that K1 is maintained in an activated state by oligomerization of the K1 ectodomain and subsequent phosphorylation of the ITAM tyrosines by Src family kinases [49].

K1 has a role in KSHV-induced tumor development. K1 expression immortalizes primary endothelial cells, transforms rodent fibroblasts, and K1 transgenic mice develop spindle cell sarcomatoid tumors and plasmablastic lymphoma, suggesting that the K1 protein is important for KSHV-induced tumor

development [54-56]. These cancerous phenotypes may be due to K1's modulation of cellular proteins in signaling pathways that are important for cell survival. We and others have previously shown that K1 activates the PI3K/Akt/mTOR pathway and protects against Fas-mediated apoptosis [51-53].

In our current studies, we observed that cells infected with KSHV viruses containing a wild-type K1 gene (KSHV-$K1_{WT}$ and KSHV-$K1_{REV}$) displayed a survival advantage under conditions of nutrient deprivation compared to viruses containing mutant K1 genes (KSHV-$K1_{5XSTOP}$ and KSHVΔK1). To understand the underpinnings of this phenotype, we performed tandem affinity purification and mass spectrometry to identify K1 binding proteins. We found that KSHV K1 associates with the gamma subunit of 5'adenosine monophosphate-activated protein kinase (AMPKγ1).

AMPK is a heterotrimeric serine/threonine kinase composed of an alpha catalytic sub-unit and two regulatory subunits, beta and gamma [85]. Each subunit is part of a larger isoform family including the following subunit isoforms: α1, α2, β1, β2, γ1, γ2, and γ3 [130-133]. The isoforms of each subunit are found in different compartments within the cell. AMPKα1 and AMPKα2 localize to the cytoplasm. AMPKα2 also localizes to the nucleus in rat pancreatic and HeLa cells [134]. AMPKα1 and AMPKβ1 are in the perinuclear region in HEK-293 cells [135]. In mammalian neuron nuclei, AMPKα2, AMPKβ1, and AMPKγ1 are located in the nucleus [136]. The subunit isoforms can come together in various combinations to form different heterotrimers. The differences in function of each heterotrimer are still under investigation. The presence of the three subunits is necessary for full

activation of AMPK, and the regulatory subunits stabilize expression of the catalytic α subunit [137].

AMPK responds to stresses that reduce ATP levels by inhibiting anabolic and activating catabolic pathways to maintain energy homeostasis [86]. Binding of adenosine monophosphate (AMP) to the gamma subunit allosterically activates AMPK and promotes phosphorylation of AMPKα at Thr172 by upstream kinases [88-90]. AMPK also responds to environmental stress factors that reduce cellular ATP levels such as hypoxia [111, 138-140].

The role of AMPK as a tumor promoter is actively being explored [102, 103]. Some studies suggest that AMPK promotes tumor cell survival in vitro and in vivo. Inhibition of AMPK reduces prostate cell survival and increases apoptosis under normal and stressed conditions [104, 105]. AMPK promotes survival in multiple myeloma, colorectal and glioma cancer cell lines [107-109]. In vivo, AMPK signaling is elevated in developing tumors in a glioblastoma rat model [110]. Moreover, xenografts that have been prepared from AMPKα1/α2-null MEFs exhibit reduced tumor growth in comparison to wild-type (WT) MEFs [111]. Thus, there is accumulating evidence suggesting that AMPK may promote cancer cell survival and tumor development.

Here we report that K1 binds AMPKγ1 and that this interaction is important for K1's ability to enhance cell survival.

RESULTS

Cells infected with KSHV containing WT K1 display increased survival.

BAC16 recombinant viruses containing WT K1 (KSHV-$K1_{WT}$ and KSHV-$K1_{REV}$) were

made as previously described [141]. Immortalized human umbilical vein endothelial cells (HUVEC) [55] or iSLK cells were infected with BAC16 recombinant viruses containing WT K1 (KSHV-K1$_{WT}$ and KSHV-K1$_{REV}$) or mutant K1 (KSHV-K1$_{5XSTOP}$ and KSHVΔK1) genes [141]. These recombinant BAC16 viruses contain a GFP marker to monitor cell infectivity [141]. Both HUVEC and iSLK cells were stably selected until 100% of cells were green indicating that all cells were infected with these viruses.

Each HUVEC cell line was then subjected to stress by withdrawing serum and growth factors. KSHV-K1$_{WT}$ and KSHV-K1$_{REV}$ (revertant) harbor a wild type K1 gene while the KSHV-K1$_{5XSTOP}$ and KSHVΔK1 lack K1 (Fig. 3.1A). We evaluated cell viability at various time-points by MTS ([3-(4,5-dimethylthiazol-2-yl)-5-(3-carboxymethoxyphenyl)-2-(4-sulfophenyl)-2H-tetrazolium, inner salt), which is a measurement of metabolic activity, and trypan blue exclusion assay. At 24, 48, and 72 hours following nutrient deprivation, HUVEC infected with KSHV-K1$_{WT}$ and KSHV-K1$_{REV}$ had more viable cells compared to the KSHV-K1$_{5XSTOP}$ and KSHVΔK1 HUVEC as observed using the MTS assay (Fig. 3.1B). The differences were greatest at 72 hours post-nutrient deprivation.

To further substantiate these results, we also performed trypan blue exclusion assays and observed that the KSHV-K1$_{WT}$ and KSHV-K1$_{REV}$ infected cells were more viable compared to the cells infected with KSHV-K1$_{5XSTOP}$ and KSHVΔK1 infected cells at 48 and 72 hours (Fig. 3.1C). Similar to the MTS assay results, we observed reductions in cell viability in KSHV-K1$_{5XSTOP}$ and KSHVΔK1 infected cells

compared to KSHV-$K1_{WT}$ and KSHV-$K1_{REV}$ infected cells at 24, 48, and 72 hours post-starvation (Fig. 3.1C).

Furthermore, iSLK cell lines stably infected with these same viruses (KSHV-$K1_{WT}$, KSHV-$K1_{REV}$, KSHV-$K1_{5XSTOP}$ and KSHVΔK1) were also evaluated following serum withdrawal. Every two days for a total of 12 days, we evaluated cell viability by trypan blue exclusion. At all time-points following serum withdrawal, we observed that KSHV-KT_{WT} and KSHV-$K1_{REV}$ infected iSLK cells had increased viability compared to KSHV-$K1_{5XSTOP}$ and KSHVΔK1 iSLK cells (Fig. 3.1D). These findings suggest that K1 promotes KSHV-infected cell survival in the context of the whole genome and under conditions of nutrient deprivation.

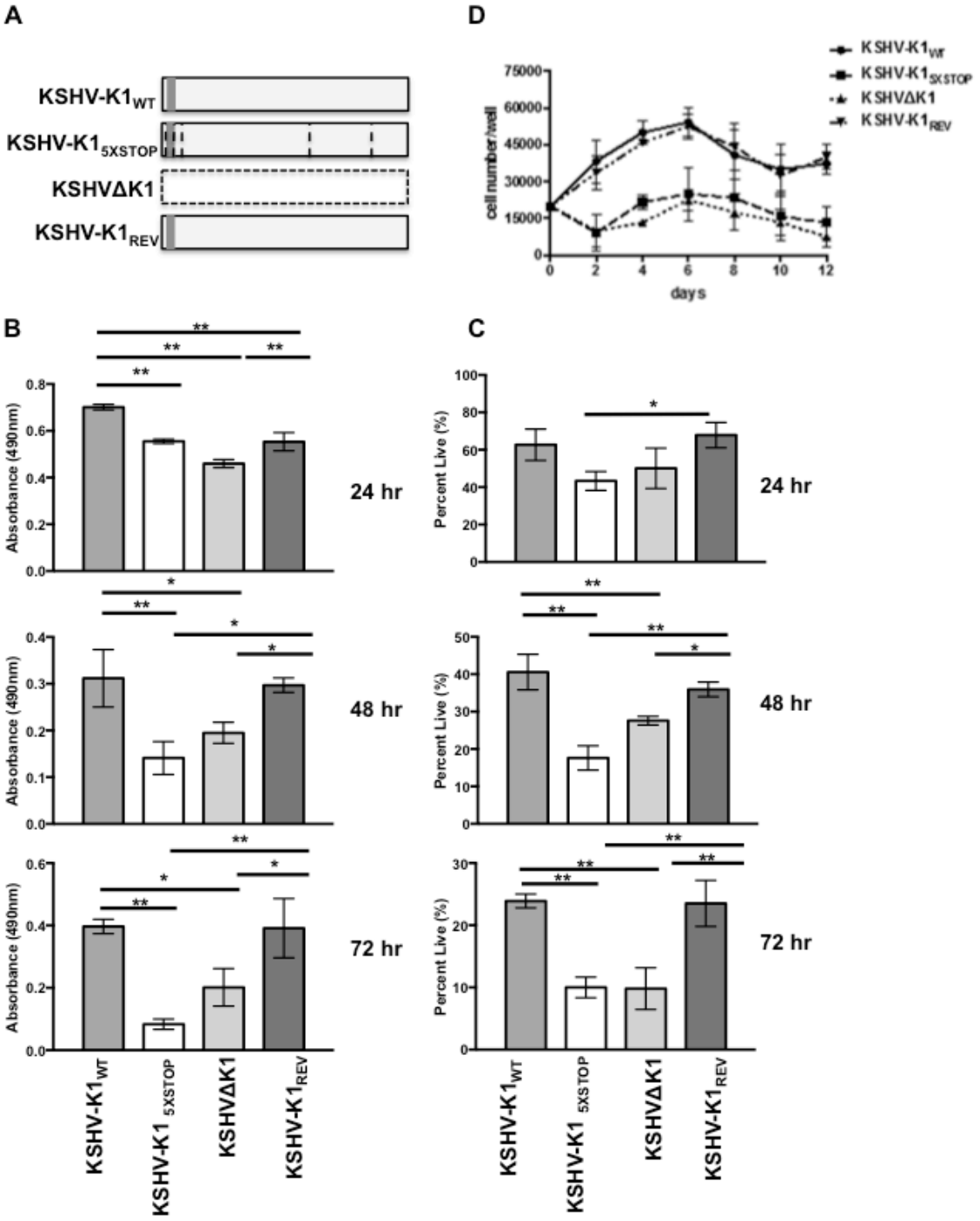

Figure 3.1. KSHV K1 mutant infected cells exhibit decreased survival following nutrient deprivation. (A) KSHV-K1$_{WT}$ and KSHV-K1$_{REV}$ (revertant) harbor a wild type K1 gene. The KSHV-K1$_{5XSTOP}$ has a K1 mutant gene that contains 5 stop codons. Three of the stop codons follow the first start codon of the K1 gene. The other two stop codons replace

two downstream ATG codons at positions 481 and 763 in the K1 gene. The KSHVΔK1 mutant has had the K1 gene replaced by a RpsL-Neo cassette. Hence, the KSHV-$K1_{5XSTOP}$ and KSHVΔK1 are not able to express the K1 protein. The grey box represents FLAG and horizontal lines represent the stop codons in KSHV-$K1_{5XSTOP}$. HUVEC infected with KSHV-$K1_{WT}$, KSHV-$K1_{5XSTOP}$, KSHVΔK1 or KSHV-$K1_{REV}$ were starved of serum and growth factors for 24, 48 and 72 hours. (B) The proportion of viable cells within each group was determined using an MTS assay. (C) The number of viable cells/well for each group was determined by trypan blue exclusion assay. Error bars are the standard deviation of biological triplicates. (D) KSHV-$K1_{WT}$, KSHV-$K1_{5XSTOP}$, KSHVΔK1, and KSHV-$K1_{REV}$ infected iSLK cells were cultured without serum. Cell viability was determined by trypan blue exclusion. Error bars are the standard deviation of biological triplicates. GraphPad Prism was used to determine one-way ANOVA and Tukey's post-test. *$P<0.05$,**$P<0.005$

A major regulator of metabolic stress is AMP-activated protein kinase (AMPK). AMPK responds to metabolic stress by activating catabolic pathways and inhibiting anabolic cell signaling pathways to maintain energy homeostasis [142]. Because we observed that cells infected with KSHV expressing a WT K1 gene had a survival advantage compared to cells infected with KSHV K1 mutant viruses following exposure to metabolic stress, and AMPK is involved in maintaining metabolic homeostasis, we hypothesized that K1 might modulate AMPK function. To explore this possibility, we compared cell survival in HUVEC infected with KSHV-$K1_{WT}$ and KSHV-$K1_{REV}$ wild-type viruses to KSHV-$K1_{5XSTOP}$ and KSHVΔK1 mutant viruses following treatment with the AMPK inhibitor, compound C. Compound C is a reversible and competitive inhibitor of ATP [143]. In the presence of 5μM ATP and

absence of AMP, compound C has a Ki of 109 ± 16 nM [143]. Compound C significantly prevents AMPK activation *in vitro* at 20 μM and 40 μM in cells treated with the AMPK activators metformin or AICAR [143]. According to Zhou et al., compound C has minimal impact on structurally related kinases such as ZAPK, SYK, PKCθ, PKA and JAK3 [143]. Inhibition of AMPK by compound C has been shown to induce cell death in various cell lines [105, 144].

We observed increased cell viability in KSHV-K1$_{WT}$ and KSHV-K1$_{REV}$ infected cells compared to KSHV-K1$_{5XSTOP}$ infected cells by MTS assay (Fig. 3.2A). Corroborating these results, we also observed increased cell viability in KSHV-K1$_{WT}$ and KSHV-K1$_{REV}$ compared to KSHVΔK1 infected cells, suggesting that cells infected with WT K1 virus are less sensitive to the stress induced by AMPK inhibition than cells infected with the KSHV K1 mutants (Fig. 3.2B). As expected, cell viability between KSHV-K1$_{WT}$ and KSHV-K1$_{REV}$ infected cells was essentially the same (Figs. 3.2A and 3.2B).

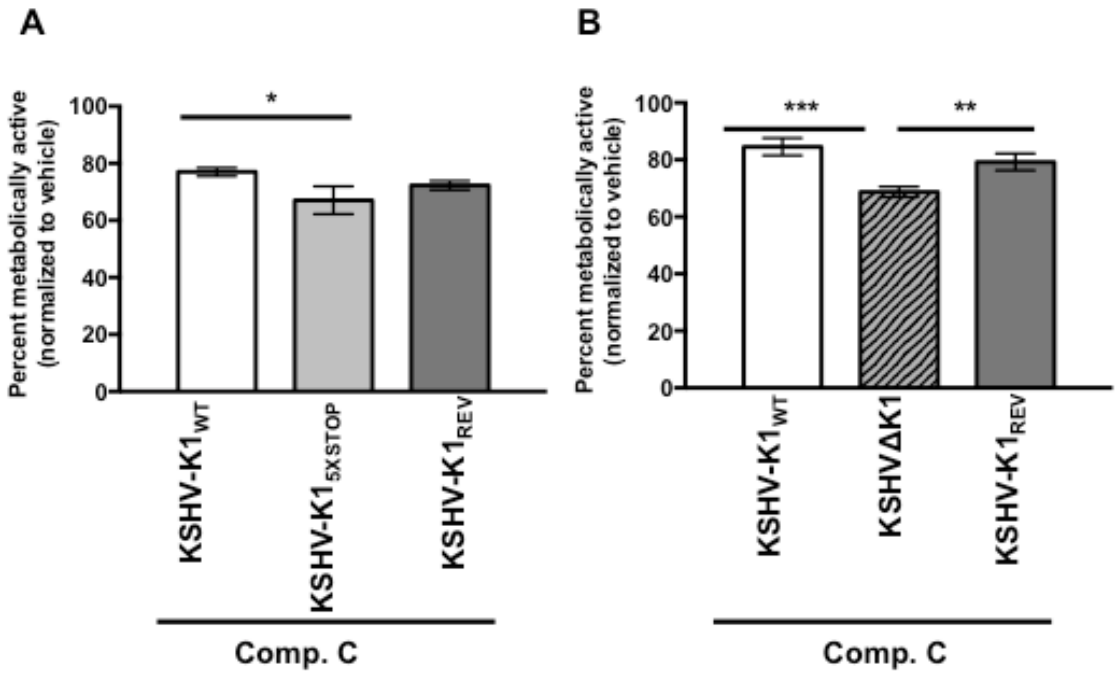

Figure 3.2. Cells infected with KSHV containing WT K1 are more resistant to AMPK inhibition than cells infected with KSHV K1 mutants. HUVEC infected with viruses containing a WT or mutant K1 gene were treated with 20 μM of compound C or vehicle control (DMSO = 0.2%) for 48 hours. The percent of metabolically active cells was determined using an MTS assay. Percentages were derived from normalization to vehicle treated samples. (A) The percent of metabolically active HUVEC stably infected with the recombinant viruses KSHV-$K1_{WT}$, KSHV-$K1_{5XSTOP}$, and KSHV-$K1_{REV}$. (B) The percent of metabolically active of HUVEC stably infected with KSHV- $K1_{WT}$, KSHVΔK1, and KSHV-$K1_{REV}$. Error bars represent the standard deviation of biological triplicates. GraphPad Prism was used to determine one-way ANOVA and Tukey's post-test. *P<0.02, **P<0.01, ***P<0.001.

To evaluate the impact of K1 expression by itself on cell survival following treatment with the AMPK inhibitor, compound C, we created FLAG epitope-tagged K1 (K1) or empty vector (EV) HEK-293 stable cell lines. The EV or K1 HEK-293 cells were treated with increasing concentrations of compound C, and cell viability was evaluated by trypan blue exclusion assay. We observed an increased number of viable cells in the K1 expressing cells compared to EV expressing cells using two different concentrations (10 μM and 20 μM) of compound C (Fig. 3.3A). We observed this difference at both 8 and 24 hours following incubation of the cells with 10 μM compound C (Fig. 3.3B). In order to determine whether K1 protected from apoptosis induced by AMPK inhibition, we also performed an assay to detect active caspase-3, which is an indicator of apoptosis. Active caspase-3 levels were remarkably elevated in EV cells compared to K1 expressing cells, suggesting that K1 protects cells from apoptosis when AMPK is inhibited (Fig. 3.3C). K1 expression in these cells was confirmed by a Western blot (Fig. 3.3D). This data suggests that K1 expression can keep cells alive by diminishing the effects of AMPK inhibition.

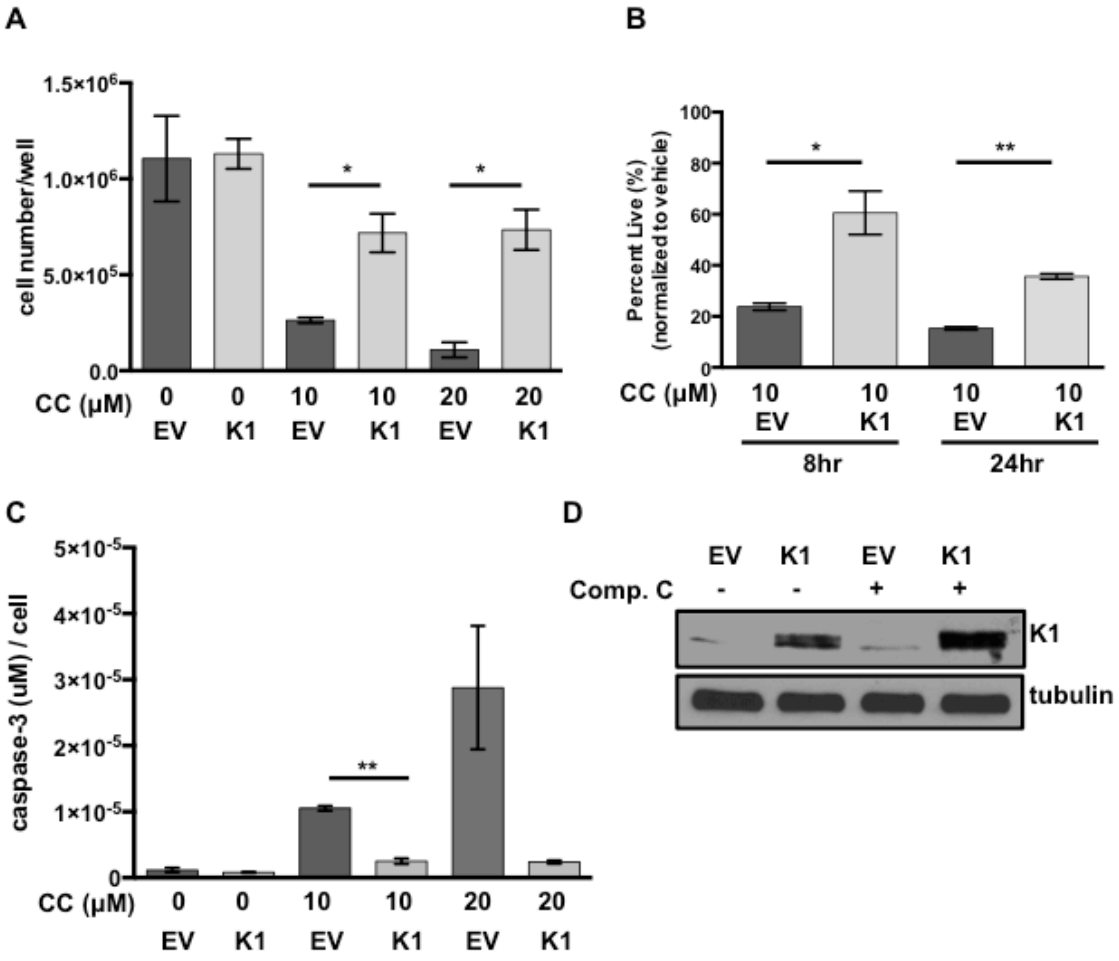

Figure 3.3. K1 expression provides a survival advantage in cells treated with compound C. (A) HEK-293 cells stably expressing empty vector (EV) or FLAG-K1 (K1) were treated in duplicate with 0 μM/ DMSO (0.2%), 20 μM compound C (CC) or 10 μM compound C for 6-8 hours. (B) HEK-293 cells stably expressing EV or K1 were treated in duplicate with 0 μM/DMSO (0.1%) or 10 μM compound C (CC) for 8 and 24 hours. Cell viability was determined by trypan blue exclusion assay. Percentages were derived from normalization to vehicle treated samples. (C) The level of caspase-3 activity was determined and normalized to cell number. (D) EV or K1 HEK-293 cells treated with either 0 μM/DMSO (0.1%) or 10 μM compound C for 6 hours and immunoblotted for K1 and tubulin. Statistical significance was evaluated by Student's t test. *P<0.05, **P<0.005

The KSHV K1 protein associates with the gamma subunit of AMPK (AMPKγ1). To investigate how K1 may be promoting cell survival following exposure to metabolic stress, we wanted to determine cellular proteins associated with K1. We identified K1-associated cellular proteins by performing tandem affinity purification of K1 from HEK-293 cells and subjecting cellular proteins bound to K1 to mass spectrometry.

Stable cell lines expressing a FLAG and HA double epitope-tagged version of K1 and EV HEK-293 cells were generated as previously described [145]. For tandem affinity purification, FLAG-HA-K1 or EV HEK-293 expressing cells were lysed with NP40 buffer. The clarified lysates were incubated with anti-FLAG M2 affinity gel, washed with NP40 buffer, and then eluted with 3X FLAG peptide. The eluates were subsequently incubated with an anti-HA resin, washed with NP40 buffer and eluted. The eluates were resolved by sulfate polyacrylamide gel electrophoresis (SDS-PAGE) and Coomassie stained. Only bands that were present in the K1 lane and absent in the EV lane were isolated and submitted for MALDI/TOF/TOF mass spectrometry (Fig 3.4A).

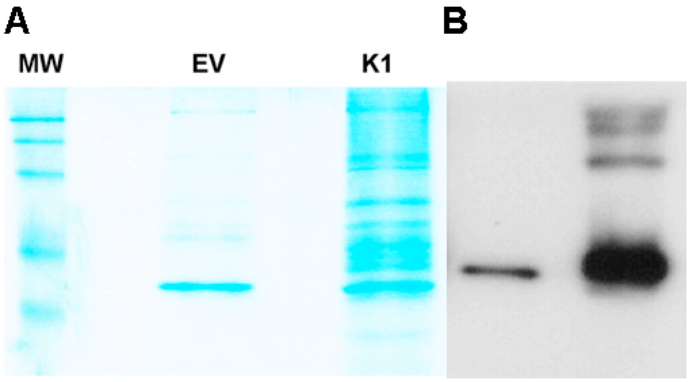

C

HSP90 unique peptides (HSP90AB1_IPI:IPI00414676.6)

EQVANSAFVER
FYEAFSK
HLEINPDHPIVETLR
HSQFIGYPITLYLEK
KHLEINPDHPIVETLR
LGIHEDSTNR
LGLGIDEDEVAAEEPNAAVPDEIPPLEGDEDASR
SIYYITGESK
ADHGEPIGR
DNSTM*GYM*M*AK
NPDDITQEEYGEFYK
RAPFDLFENK
YHTSQSGDEM*TSLSEYVSR

D

PRKAG1 unique peptides (PRKAG1_IPI:IPI00413318.4)

LPVIDPESGNTLYILTHK
LVVVDENDVVK
LVEAEVHR
TTTPVYVALGIFVQHR
FDVINLAAEK
AAPLWDSK
CYDLIPTSSK

Figure 3.4. K1 associating proteins determined by mass spectrometry. A) Stable cell lines expressing a FLAG and HA double epitope-tagged version of K1 and EV HEK-293 cells were subjected to tandem affinity purification. FLAG-HA-K1 or EV HEK-293 expressing

cells were lysed and the lysates were incubated with anti-FLAG M2 affinity gel, washed and eluted with 3X FLAG peptide. The eluates were subsequently incubated with an anti-HA resin, washed with NP40 buffer and eluted. The eluates were resolved by sulfate polyacrylamide gel electrophoresis (SDS-PAGE) and Coomassie stained. (B) The eluates from (A) were also subjected to SDS-PAGE and Western blot analysis with an anti-FLAG antibody to detect the presence of the monomer and oligomeric forms of K1. (C and D) Mass spectrometry analysis identified HSP90 (C) and AMPKγ1 also known as PRKAG1 (D) as K1 associating proteins. The peptide sequences of Hsp90 and AMPKγ1 identified by mass spectrometry are shown. Asterisk indicates modified amino acids.

We also confirmed successful pull-down of FLAG-HA-K1 by detecting FLAG by SDS-PAGE and Western blot (Fig. 3.4B). Using mass spectrometry, we found AMPKγ1 associated with K1 (Figs. 3.4D and 3.5A). We also observed an association between K1 and heat-shock protein 90 (HSP90) (Figs. 3.4C and 3.5A), which confirmed our previous report on the association of K1 with HSP90 [145].

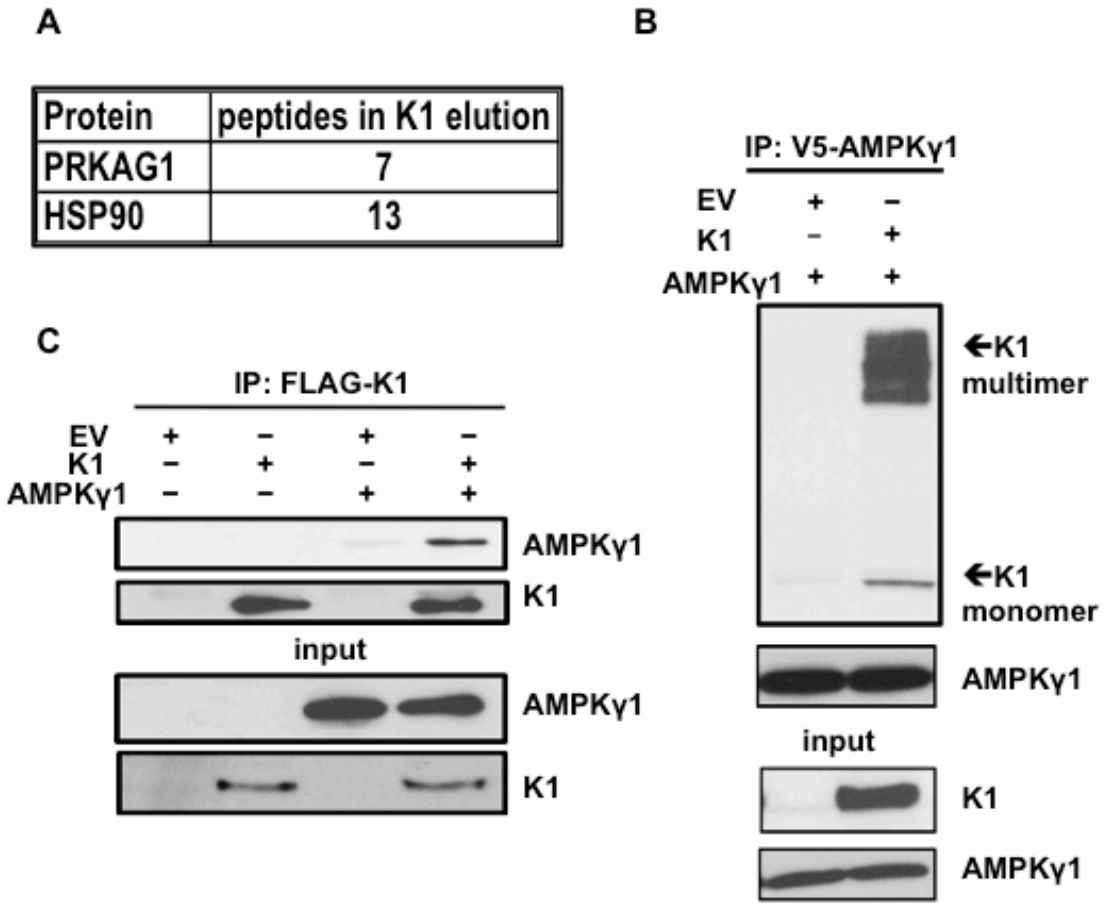

Figure 3.5. K1 associates with AMPKγ1. (A) Number of PRKAG1 (AMPKγ1) and HSP90 peptides identified in association with K1 by mass spectrometry. (B) HEK-293 cells stably expressing empty vector (EV) or FLAG-K1 (K1) were transfected with V5-AMPKγ1 (AMPKγ1). AMPKγ1 was immunoprecipitated, and immunoblotted for K1 or AMPKγ1. (C) HEK-293 cells stably expressing EV or K1 were transfected with AMPKγ1 or EV (pcDNA3). K1 was immunoprecipitated and immunoblotted for AMPKγ1 or K1.

Next, we constructed a V5 epitope-tagged AMPKγ1 (AMPKγ1) in pcDNA3 vector. To confirm the association between K1 and AMPKγ1 as determined by mass

spectrometry, we transiently expressed AMPKγ1 in HEK-293 cells stably expressing EV or FLAG epitope-tagged K1 (K1). We performed a co-immunoprecipitation by incubating EV- or K1-expressing HEK 293 clarified lysates containing equal amounts of protein with anti-V5 antibody to pull down the V5 epitope-tagged AMPKγ1. We detected the multimer and monomer forms of K1 co-immunoprecipitating with AMPKγ1 in K1-expressing cells, but not from EV control cells (Fig. 3.5B). To further substantiate the association between K1 and AMPKγ1, we performed the reverse immunoprecipitation and immunoprecipitated K1. We observed that AMPKγ1 co-immunoprecipitated with K1 from K1-expressing cells but not from EV control cells (Fig. 3.5C).

In the cell, AMPKγ1 complexes with AMPKα1 and AMPKβ1. In addition to AMPKγ1, we next wanted to determine whether the other AMPK subunits were part of the protein complex associated with K1. We transfected V5-AMPKγ1 in HEK-293 cells stably expressing empty vector (EV) or FLAG-K1 (K1), immunoprecipitated V5-AMPKγ1, and probed for endogenous AMPKα1 and AMPKβ1. In addition to detecting K1 as we previously observed, we also observed the expression of AMPKα1 and AMPKβ1 (Fig. 3.6A), suggesting that there is an association between K1 and the three subunits of AMPK. Next we wanted to determine whether we could detect association of K1 and endogenous AMPK. Because our antibody for AMPKγ1 was not appropriate for immunoprecipitation, and we had detected AMPKβ1 in the complex with AMPKγ1 and K1; we immunoprecipitated endogenous AMPKβ1 and probed for K1 (Fig. 3.6B). Upon AMPKβ1 immunoprecipitation, we detected K1,

further confirming an association between K1 and the endogenous AMPK complex (Fig. 3.6B).

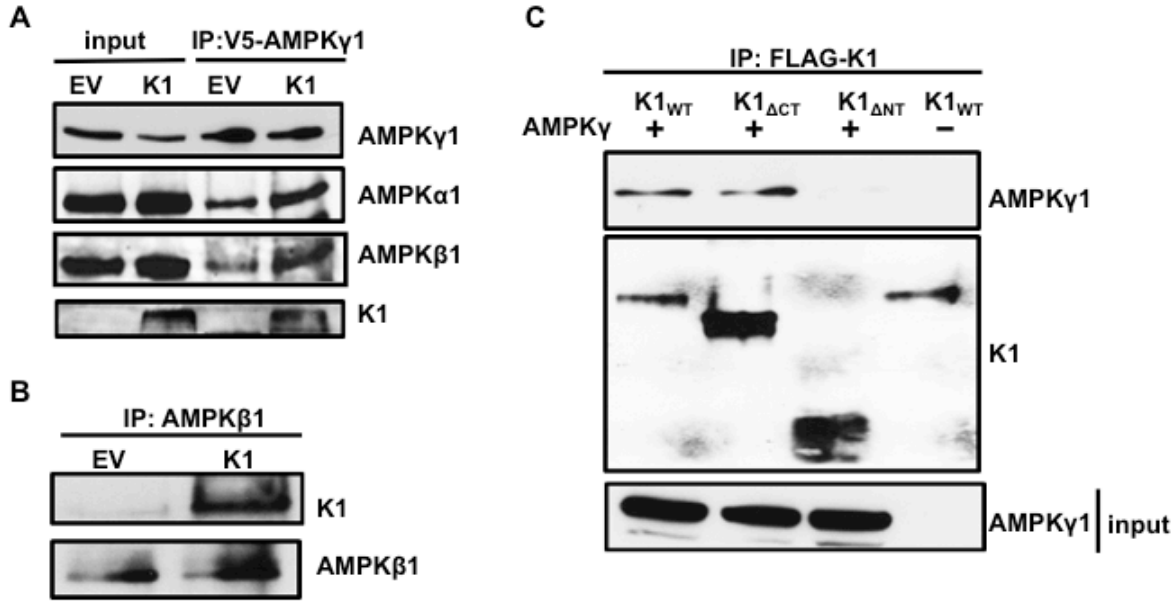

Figure 3.6. The K1 N-terminus is important for association with AMPKγ1. (A) HEK-293 cells stably expressing empty vector (EV) or FLAG-K1 (K1) were transfected with V5-AMPKγ1 (AMPKγ1). AMPKγ1 was immunoprecipitated, and blots were probed for AMPKγ1, endogenous AMPKα1, endogenous AMPKβ1 and K1. (B) Endogenous AMPKβ1 was immunoprecipitated from EV or K1 expressing HEK-293 cells. The blots were probed for K1 or AMPKβ1. (C) HEK-293 cells were transiently transfected with AMPKγ1 and with one of the following: $K1_{WT}$, $K1_{\Delta CT}$ or $K1_{\Delta NT}$. An equivalent amount of EV (pcDNA3) was also transfected along with $K1_{WT}$. We immunoprecipitated the various K1 domain mutants, and immunoblotted for AMPKγ1 or K1.

K1 has an immunoglobulin-like N-terminus, a transmembrane region, and a cytoplasmic tail containing an ITAM. To identify the region of K1 that associates with AMPKγ1, we performed co-immunoprecipitations of various FLAG-tagged K1

domain deletion mutants and V5-tagged AMPKγ1. We transiently expressed V5-AMPKγ1 (AMPKγ1) along with one of the following in HEK-293 cells: $K1_{WT}$, K1 lacking the C-terminus ($K1_{\Delta CT}$), or lacking the N-terminus ($K1_{\Delta NT}$). We also transfected an equivalent amount of EV (pcDNA3) and $K1_{WT}$ as a control. The construction of the FLAG-tagged K1 mutants has previously been described [145]. We immunoprecipitated $K1_{WT}$, $K1_{\Delta CT}$, or $K1_{\Delta NT}$ and probed for V5-tagged AMPKγ1 (Fig. 3.6C). As previously observed, we detected co-immunoprecipitation of AMPKγ1 and $K1_{WT}$ (Fig. 3.6C, lane 1). We also detected co-immunoprecipitation of AMPKγ1 and $K1_{\Delta CT}$ indicating that the K1 C-terminus is not important for K1 and AMPKγ1 association (Fig. 3.6C, lane 2). We did not observe co-immunoprecipitation of AMPKγ1 and $K1_{\Delta NT}$ suggesting that AMPKγ1 associates with K1 via the K1 N-terminus (Fig. 3.6C, lane 3).

K1 and AMPK subunits are localized to cellular membranes. About 10-20% of K1 is localized to the plasma membrane with the major fraction of K1 being found in the endoplasmic reticulum [46]. K1 can also be internalized and internalization is associated with K1 signaling [146]. Additionally, all three subunits of AMPK have been shown to localize to the cellular membrane fraction [135]. We wanted to evaluate the localization of the endogenous AMPK subunits in EV- and K1-expressing stable HEK-293 cells. We lysed equal numbers of EV- and K1-expressing HEK-293 cells and separated the cellular fractions. The fractions were then resolved by SDS-PAGE and Western blot. The blots were probed using antibodies specific for each AMPK subunit and isoform. In addition to being localized to the cytoplasm, we observed that AMPKα, AMPKβ1, and AMPKγ1 were detected

in the cellular membrane fraction (Fig. 3.7A). Along with the AMPK subunits, K1 was also found in the membrane fraction (Fig. 3.7A). We evaluated the purity of the cytoplasmic, membrane, and nuclear fractions by probing for MEK1/2, K1, and histone H3 respectively (Fig. 3.7A). These proteins are restricted to each of these fractions. Based on these findings, we conclude that K1 and multiple AMPK subunits and isoforms (without over expression) are localized to the cellular membrane fraction, suggesting that K1 associates with AMPK in the cellular membrane.

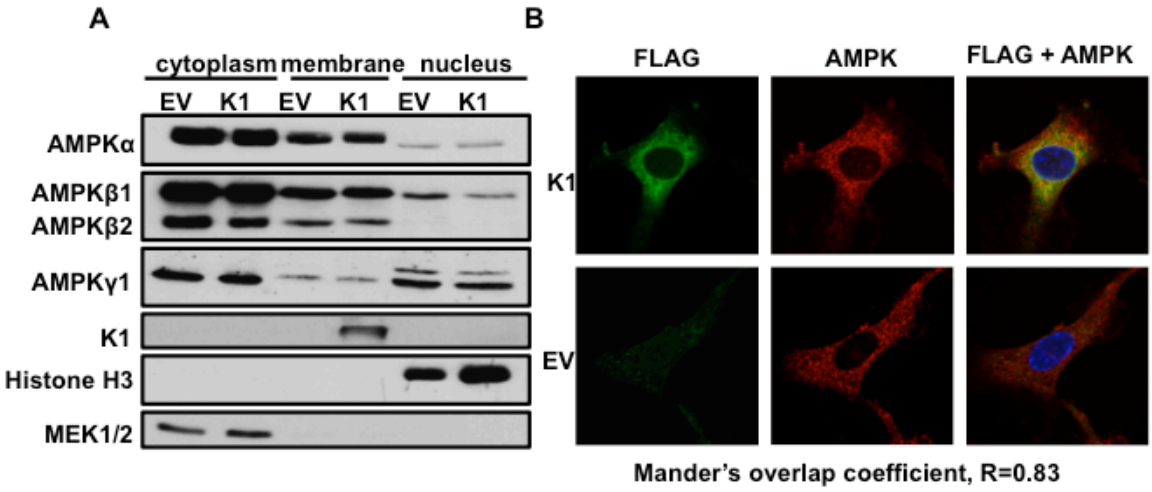

Figure 3.7. K1 and AMPK are visualized in membranes and the perinuclear area of the cell. (A) HEK-293 cells stably expressing empty vector (EV) or FLAG-K1 (K1) were lysed and fractionated into cytoplasmic, membrane and nuclear fractions. Immunoblots were probed for endogenous AMPK subunit and isoforms. (B) HUVEC stably expressing empty (EV) or FLAG-K1 (K1) were fixed and permeabilized. Cells were then stained with anti-FLAG directly conjugated to FITC antibody, and an AMPKβ1/2 antibody, followed by an anti-rabbit conjugated to Alexa Fluor 647. Nuclei were stained with DAPI. Stained HUVEC were evaluated with a Zeiss 700 confocal microscope using a 63X oil objective. Mander's overlap coefficient for this image (R = 0.83) was generated using ImageJ.

We subsequently evaluated localization of FLAG-K1 (K1) and endogenous AMPK by immunofluorescence staining. Because our AMPKγ1 antibody is not appropriate for immunofluorescence staining, and we had determined that AMPKβ1 co-localized with K1 (Fig. 3.6B), we stained for K1 and endogenous AMPKβ1/2 in EV- or K1- stably expressing HUVEC. We fixed the cells with formaldehyde, washed and then permeabilized the cells with Triton-X-100. We stained cells with FLAG-K1-FITC and AMPKβ1/2 antibodies followed by an anti-rabbit Alexa Fluor 647 secondary antibody. By confocal microscopy, we acquired z-stacks on fully stained EV and FLAG-tagged K1 HUVEC (Fig. 3.7B). We also completed z-stacks on controls containing only the secondary anti-rabbit AF647 in order to demonstrate that the staining for AMPKβ1/2 is specific and not due to non-specific secondary staining. We observed co-localization of K1 and endogenous AMPKβ1/2 in the perinuclear area (Fig. 3.7B) as determined by a Mander's overlap coefficient of 0.83, which was determined using ImageJ software. The EV transfected cells stained positive for AMPKβ1/2 but not K1, as expected.

In Fig. 3.6C we had observed that $K1_{\Delta NT}$ does not associate with AMPKγ1 by co-immunoprecipitation. $K1_{\Delta NT}$, lacks the signal peptide sequence, therefore we wanted to confirm that its lack of association with AMPKγ1 is not due to being mislocalized in the cell. Thus, we transiently expressed $K1_{\Delta NT}$, and fractionated the cell lysates into cytoplasmic, membrane and nuclear components. We then evaluated $K1_{\Delta NT}$ expression in the membrane fraction by immunoblotting for $K1_{\Delta NT}$. We observed that $K1_{\Delta NT}$ is in the membrane fraction (Fig. 3.8A). We also evaluated

the fractionation efficiency by immunoblotting for MEK1/2, AIF, and Histone H3, indicators for the cytoplasm, membrane and nucleus, respectively. To corroborate our previous findings, we confirmed that $K1_{WT}$ and AMPKγ1 associate in the membrane fraction and that there is loss of $K1_{\Delta NT}$ and AMPKγ1 association in the membrane fraction by co-immunoprecipitation. Thus, we immunoprecipitated EV (pcDNA3), $K1_{WT}$, $K1_{\Delta CT}$, or $K1_{\Delta NT}$ and probed for V5-tagged AMPKγ1. We detected $K1_{WT}$ and AMPKγ1 association, and we did not detect $K1_{\Delta NT}$ and AMPKγ1 association in the membrane fraction (Fig. 3.8B).

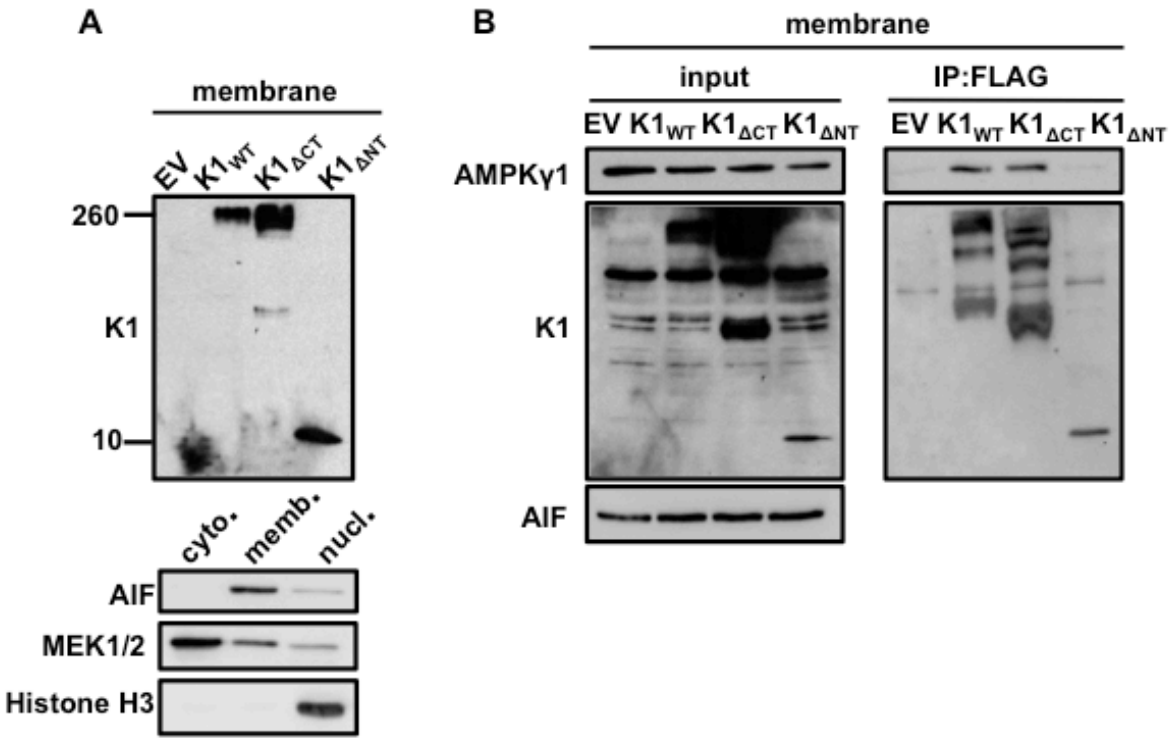

Figure 3.8. K1 N-terminus is important for K1 association with AMPKγ1 in the membrane fraction. (A) HEK-293 cells were transfected with EV (pcDNA3), $K1_{WT}$, $K1_{\Delta CT}$, and $K1_{\Delta NT}$, and then fractionated into cytoplasmic (cyto.), membrane (memb.) and nuclear (nucl.) fractions. FLAG was detected in the membrane fraction by Western blot. The

fractionation efficiency was evaluated by detecting AIF (membrane), MEK1/2 (cytoplasm), and Histone H3 (nucleus). (B) HEK 293 cells were transfected as described in (A) with the addition of V5-AMPKγ1. The cells were fractionated, and FLAG was immunprecipiated using the membrane fraction. V5-AMPKγ1 was detected by immunoblot.

K1 and AMPK association is important for cell survival following exposure to stress. Thus far, we have observed that KSHV K1 promotes survival in stressed cells, and K1 associates with AMPK via the K1 N-terminus. We next wanted to determine whether the association of K1 and AMPK is important for the survival advantage observed in stressed cells. We generated lentivirally transduced HEK-293 cells stably expressing FLAG epitope-tagged $K1_{WT}$, $K1_{\Delta CT}$, $K1_{\Delta NT}$ and empty vector (EV). We treated these cells with the AMPK inhibitor, compound C, and evaluated cell viability using the MTS assay. We observed an increased percentage of viable $K1_{WT}$ expressing cells when AMPK was inhibited, compared to cells expressing $K1_{\Delta NT}$. This result suggests that the association between K1 and AMPK is important for survival in stressed cells (Fig. 3.9A). Surprisingly, we also observed that $K1_{\Delta CT}$ expressing cells appear sensitive to AMPK inhibition, indicating that the K1-C terminus is also important for survival in stressed cells (Fig. 3.9A). We confirmed expression of the various K1 constructs by completing a Western blot using an anti-FLAG antibody or an anti-K1 antibody (Fig. 3.9B). When we immunoblotted with an anti-FLAG antibody, we observed low levels of $K1_{\Delta NT}$. Thus, we re-probed this blot using an anti-K1 antibody, and saw expression of $K1_{\Delta NT}$

expression but no $K1_{\Delta CT}$ expression since the K1 antibody is directed towards an epitope on the K1 C-terminus (Fig. 3.9C).

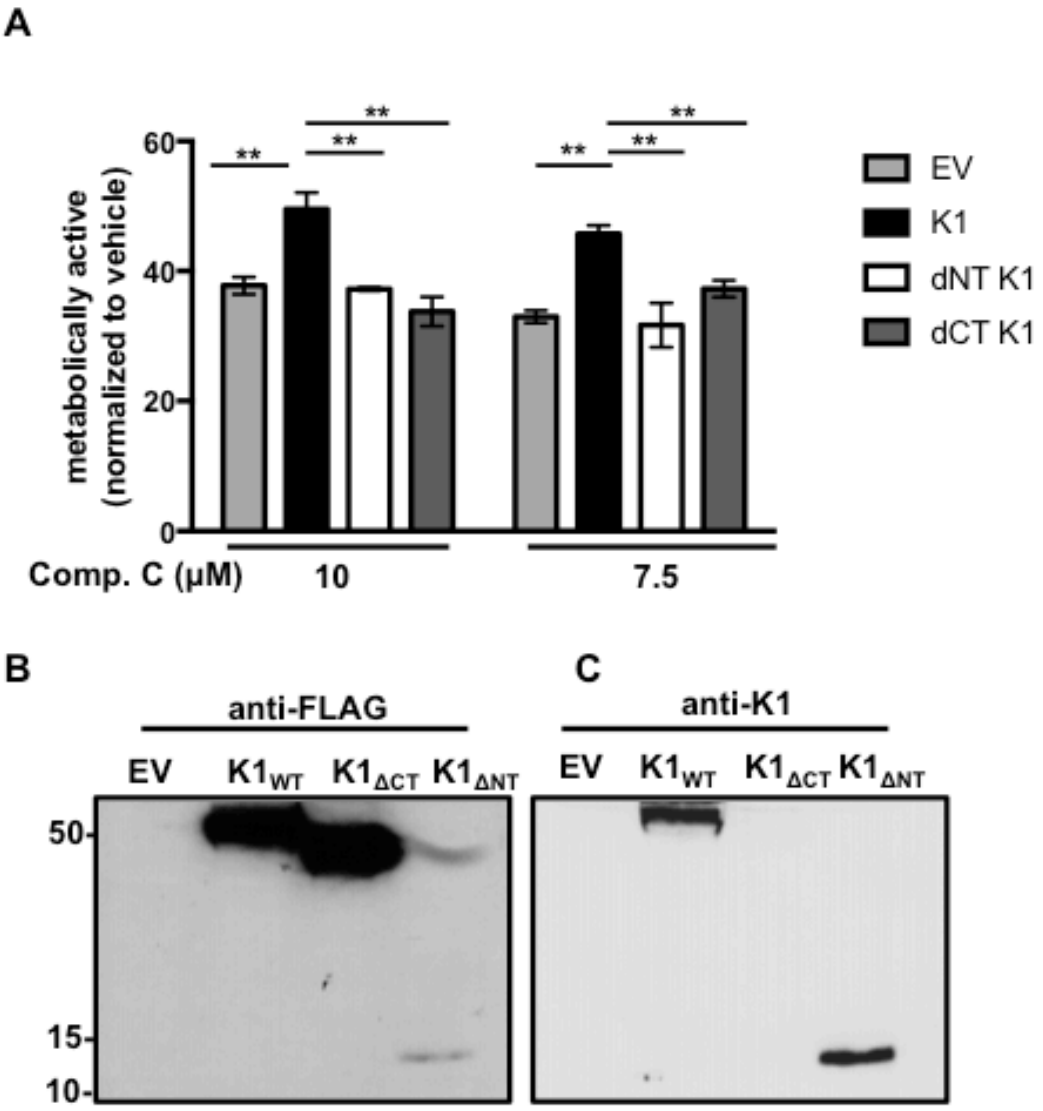

Figure 3.9. K1 and AMPK association is important for cell survival following exposure to stress. (A) HEK-293 cells stably expressing FLAG-tagged $K1_{WT}$, $K1_{\Delta CT}$, $K1_{\Delta NT}$ or empty vector (EV = pLenti CMV) were treated with 10 or 7.5 μM compound C for 48 hours. Cell viability was determined using the Promega MTS assay. The percent of metabolically active

cells was determined by normalization to the DMSO (0.1%) control. Error bars represent the standard deviation of biological triplicates. (B) Western blot showing expression of EV, $K1_{WT}$, $K1_{\Delta CT}$, and $K1_{\Delta NT}$ using an anti-FLAG antibody. (C) Western blot from (Fig. 7B) was stripped and probed for K1 using an anti-K1 antibody. GraphPad Prism was used to determine one-way ANOVA and Tukey's post-test **P<0.005

K1 facilitates AMPK activity in stressed cells. We found that K1 associates with AMPK and this association is important for the survival advantage in stressed cells. We next wanted to determine the status of AMPK activity in stressed EV and K1 expressing cells. We exposed HUVEC stably expressing empty vector (EV) or FLAG-tagged K1 (K1) to media without serum and growth factors containing either compound C or DMSO control for 24 hours. We then performed an AMPK-specific kinase activity assay. We incubated lysate from EV or K1 expressing HUVEC with or without an AMPK substrate, a synthetic peptide called SAMS peptide (HMRSAMSGLHLVKRR), AMP, and radiolabeled γ-32P-ATP [147]. We next evaluated the incorporation of radiolabeled phosphate from γ-32P-ATP into SAMS peptide. Compound C treatment resulted in an overall reduction in AMPK activity in both EV and K1 expressing cells compared to untreated cells. However, in the presence of compound C, we observed a higher degree of AMPK activity in K1 expressing cells compared to EV expressing cells (Fig 3.10A). This data suggests that K1 expression promotes AMPK activity in stressed cells. We also confirmed that K1 expression is not altered by nutrient deprivation and compound C treatment by Western blot analysis (Fig 3.10B).

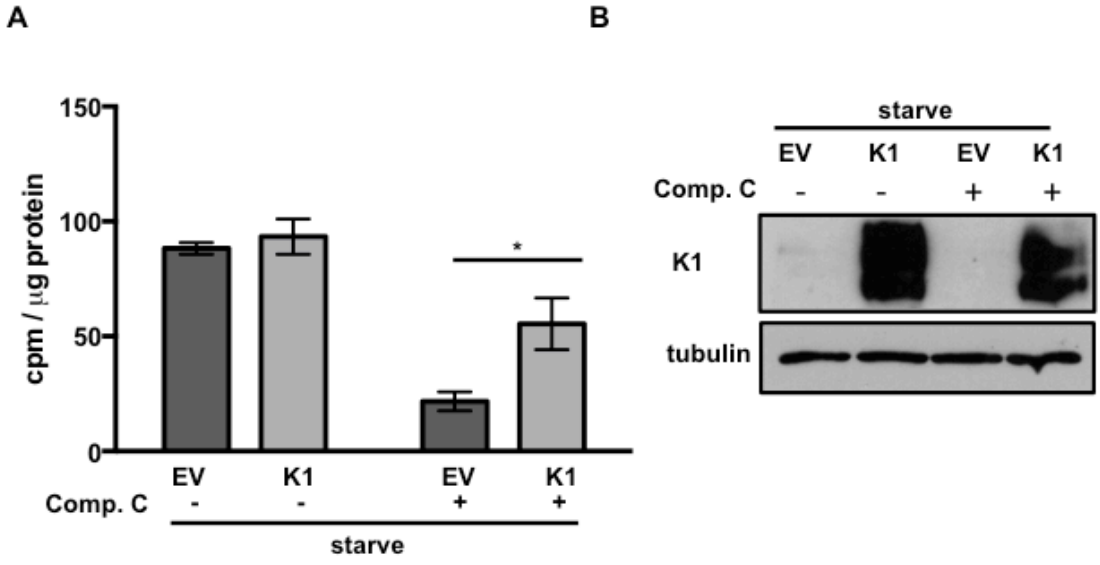

Figure 3.10. K1-expression facilitates AMPK activity in stressed cells. (A) HUVEC stably expressing empty vector (EV) or FLAG-K1 (K1) were deprived of serum and growth factors (starve) for 24 hours. At the time of starvation, 5 μM compound C or DMSO (0.05%) was added. Each condition for EV and K1 was completed in triplicate. AMPK-specific activity was determined by subtracting counts per minute (cpm) derived for each sample incubated without SAMS peptide from cpm derived from each sample incubated with SAMS peptide. These values were then normalized to total protein for each sample. The error bars represent the standard deviation of triplicates. (B) Western blot of K1 and tubulin using lysate from the AMPK activity assay. *P<0.05 Student's t test

K1 maintains PI3K pathway despite AMPK activation. Because K1 activates the PI3K pathway via its ITAM in the C-terminus, we wanted to know whether the pathway remains active when cells are exposed to serum starvation, a condition that activates AMPK. Activated AMPK inhibits mTORC1 in two ways. AMPK phosphorylates tuberous sclerosis 2 (TSC2) and raptor; both events ultimately result

in the inhibition of mTORC1 [148, 149]. We either serum starved for 8 hours or treated HUVEC cells stably expressing EV or K1 with vehicle or oligomycin, an ATP synthase inhibitor and an AMPK activator. We then evaluated AMPK and S6K activity by completing SDS-PAGE and Western blot. With serum starvation and oligomycin treatment, we observed an increase in phosphorylated levels of AMPK compared to vehicle treated cells (Fig. 3.11). We also observed a slight increase in AMPK activity in K1-expressing cells compared to EV (Fig 3.11). Following serum starvation, there is an overall decrease in phosphorylated S6K in both EV and K1-expressing cells compared to vehicle treated, but there is greater S6K activity with K1 expression than EV (Fig. 3.11). This data suggests that despite AMPK activity, K1 maintains PI3K pathway activation under certain conditions.

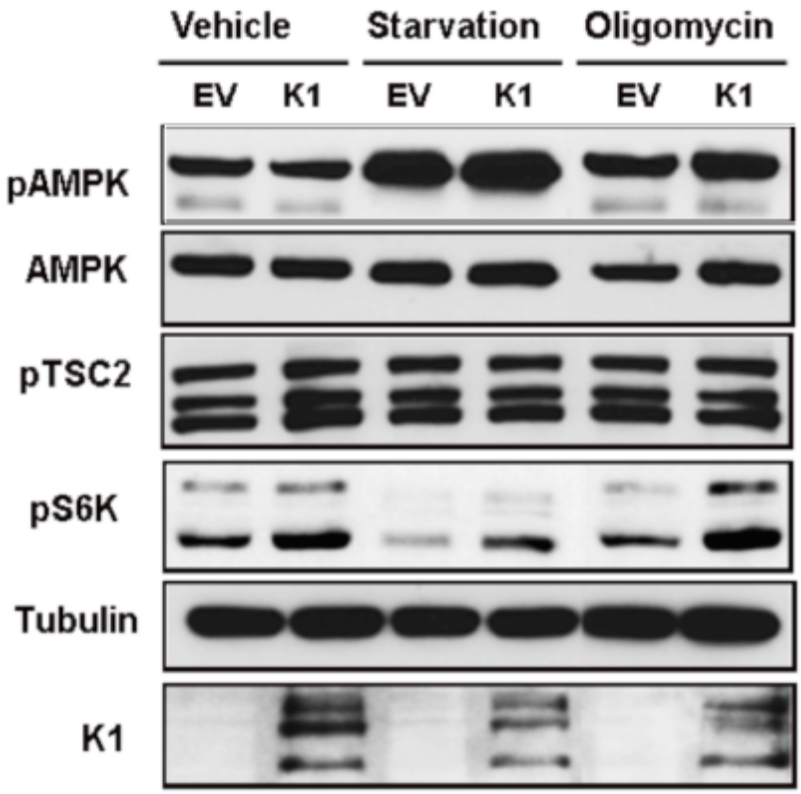

Figure 3.11. K1 maintains an active PI3K pathway despite AMPK activation following 8 hours of serum starvation. HUVEC stably expressing EV or K1 were treated with vehicle (DMSO), serum starved for 8 hours, or treated with 2 μM oligomyicn, an ATP synthase inhibitor one hour prior to cell harvest. The levels of phosphorylated and total proteins were determined by Western blot.

DISCUSSION

Cell survival during KSHV infection is paramount to the establishment of life-long infection. Upon infection, KSHV primarily enters a latent state. During latency, KSHV expresses a limited number of proteins and microRNAs that enable it to successfully persist in the cell by avoiding the immune response and by promoting cell survival [150]. When KSHV reactivates and enters the lytic stage, the cell must remain viable throughout viral replication and virion assembly so that infectious virions are generated. Cell death prior to completion of the lytic program would result in defective viral replication.

We observed that KSHV infected cells containing a WT K1 gene had a survival advantage compared to cells infected with KSHV K1 mutants following exposure to stress. To explore the underpinnings of this phenotype, we completed tandem affinity purification and mass spectrometry to identify K1-associating proteins. We identified AMPKγ1 as a K1-associating protein. We corroborated this finding independently and found that K1 co-immunoprecipitated with AMPKγ1. By performing co-immunoprecipitations of AMPKγ1 and K1 domain mutants, we found that the K1 N-terminus is important for K1 and AMPKγ1 association. The association

between K1 and AMPK is important for the survival advantage in stressed cells because we observed reduced cell viability in cells expressing $K1_{\Delta NT}$ compared to $K1_{WT}$. Our studies indicate that KSHV K1 promotes survival via its association with AMPK, and KSHV K1 facilitates AMPK activity in stressed cells.

Under normal culture conditions, our lab and others have shown that K1 activates the PI3K/Akt/mTOR pathway [50, 51]. It has been reported that cells having overly active Akt and consequently a high glycolytic rate are more sensitive to cell death following starvation compared to control cells [151]. Moreover, when starved-cells are treated with an activator of AMPK, cells with active Akt are protected from cell death [151]. KSHV-infected cells also have an active PI3K/Akt/mTOR pathway and a high glycolytic rate [80, 152, 153]. Furthermore, simultaneous activation of AMPK, Akt and mTOR, has been observed in liver cancer cells following nutrient starvation [154]. Thus, low levels of AMPK activation may promote metabolic adaptation and consequently, increase KSHV-infected cell survival. We propose that K1 promotes AMPK activity during metabolic stress and in this way enhances KSHV-infected cell survival.

Among others, we identified another K1-associating protein, the endoplasmic reticulum calcium ATPase 2 (SERCA) by mass spectrometry. SERCA is a calcium pump that controls calcium levels by pumping Ca2+ in an ATP-dependent manner from the cytosol into the ER [155, 156]. Homeostatic movement of intracellular Ca2+ from the cytosol into the ER via SERCA and from the ER towards the mitochondria via inositol 1, 4, 5-triphosphate receptors (IP3Rs) is critical for the function of cellular processes including autophagy and apoptosis [155]. The function or expression of

SERCA and/or IP3Rs can be modulated by pro-tumorigenic factors such as BCL-2 and myc, thus, promoting cell survival in a changing tumor microenvironment [155].

AMPKα2 expression promotes SERCA activity and reduces ER stress in HUVEC cells [157]. Although interaction between K1, SERCA and AMPK has not been confirmed by co-immunoprecipitations, we speculate that K1 modulates SERCA activity by altering AMPK activity and consequently, alleviates ER stress. Increased ER stress can be detrimental to the cell and result in apoptosis [158].

The role of AMPK during herpesvirus infection is complicated, and whether it promotes viral replication or inhibits it may depend on a variety of factors. During human cytomegalovirus (HCMV) infection, AMPK has been found to promote a metabolic environment that is conducive to viral replication [159, 160]. AMPK inhibition blocks increased glycolysis that is induced by HCMV infection and inhibits viral DNA synthesis [160]. Interestingly, treatment of HCMV-infected fibroblasts with the AMPK activator, AICAR [159, 161] or the inhibitor, compound C, results in reduced HCMV replication [159]. During human herpes simplex virus-1 (HSV-1) infection, AMPK activity facilitates neuron survival and reduces viral production [162]. Thus, AMPK appears to impact viral production differently during HCMV and HSV-1 infection.

Recently, Cheng et al. observed that endogenous AMPKα1 inhibits KSHV replication following primary infection [163]. AMPK does not seem to affect KSHV infectivity nor trafficking to the nucleus but it does have an inhibitory affect on KSHV lytic gene expression since knock down of AMPK results in increased expression of

some KSHV lytic genes and corresponding proteins [163]. Thus, AMPK inhibits the KSHV lytic cycle but not the establishment of latency.

Our studies examined the role of AMPK in latently K1 WT or mutant KSHV-infected cells that had been subjected to stress. Our results do not contradict those results of Cheng et al. because we are each examining very different phases of the KSHV life cycle. Because AMPK can be activated by a variety of cellular stresses and can impact multiple cell signaling pathways, we will most likely observe that AMPK can differentially impact the infected-cell and the KSHV life cycle as we investigate further the role of AMPK during KSHV infection. Another layer of complexity is that there are multiple isoforms of the AMPK subunits. Therefore, different combinations of these isoforms can form different heterotrimeric complexes. We do not yet understand how the different combinations may result in altered functions of AMPK.

MATERIALS AND METHODS

Cell culture, transfections, and chemical compounds. HEK-293 (ATCC, CRL-1573) and iSLK cells [141] were maintained in Dulbecco's Modified Eagle Medium (DMEM) and human telomerase-reverse transcriptase-immortalized human umbilical vein endothelial cells (hTERT-HUVEC) [55] were cultured in endothelial growth basal medium (EBM-2) from Lonza and supplemented with an endothelial cell growth medium (EGM-2) bullet kit without heparin and ascorbic acid supplements. All cell lines were supplemented with 10% heat-inactivated fetal bovine serum (HI-FBS), 1% penicillin-streptomycin (PS), and 1% L-glutamine and maintained at 37°C and 5% CO2. Additionally, EV (pcDNA3) or FLAG-K1 stably

expressing HEK-293 cells were maintained in 1 mg/mL G418. For transfection of HEK-293 cells, cells were transfected with 10 µg pcDNA3-V5-AMPKγ1 or vector per 10 cm plate using XtremeGENE HP reagent according to the manufacturer's instructions. The AMPK inhibitor, compound C, was purchased from Calbiochem and suspended in dimethyl sulfoxide (DMSO).

Constructs. HEK-293 cells stably expressing EV or FLAG-HA-K1 were made as previously described [145]. Briefly, FLAG-HA was cloned following the signal peptide sequence on the N-terminus of K1 (Accession# AF170531). The FLAG-HA-K1 was then cloned into the pcDNA3 vector. A V5-epitope tag was added to the N-terminus of PRKAG1 (NP_002724) by PCR and then cloned into the pcDNA3 vector. The pcDNA3-K1 domain mutants were prepared as previously described [145]. The pcDNA3-K1 WT construct was used as a template for making the lentiviral K1 WT and mutant constructs. pLenti-FLAG-K1 domain mutants were generated using Q5 Site-Directed Mutagenesis kit (Q5) by New England Biolabs Inc and appropriate primer sets were designed according to the Q5 kit specifications. FLAG-K1, FLAG-$K1_{\Delta CT}$, and FLAG-$K1_{\Delta NT}$ were cloned into the lentiviral vector, pLenti CMV Puro DEST. Empty vector is pLenti CMV Puro. DEST. pLenti-FLAG-K1 domain mutants were generated using Q5 Site-Directed Mutagenesis kit by New England Biolabs Inc.

Generation of stable cell lines. pcDNA3-FLAG-HA-K1 or pcDNA3 empty vector were transfected into HEK-293 cells and selected in media containing 1 mg/mL G418. All lentiviruses were prepared using the Virapower lentiviral expression system as per the manufacturer's instructions (Invitrogen). hTERT-

HUVEC or HEK-293 cells were cultured to approximately 80% confluency in a 6-well dish. At the time of lentiviral transduction, cells were rinsed with PBS and 2 mLs of lentivirus (unconcentrated) was added in the presence of 10 μg/mL polybrene. The cells were centrifuged for 90 minutes at 3000 RCF at 30°C. The cells were then incubated overnight at 37°C and 5% CO2. The media containing lentivirus was replaced with the appropriate fresh media the following day. Forty-eight hours following lentiviral transduction, HUVEC cells underwent selection with 0.5 μg/mL puromycin for 1 week. Transduced HEK-293 cells underwent selection with 1 μg/mL puromycin for 1-2 weeks.

Tandem affinity purification. EV (pcDNA3) or FLAG-HA-K1 (pcDNA3) HEK-293 cells were washed with cold phosphate buffered saline (PBS) and then lysed in NP40 lysis buffer containing phosphatase and protease inhibitor cocktails (Roche). Following lysis, clarified supernatants were subjected to tandem affinity purification using FLAG HA Tandem Affinity Purification Kit (Sigma). Following tandem affinity purification, the eluates were resolved on a 12% NPAGE Novex Bis-Tris Mini gel (Invitrogen). The gel was Coomassie stained and bands present in the K1 sample but absent in the EV were submitted to the Harvard Mass Spectrometry core for MALD/TOF/TOF mass spectroscopy analysis.

Trypan blue exclusion assay. EV or FLAG-HA-K1 stably expressing HEK-293 cells were plated at 650,000 cells/well in a 6-well dish or at 60,000/well in a 24-well dish. The next day, the media was removed and replaced with complete media containing the relevant concentration of compound C. Six to eight hours later the media from each well was collected; the cells were gently washed with PBS and

trypsinized. The cells were pelleted and resuspended in 0.6-1 mL complete media. An aliquot was removed for the trypan blue exclusion assay. The cells were then pelleted, the supernatant was discarded and the pellets were immediately frozen and maintained at -80°C until utilized for the caspase-3 assay. HUVEC infected with KSHV containing WT K1 or mutant K1 were plated at 20,000 cells per well of a 24-well plate in EBM-2 without serum and growth factors. iSLK cells containing WT K1 or mutant K1 were plated in a similar manner, but in complete media. The next day, the iSLK media was replaced with serum-free DMEM. At the time of counting, cells were trypsinized and cell suspension was then combined with trypan blue (0.4% Sigma Aldrich) at a 1:1 dilution. Each sample was counted in duplicate or triplicate using a hemacytometer.

Active caspase 3 assay. The previously frozen cell pellets were thawed on ice. The caspase-3 assay was then completed based on the manufacturer's instructions (ApoAlert Caspase-3 Fluorescent Assay by Clontech Laboratories). Briefly, the pellets were lysed and maintained on ice followed by centrifugation. The clarified supernatant was then assayed for active caspase-3 and fluorescence was determined using the CLARIOstar plate reader (BMG Labtech). Active caspase-3 concentrations were determined using a standard curve, and active caspase-3 values were then further normalized to cell number.

MTS assay. Five thousand cells per 100 µL were counted and resuspended in EBM-2 containing 30 µg/mL hygromycin but lacking all other supplements. Cells were plated in triplicate and incubated for 24, 48 and 72 hours. Cell proliferation was determined using the Cell Titer 96 Aqueous One Solution Cell Proliferation Assay

(Promega) according to the manufacturer's instructions. Stored aliquots of previously frozen MTS were thawed in a water bath at 37°C. Twenty microliters of MTS reagent was then dispensed into each well using a multichannel pipet. The plate was then gently shaken for 30 seconds and placed in an incubator at 37C° for 2-3 hours. At the end of incubation, the plate was gently tapped to mix the formazon product. The absorbance was then immediately measured at 490 nm using a CLARIOstar plate reader (BMG Labtech). Elevated absorbance values are indicative of metabolically active cells.

Cell Fractionation. HEK-293 stably expressing EV (pcDNA3) or FLAG-HA-K1 (pcDNA3) were washed, trypsinized, centrifuged and counted. Five million cells were prepared using a cell fractionation kit according to the manufacturer's instructions (Cell Signaling Technology). Equal volumes of each lysate from each fraction for EV and K1 were loaded and resolved by sodium dodecyl sulfate-polyacrylamide gel electrophoresis (SDS-PAGE) and then transferred to a nitrocellulose membrane.

Immunoblots. Cells were harvested, washed twice with PBS, and then lysed in buffer containing 0.5% NP40, 150 mM NaCl, 50 mM Tris-HCL pH 8.0, and a cocktail of proteinase (Roche) and phosphatase (Roche) inhibitors. The lysates used to evaluate K1 protein expression were frozen and thawed two times. Protein concentrations were determined by Bradford assay. To evaluate phosphorylated proteins, equal amounts of protein (15-25 μg) were loaded per lane and resolved by SDS-PAGE and then transferred to a nitrocellulose membrane. The following antibodies from Cell Signaling Technology were used: phospho-AMPKα (Thr172) #2535, AMPKα #2603, AMPKα1 #2795, AMPKα2 #2757, AMPKβ1 #12063,

AMPKβ1/2 #4150, AMPKγ1#4187, phospho-p70 S6K #9204, phospho-TSC2 #5584, HRP-linked anti-rabbit IgG #7074 and HRP-linked anti-mouse IgG #7076. In some experiments K1 expression was confirmed by immunoblotting with an HRP-conjugated mouse monoclonal anti-FLAG M2 antibody from Sigma #F1804. In other experiments, K1 expression was confirmed by immunobloting with an in-house monoclonal K1 antibody, followed by incubation with an HRP-conjugated anti-mouse antibody. The K1 monoclonal antibody was made by Abmart Inc., Shanghai, China (www.ab-mart.com). The epitope used to make this antibody is KQRDSNKTVP, protein ID#AAB71616 and gene accession #U86667.

Co-immunoprecipitations. Lysates containing equal amounts of protein as determined by the Bradford assay were combined with EZview Red anti-FLAG M2 affinity gel (Sigma, F2426) as per the manufacturer's instructions. For V5-AMPKγ1 immunoprecipitation, protein A/G agarose (Santa Cruz, sc-2003) was combined with monoclonal anti-V5 antibody (Sigma, V8012), which was used at 1ug of antibody/1 mg of protein, and rotated overnight at 4°C. The next day, the supernatant was removed and the affinity gel or agarose pellets were washed 4X, each with 1mL of 0.1% NP40 lysis buffer. For immunoprecipitation using the membrane fraction, affinity gel pellets were washed with 1mL of 0.1% NP40 lysis buffer, followed by 5 minutes rotation at 4°C for 3 times and with 1mL 0.5% NP40 lysis buffer followed by 5 minutes rotation at 4°C for one time. Detergent was then removed from the membrane fraction using Pierce Detergent spin columns. FLAG-HA-K1 and/or FLAG-K1 domain deleted mutants was eluted using 3X FLAG peptide (Sigma, F4799) as per the manufacturer's instructions. Laemmli buffer (2X) was added to the

FLAG-HA-K1 eluate or directly to the V5-AMPKγ1/agarose samples (1:1) and all samples were heated at 100°C for 6 minutes. Proteins were resolved by SDS-PAGE followed by Western blot.

AMPK activity assay. HUVEC stably expressing EV or FLAG-K1 were incubated in EBM-2 without serum and growth factors for 24 hours. Either 5 uM compound C or DMSO (0.05%) control was added at the start of starvation. Cells were washed with cold PBS and then lysed with a buffer containing 50mM Tris-HCL pH 7.4, 1 mM EDTA, 1 mM EGTA, 250 mM mannitol, 1% Triton X-100 and proteinase (Roche) and phosphatase inhibitors (Roche). Lysates were then clarified by centrifugation. For the AMPK activity assay, reagents were purchased from SignalChem and the manufacturer's protocol followed. Briefly, 10 µLs of cell lysate was incubated with 5 µL of 1 mg/mL SAMS or peptide substrate solution, 5 µLs 0.5 mM AMP solution and 5 µLs γ-32P-ATP assay cocktail. Gamma-32P-ATP was purchased from Perkin Elmer. The mixture was incubated at room temperature for 30 minutes and then 20 µLs was added to phosphocellulose paper and washed 2 times in 1% phosphoric acid solution. Counts per minute (cpm) were acquired using a PerkinElmer liquid scintillation analyzer.

Immunofluorescence and confocal microscopy. Approximately 120,000 HUVEC cells stably expressing EV or FLAG-K1 were plated in MatTek 35 mm glass-bottom dishes. Cells were washed with PBS and fixed by 15-minute incubation in 3.7% formaldehyde at room temperature. Cells were washed 3X with PBS and then permeabilized by 15-minute incubation at room temperature in 0.2% Triton-X 100/PBS. Cells were then washed again 3X with PBS and then blocked in 10%

bovine serum albumin (BSA) PBS for 30 minutes. Cells were stained 1:200 with a directly conjugated FITC-ECS (DDDDK) polyclonal antibody (Bethyl laboratories) and anti-AMPKβ1/2 (1:50, Cell Signaling) in 10% BSA for 1 hour at room temperature. Cells were washed 2X quick followed by 3X 5-minute washes. Samples were then incubated with anti-rabbit Alexa Fluor 647 (1:600) secondary antibody in 10% BSA at room temperature for 1 hour. All samples were then stained with DAPI for 1 minute and washed. Fluorescent images were acquired by taking z-stacks using a 63X oil objective on a Zeiss 700 confocal microscope. The overlap coefficient according to Manders (R) was determined using ImageJ.

Generation of WT or mutant K1 recombinant viruses. The construction of the KSHV WT and mutant recombinant viruses has previously been described in detail [141]. Briefly, the BAC 16 was kindly provided by Dr. Jae U. Jung. pcDNA3 WT and mutant K1 constructs were used as templates for construction of recombinant viruses. pcDNA3 WT K1 FLAG, which has a FLAG tag at the N-terminus, was constructed as previously described [164]. The pcDNA3-$K1_{5XSTOP}$ construct has 3 stop codons following the start codon of WT K1FLAG and two TGA stop codons replacing ATG start codons at positions 481 and 763. $K1_{5XSTOP}$ was inserted into BamHI and EcoRI sites of pcDNA3-FLAG K1WT. The original K1 gene is located within the BAC16 genome at position 105 to 959. The recombinant viruses containing KSHV-$K1_{WT}$, KSHV-$K1_{5XSTOP}$, KSHVΔK1 and KHSV-$K1_{REV}$ were made utilizing the Red/ET recombination system (Gene Bridges Inc) as per the manufacturer's instructions. KSHVΔK1 was constructed by replacing the K1 gene with the linear RpsL-neo cassette that is flanked by homologous arms [141].

Establishment of cells stably infected with WT or mutant K1 recombinant viruses. Five × 10^5 cells of WT or recombinant virus infected iSLK cells were plated in one well of a 6- well plate overnight after which cells were reactivated with 3 μg/ml doxycycline and 1 mM sodium butyrate for 3 days. Supernatant was collected and cleared by centrifugation at 950g for 10 min and filtered through a 0.45 μm filter. iSLK cells were infected as previously described [141] and maintained in the presence of 1 μg/ml puromycin, 250 μg/mL G418, and 1.2 mg/mL hygromycin [141]. In order to infect HUVEC, the filtered viral supernatants from reactivated iSLK cells were incubated with the immortalized HUVEC cells in the presence of 8 μg/ml of polybrene and centrifuged for 2 hours at 3000 RCF at 30°C. The cells were then placed in an incubator with 5% CO2 at 37°C. At 48 hours post-infection, 30 μg/ml hygromycin was added to the media to select for HUVEC stably infected with KSHV-$K1_{WT}$, KSHV-$K1_{5XSTOP}$, KSHVΔK1 or KSHV-$K1_{REV}$ (revertant) recombinant viruses. The infected HUVEC cells were also maintained in the presence of 30 μg/ml hygromycin.

Acknowledgements. We would like to thank Dr. Jae Jung for the original KSHV BAC16 construct. We thank the UNC Microscopy Service Laboratory members, particularly Dr. Robert Bagnell, for their assistance. We also thank Damania lab members for helpful advice. BD is a Leukemia and Lymphoma Society Scholar, and a Burroughs Wellcome Fund Investigator in Infectious Disease.

CHAPTER 4. THE KSHV ORF36 PROTEIN KINASE AUGMENTS TUMORIGENESIS IN A MOUSE MODEL SYSTEM[3]

OVERVIEW

We generated a novel vPK transgenic mouse by cloning human vPK into a vector under the control of the ubiquitin promoter. vPK transgenic mice were made and mice were screened for vPK expression. We were able to detect vPK protein in liver, spleen, kidney, heart, lung, thymus and lymph node of transgenic mice.

We initially compared the splenic lymphocyte subsets in vPK transgenic mice to those of wild-type (WT) mice by flow cytometry. We observed increased percentages of CD4+ T cells, increased activated T and B cells, and increased germinal center B cells in spleens from vPK transgenic mice compared to WT mice. This suggests that vPK can activate signal transduction pathways in B and T cells. Furthermore, when we immunized vPK and WT mice with antigen and evaluated splenic lymphocyte activation by flow cytometry, we found that antigen administration in vPK mice did not result in additional lymphocyte activation compared to vehicle vPK controls, since the vPK mice already display a high level of lymphocyte activation. Our results suggest that naïve vPK mice have a higher baseline level of B and T cell activation without any prior immunization. We plan to

[3] Anders P., Bhatt A., Montgomery N., Montgomery S., Perkowski E., Dittmer D., and Damania B., Manuscript in preparation.

compare the proliferative response of B cells from vPK and WT mice following exposure to various stimulants *ex vivo*.

Inflammation has been found to play an integral part in the development and progression of Kaposi's sarcoma (KS). In the early stages of KS, there is an influx of CD8+ and CD4+ T cells along with the production of inflammatory cytokines. Inflammatory cytokines reactivate KSHV from latency and stimulate endothelial cells to produce angiogenic factors thereby promoting KS progression. Activation of cell signaling pathways such as PI3K/mTOR/S6K is also important for the development of B cell lymphomas. Hence, vPK's ability to enhance B cell activation may also contribute to lymphomagenesis.

INTRODUCTION

Kaposi's sarcoma-associated herpesvirus (KSHV) is a double-strand DNA herpesvirus that is associated with the endothelial cell cancer, Kaposi's Sarcoma (KS) and two B cell lymphomas including PEL and MCD. These KSHV-associated diseases mainly occur in immune-suppressed individuals such as those who are HIV positive or are transplant recipients.

Unlike K1, which is unique to KSHV, vPK, also known as ORF36, is a viral serine/threonine kinase that is conserved among herpesviruses, underscoring the importance of this kinase in herpesvirus infection and KSHV biology. Although vPK is conserved, there are still significant differences in cellular localization and function of these viral kinases among different herpesviruses. Herpesvirus orthologs to KSHV ORF36 include UL13 (HSV-1, -2), ORF47 (VZV), UL97 (HCMV), U69 (HHV-6, -7), and BGLF4 (EBV) [58].

Viral protein kinase undergoes autophosphorylation, which is important for its catalytic activity, is localized to the nucleus, and is presumed to be a tegument protein [59, 60, 165]. When vPK is expressed ectopically, it localizes to the nucleus and cytoplasm [57]. Viral PK has been shown to have a multitude of functions *in vitro*. Viral PK expression results in the phosphorylation of MKK4 and MKK7 and subsequent phosphorylation of c-Jun N-terminal kinase (JNK) [59]. In human and mouse cell lines, vPK inhibits the activation of the IFNβ promoter and the production of IFNβ [61]. Moreover vPK has cyclin-dependent kinase like function by inducing the phosphorylation of Rb and lamin A thereby promoting cell cycle progression [57].

Our lab has recently shown that vPK resembles and mimics the activity of the cellular protein S6 kinase (S6KB1) [62]. S6KB1 is downstream in the PI3K/mTOR pathway and is phosphorylated by mTOR. Activated S6KB1 phosphorylates multiple targets some of which are involved in protein synthesis such as ribosomal S6 protein, a protein that is part of the 40S ribosome; and eIF4B, a protein that is part of the translation pre-initiation complex [63]. Expression of vPK results in increased de novo protein synthesis, tubule formation, and anchorage independent growth, compared to empty vector suggesting that vPK may be an oncogenic protein [62].

Until most recently, our understanding of vPK function was based on data obtained from *in vitro* systems. We wanted to determine whether vPK-expressed *in vivo* would reveal either a novel function for vPK and/or support *in vitro* observations; therefore, we generated two lines of vPK transgenic mice along with C57BL/6 littermate controls.

RESULTS

A vPK gene was inserted downstream of the ubiquitin promoter (Ub) in the vector, pBS.Ub.hGH (Fig. 4.1A). The transgene fragment was microinjected into fertilized embryos of C57BL/6 mice and subsequently implanted into pesudopregnant females. We screened the pups for vPK transgene expression by isolating mouse genomic DNA and polymerase chain reaction (PCR)(Fig. 4.1B). We next detected vPK protein expression in spleens from vPK and littermate WT controls (Fig. 4.1C). Because vPK expression is under an ubiquitin promoter and should be expressed in all tissues, we wanted to determine whether vPK is expressed throughout the body. We found vPK protein expression in multiple organs including liver, spleen, kidney, heart, lung, thymus and lymph nodes but not in WT littermate control organs (Fig. 4.1D).

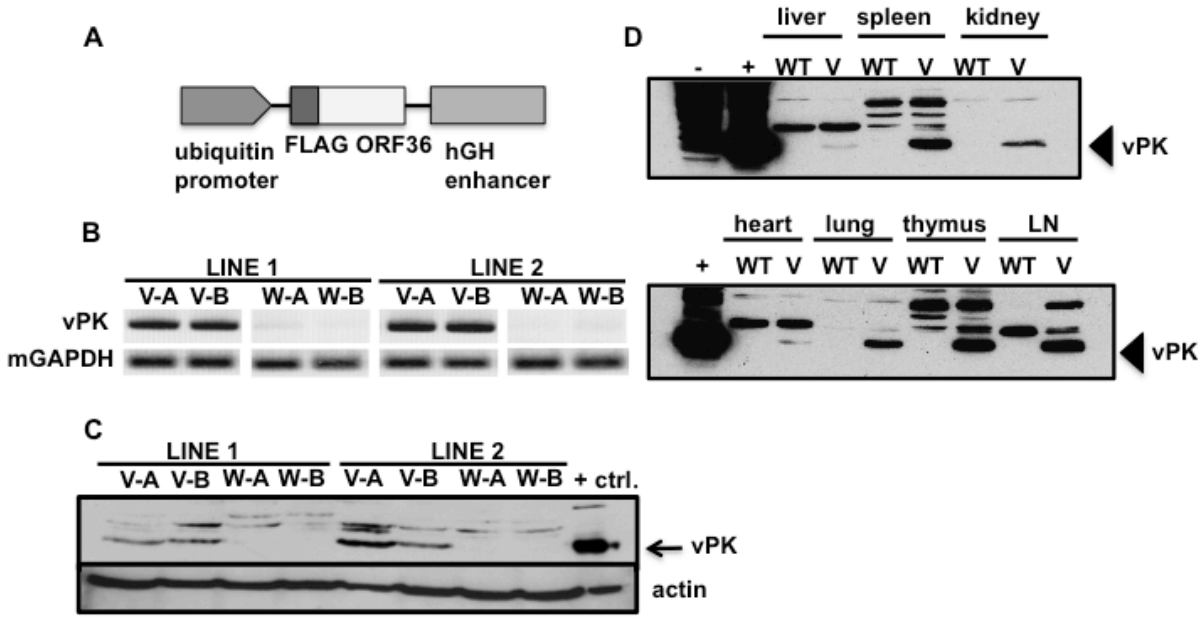

Figure 4.1. Development of a vPK transgenic mouse model system. (A) Schematic of the transgene fragment used to make the vPK transgenic, which includes an ubiquitin promoter, the FLAG-tagged vPK/ORF36 sequence, and a stabilization sequence (hGH enhancer). (B) Viral PK expression in mouse genomic DNA obtained from 2 transgenic lines and littermate WT controls. (C) Viral PK protein expression in spleens from 2 vPK transgenic lines and littermate WT controls. (D) Viral PK protein expression in multiple organs from a vPK transgenic mouse (Line 1) and WT littermate control. LN indicates lymph node.

Characterization of immune cell subsets in vPK transgenic mice. Because this is the first expression of KSHV vPK *in vivo*, we began characterizing the immune cell subsets in the spleens from the two lines of vPK transgenic mice and WT littermate controls by flow cytometry. Because KSHV infects B cells and causes B cell lymphomas in humans, we are particularly interested in the B cell compartment within the spleens of vPK transgenic mice.

We evaluated T and B cells subsets in the spleens from vPK (lines 1 and 2) transgenic and WT mice by flow cytometry. Interestingly, we observed an increase in CD19+IgD-IgM- percentages in both vPK lines compared to WT littermates (first highlighted row in Table 4.1).

When activated, naïve B cells undergo class switch recombination (CSR), also called isotype switching, in which the heavy chain DNA is recombined from IgM and IgD to IgG, IgA or IgE [166]. Following CSR, B cells lose expression of IgM and IgD. Thus, a subset of B cells that is negative for these markers may be class switched B cells [167].

Table 4.1: Immune cell subsets in spleens from WT and vPK transgenic mice.

		WT			vPK 1				vPK 2			
Class (cells)	Marker	%	SD	n	%	SD	n	*P*	%	SD	n	*P*
B	CD19+	55.4	5.0	8	43.4	9.8	6	0.003	49.8	3.3	4	0.013
mature B	CD19+IgD+IgM+	82.4	2.1	8	76.1	8.2	6	0.012	77.3	4.9	4	0.003
immature B	CD19+IgD-IgM+	10.8	1.5	8	14.4	5.2	6	NS	11.2	1.6	4	NS
	CD19+IgD-IgM-	5.3	0.7	8	7.6	2.6	6	0.001	9.0	5.1	4	0.010
marginal B	CD19+CD21+CD23-	11.6	3.6	8	12.8	3.8	6	NS	8.8	1.9	4	NS
follicular B	CD19+CD21-CD23+	78.3	4.4	8	73.7	7.1	6	NS	73.7	3.0	4	NS
T	CD3+	35.4	4.1	8	38.3	5.5	6	NS	48.1	2.3	4	0.0003
T helper	CD3+CD4+	48.2	5.6	8	61.0	6.7	6	0.003	57.9	2.8	4	0.010
cytotoxic T	CD3+CD8+	40.6	3.9	8	28.2	6.6	6	0.030	32.7	3.1	4	NS

We also noted an increase in the percentages of CD4+ T cells and reduced percentages of CD8+ T cells in both lines compared to WT littermate controls (Table 4.1).

We next evaluated immune subsets in spleens from additional vPK line 2 transgenic mice and also adjusted the flow cytometry panel to include germinal center B cells, which is a subset of class switched B cells. Supporting our previous findings (Table 4.1), we observed increased percentages of class switched B cells (B220+IgM-IgD-) (Table 4.2). Although not significant, there was an increase in germinal center B cells as indicated by B220+CD95+GL-7+ cells in the spleens from vPK transgenic mice compared to WT controls (Table 4.2). We also observed an increased T helper to cytotoxic T cell ratio (Table 4.2), which was also previously observed (Table 4.1).

Table 4.2: Immune cell subsets in spleens from WT and vPK (line 2) transgenic mice.

		WT			vPK 2			
Class (cells)	Marker	%	SD	n	%	SD	n	*P*
B	B220+	44.3	4.5	3	40.5	1.4	3	NS
mature B	B220+IgD+IgM+	72.1	3.0	3	67.4	3.0	3	NS
immature B	B220+IgD-IgM+	21.0	2.6	3	19.2	2.0	3	NS
	B220+IgD-IgM-	3.9	0.4	3	8.3	2.7	3	0.050
marginal B	B220+CD21+CD23-	9.2	0.5	3	7.9	1.5	3	NS
follicular B	B220+CD21-CD23+	76.5	2.2	3	73.9	1.2	3	NS
plasmablasts	CD19+CD138+	0.3	0.047	3	0.3	0.006	3	NS
germinal center B	B220+CD95+GL-7+	0.6	0.1	3	2.4	2.2	3	NS
T	CD3+	35.7	3.7	3	41.2	2.2	3	NS
T helper	CD3+CD4+	48.5	2.5	3	57.5	5.0	3	0.050
cytotoxic T	CD3+CD8+	42.8	2.1	3	36.1	4.5	3	NS

Viral PK (line 2) mice had an increase in germinal center B cells. We corroborated this finding by evaluating the percentage of germinal center B cells in vPK (line 1) transgenic mice (Table 4.3).

Table 4.3: Immune cell subsets in spleens form WT and vPK (line 1) transgenic mice.

		WT			vPK 1			
Class (cells)	Marker	%	SD	n	%	SD	n	P
B	B220+	50.2	7.4	6	44.7	2.9	6	NS
mature B	B220+IgD+IgM-	79.8	3.0	6	67.5	6.9	6	0.003
immature B	B220+IgD-IgM+	12.4	1.9	6	11.8	3.0	6	NS
	B220+IgD-IgM-	5.3	1.5	6	13.7	4.6	6	0.002
germinal center B	B220+CD95+GL-7+	2.3	0.9	6	5.4	2.0	6	0.006
T	CD3+	34.2	4.3	6	40.6	4.0	6	0.023
T helper	CD3+CD4+	52.4	1.6	6	63.6	7.3	6	0.01
cytotoxic T	CD3+CD8+	40.2	2.1	6	30.1	6.9	6	0.01

Based on this initial characterization of splenic immune cell subsets, which suggests that naïve vPK transgenics have a mildly activated immune system, we wanted to determine whether we could exacerbate this response *in vivo* by

immunization with an antigen that induces a T-cell dependent response thereby generating a germinal center reaction [168].

T-dependent antigen response in vPK transgenic mice. To determine the primary immune response, we immunized 8-12 week old vPK transgenics (line 1) or WT littermate controls intrarperintoneally with NP (4-Hydroxy-3-nitrophenylacetyl hapten) that is conjugated to KLH (keyhole limpet hemocyanin) or PBS without adjuvant (Fig. 4.1). Since previous reports indicate the presence of a germinal center reaction as indicated by an increase in germinal center B cells occurs at around 10 days post immunization [37, 168], we sacrificed mice at 10 days following immunization.

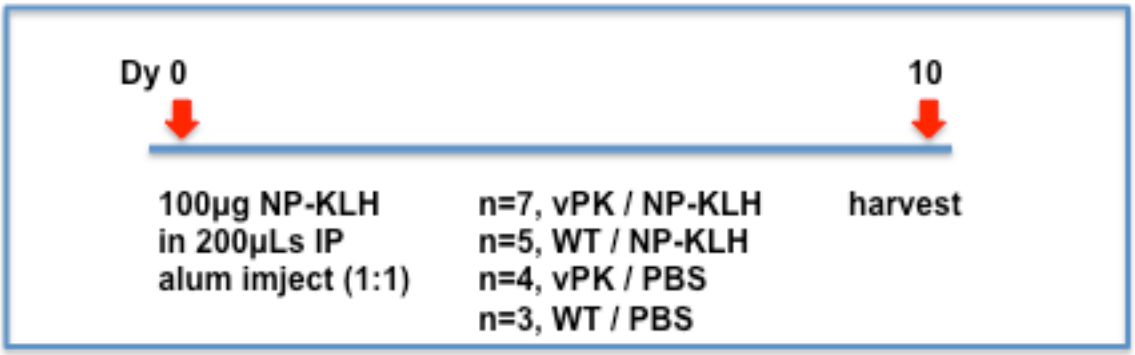

Figure 4.2. Immunization protocol for vPK transgenic and WT mice with NP-KLH or PBS

We did not observe differences in total body weight indicating that NP-KLH immunization did not impact general health in either group (Fig. 4.3A). Because NP-KLH immunization induces a primary immune response and this response may be exasperated in the vPK transgenics, there may be an influx of immune cells, resulting in spleens with greater mass than in immunized WT. We did not observe

differences in the weights of spleens between vPK and WT immunized or vehicle treated groups (Fig. 4.3B), suggesting that either there are no differences in the number of immune cells or the differences are more subtle than those observed by spleen weights alone.

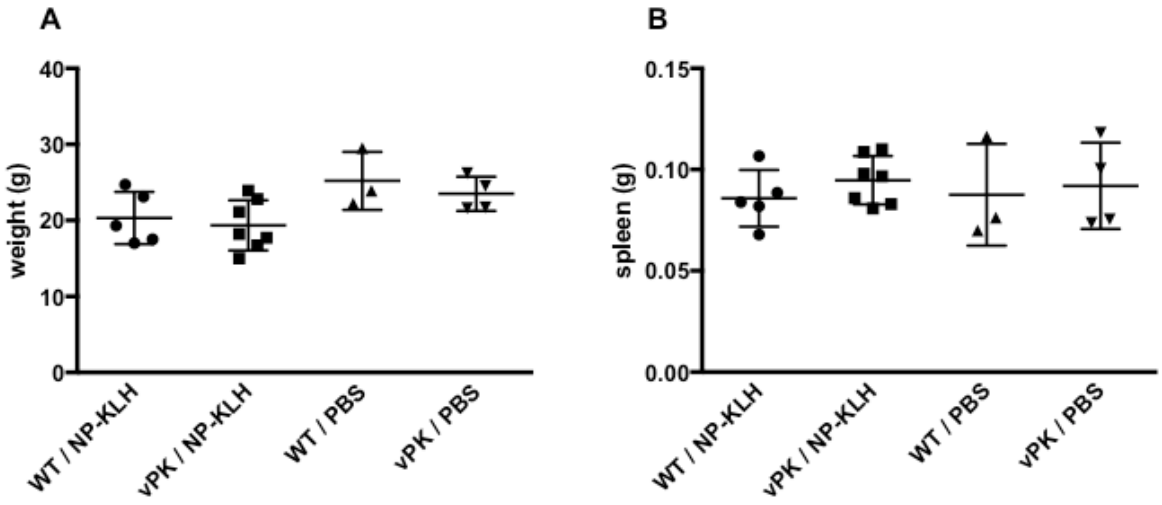

Figure 4.3. Body and spleen weights for NP-KLH immunized vPK transgenic and WT mice. Heterozygous vPK transgenic mice and littermate controls were immunized with NP-KLH and alum or PBS alone and harvested 10 days post immunization. (A) Body weights for all mice 10 days post immunization. (B) Spleen weights for all mice at 10 days following immunization.

The immune response in control vPK transgenic mice resembled the immune response in NP-KLH immunized WT mice. Next, we completed a basic evaluation of B cell subsets from the spleens of NP-KLH or PBS immunized vPK transgenics and WT mice. By flow cytometry we evaluated immature B cells, mature B cells, germinal center B cells and the activation status of B cell subsets. Our gating

strategy involved making an initial forward side scatter gate, a live cell gate, followed by a gate on B cells (B220) and subsequent gates to identify each subset as well as activation status (Fig. 4.4).

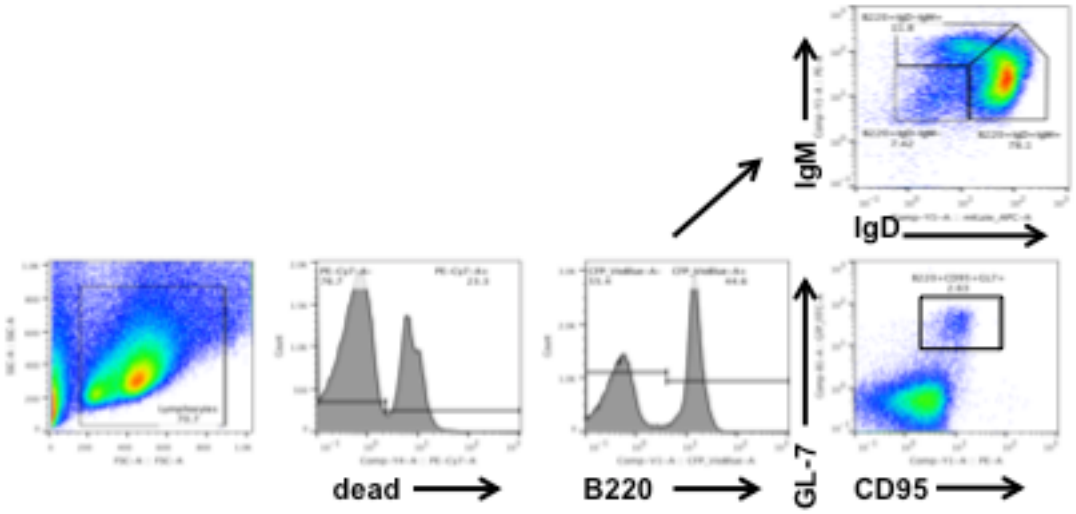

Figure 4.4. Gating strategy to identify B cell subsets. Flow cytometry was completed on spleens from NP-KLH or PBS immunized vPK transgenics and WT controls. Gates were drawn to exclude dead cells and then on B220+ cells to identify B cells. Immature B cells were determined as being B220+IgM+IgD-, mature B cells as B220+IgM+IgD+, class switched B cells as B220+IgM-IgD-, and germinal center B cells as B220+CD95+GL-7+.

Interestingly, we did not observe differences in the number of B cells and B cell subsets between vPK transgenics that had been immunized with NP-KLH compared to vPK controls that had received PBS (Fig 4.5 A, B, C, and D). The spleens from control vPK transgenics had comparable numbers of the various B cell subsets including total B cells (Fig. 4.5A), mature (Fig.4.5B) and immature (Fig. 4.5C) to the numbers from spleens of NP-KLH immunized WT mice. As we had observed in

previous experiments (Tables 4.1, 4.2 and 4.3), there were increased numbers of B220+IgM-IgD- cells or class switched B cells regardless of immunization status in vPK mice (Fig. 4.5D).

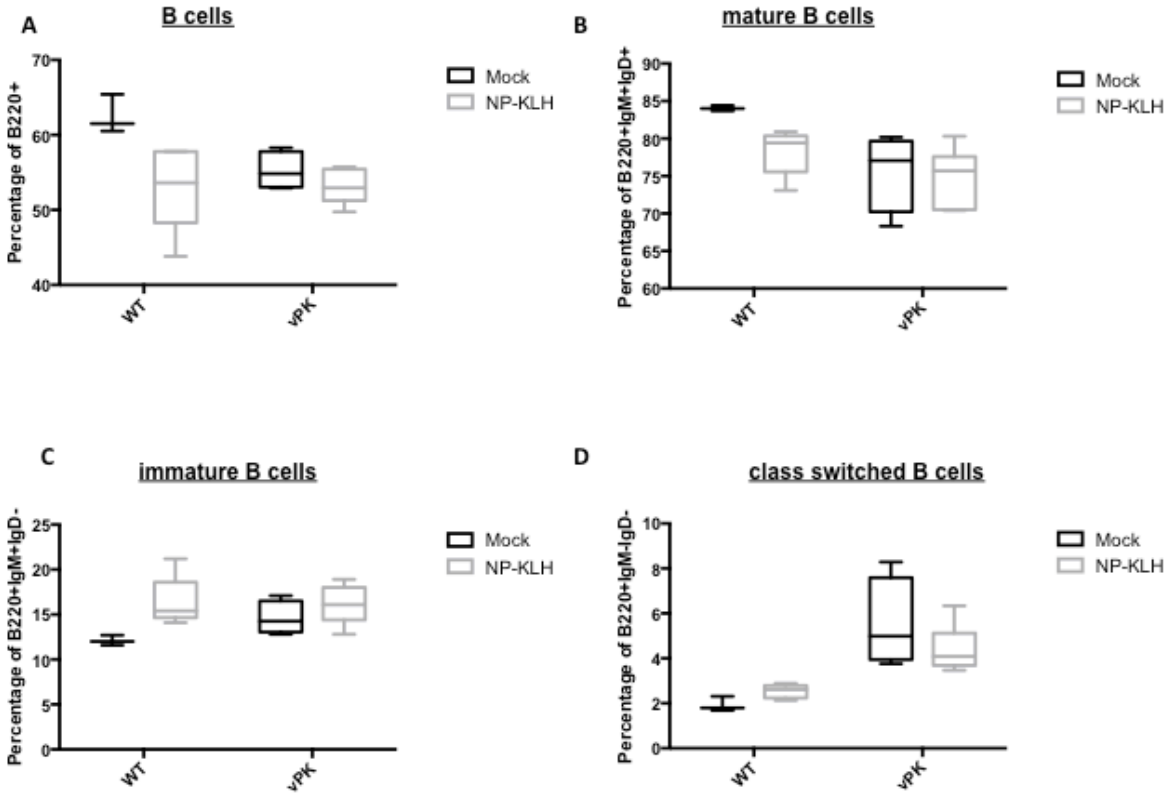

Figure 4.5. The percentages of B cells in spleens from vPK mice immunized with PBS were comparable to WT immunized with NP-KLH. Flow cytometry was completed on cells obtained from vPK transgenic or WT mice immunized with NP-KLH or PBS. (A) The percentages of B220+ cells. (B) The percentages of B220+IgM+IgD+ cells. (C) The percentages of B220+IgM+IgD- cells. (D) The percentages of B220+IgM-IgD- cells. The whiskers represent the minimum and maximum values, and the horizontal line on each box is the median. Mock = PBS.

To evaluate the activation status of the various B cell subsets, we stained for CD69, an early activation marker found on both T and B cells, and CD86. CD86 is upregulated on activated B cells and is the ligand for CD28 and CTLA-4 on T cells. The percentages of activated, as indicated by CD69 expression, on mature and immature B cells were overall low in all groups but similar between WT / NP-KLH, vPK / NP-KLH and vPK / PBS (Fig. 4.6A and B).

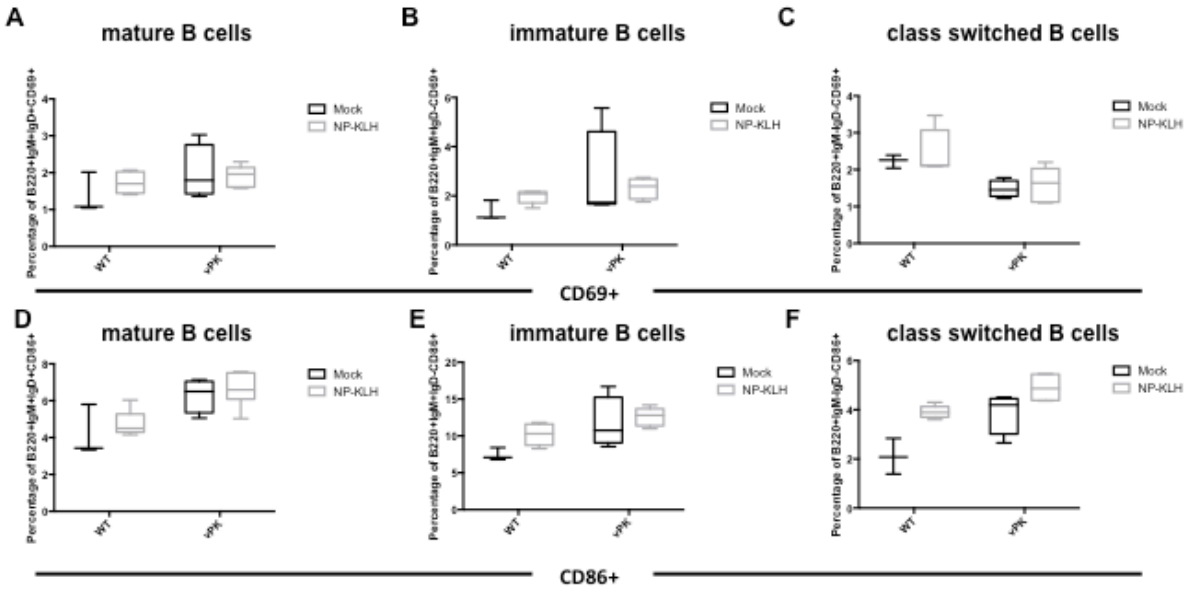

Figure 4.6. Activation status of B cell subsets from the spleens of immunized vPK transgenic and WT mice. (A) Percentages of B220+IgM+IgD+CD69+ cells. (B) Percentages of B220+IgM+IgD-CD69+ cells (C) Percentages of B220+IgM-IgD-CD69+ cells (D) Percentages of B220+IgM+IgD+CD86+ cells (E) Percentages of B220+IgM+IgD-CD86+ cells (F) Percentages of B220+IgM-IgD-CD86+ cells. The whiskers are the minimum and maximum, and the horizontal line on each box is the median. Mock = PBS.

Because we are inducing a primary immune response to NP-KLH, only a small subset of B cells should be responsive, thus the percentages of activated B cells should be fairly low. Overall, the percentages of class switched CD69+ B cells were reduced in both vPK treated groups compared to WT groups (Fig 4.6C). We observed an increase in the number of activated mature, immature, and class switched B cells expressing CD86 in vPK / PBS treated mice, and these numbers were similar to the numbers obtained from splenic NP-KLH immunized WT mice (Fig 4.6 D, E, and F), which further corroborates the idea that naïve vPK mice have an immune response to NP-KLH that is similar to NP-KLH-immunized WT mice.

As observed previously (Tables 4.2 and 4.3), we also noted increased numbers of germinal center B cells in the vPK transgenics regardless of treatment compared to WT / PBS (Fig. 4.7).

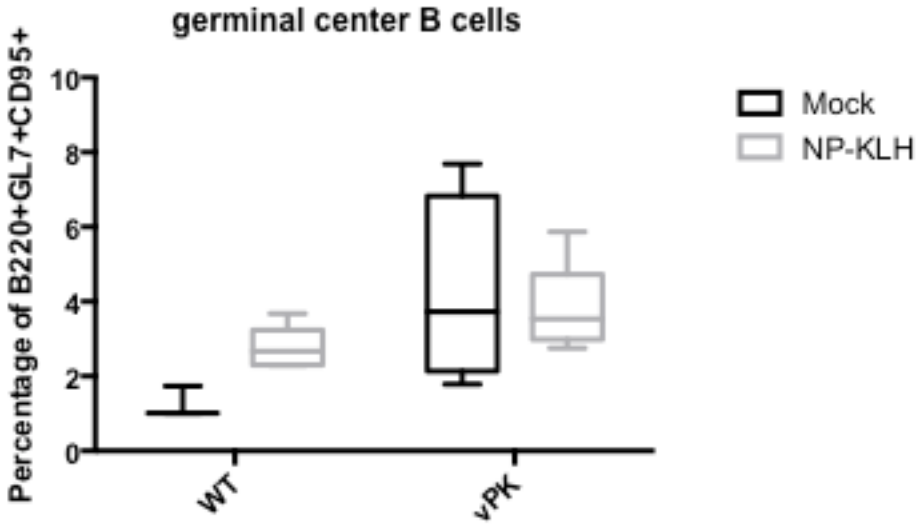

Figure 4.7. vPK transgenic mice have increased percentages of germinal center B cells. The percentages of germinal center B cells in spleens from vPK and WT mice

immunized with NP-KLH or PBS (mock) were determined using flow cytometry. Whiskers are the minimum and maximums.

We also evaluated the percentages of overall T cells, T helper cells, and cytotoxic T cells. There were no differences between vPK / NP-KLH and vPK / PBS (Fig. 4.8 A, B and C). As observed previously (Tables 4.1, 4.2 and 4.3), both vPK treated groups had increased CD3+CD4+ T cells and reduced CD3+CD8+ T cells compared to WT treated groups (Fig. 4.8 B and C).

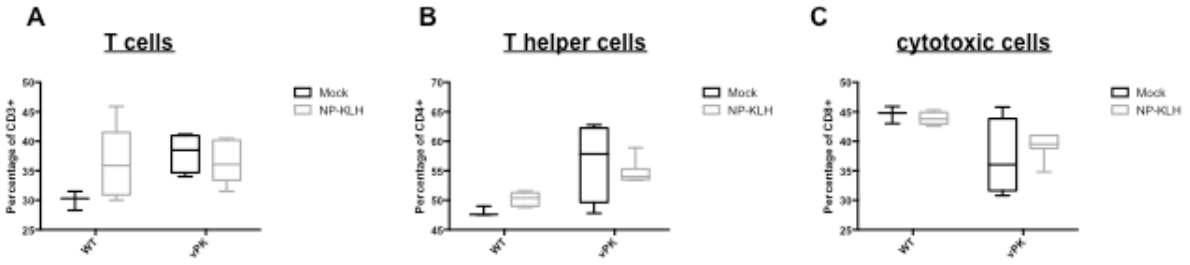

Figure 4.8. Splenic T cell subsets in immunized vPK and WT mice. Viral PK and WT mice were immunized with NP-KLH or PBS. The percentages of T cells and T cell subsets were determined by flow cytometry. (A) CD3+ cells (B) CD3+CD4+ (C) CD3+CD8+. Whiskers are the minimum and maximums. Mock = PBS.

Thus far, our data indicate that spleens from vPK mice have increased numbers of splenic class switched B cells, germinal center B cells and an increased CD4+ T:CD8+ T cell ratio compared to WT. Therefore, we were very interested to evaluate the activation status of these cells. We stained splenic cells with an antibody cocktail to identify T cells, T cell subsets, and activation status using the marker CD44, which is involved in adhesion and is up regulated on T cells upon activation [169]. Our

results using the other activation markers CD25 and CD69 were inconclusive. Viral PK transgenic mice immunized with either NP-KLH or PBS had increased percentages of activated T helper cells (CD3+CD4+CD44+) compared to WT groups (Fig. 4.9). There were no differences in activated cytotoxic T cells between groups (*data not shown*).

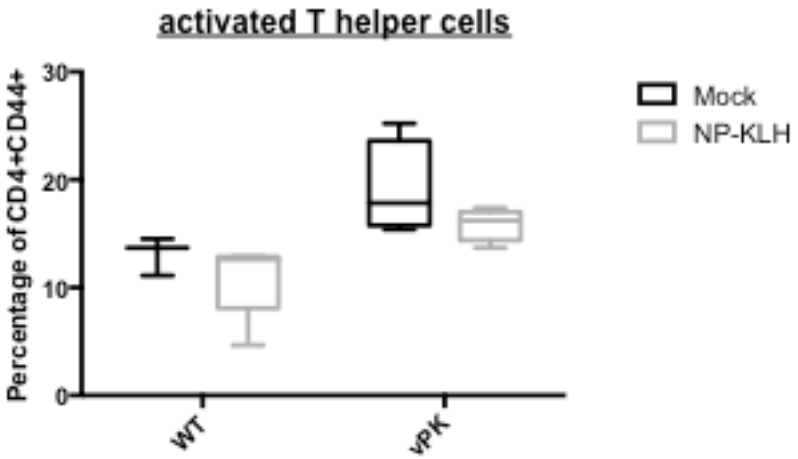

Figure 4.9. vPK spleens have increased percentages of CD44 positive T helper cells compared to WT. Viral PK transgenics and WT mice were immunized with either NP-KLH or PBS. The percentages of CD3+CD4+CD44+ cells were determined by flow cytometry. Mock = PBS.

We also evaluated splenic T cells and T cell subsets from immunized vPK and WT for differences in CD86 expression. CD86, as previously noted is the ligand for CD28 and CTLA-4. We observed that vPK transgenics, both mock and those immunized with NP-KLH or PBS, had increased numbers of CD86+ T helper (Fig. 4.10A) and cytotoxic T cells (Fig. 4.10B) compared to WT groups.

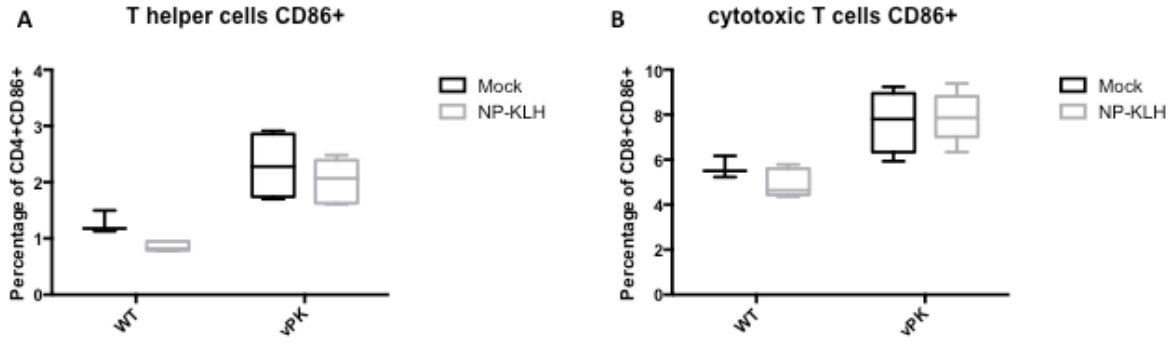

Figure 4.10. CD86 expression is increased on vPK T helper and cytotoxic T cells. Viral PK and WT mice were immunized with NP-KLH or PBS. CD86 expression was evaluated on CD3+ splenic T cells by flow cytometry. (A) Percentages of CD3+CD4+CD86 cells (B) Percentages of CD3+CD8+CD86+ cells. Whiskers are the minimum and maximum. Mock = PBS.

CD86 is predominantly expressed on antigen presenting cells (APCs). APCs modulate T cell responses via CD86 ligation of CD28 or CTLA-4 on T cells. Interestingly, there are several reports indicating that CD86 is expressed on activated effector memory human T cells [170, 171]. These CD86 expressing T cells express major histocompatibility complex class II (MHC-II), have the ability to present antigen [172], and to stimulate resting or naive T cells to proliferate and produce interferon gamma (IFN-γ) [171, 173]. MHC-II and functional CD86 are also expressed on activated mouse T cells [174, 175]. Interleukin-2 (IL-2) induces the upregulation of CD86 expression on CD4+ and CD8+ T cells and this upregulation of CD86 is partially dependent on mTORC1 signaling since treatment with rapamycin reduces CD86 expression on T cells [170]. CD86 has also been found to be upregulated on T cells in various contexts of disease such as on T cells from HIV+

individuals [176], on allergen specific T cells [177], on tumor infiltrating lymphocytes [178] and on T cells from individuals with liver disease [172].

Aged vPK expressing mice are prone to tumor development. Because we observe increased numbers of class switched and germinal center B cells *in vivo* and vPK expression facilitates cellular transformation *in vitro* [62], we hypothesized that vPK mice may be more prone to tumor development than WT mice. Interestingly, most primary effusion lymphomas (PEL), which harbor latent KSHV, appear to be derived from post-germinal center B cells.

Using a cohort of vPK and age-matched WT mice, we followed these mice for 18-24 months after birth. When we sacrificed vPK transgenic and aged-match WT mice, we collected blood to obtain serum, ear biopsy to re-confirm genotype and the following organs: lung, liver, spleen, and kidney, as well as any observed masses or ascites.

Our preliminary data suggests that aged vPK mice are more prone to tumor development than WT mice because we observed that a greater proportion of vPK mice developed tumors compared to WT mice (Fig. 4.11A).

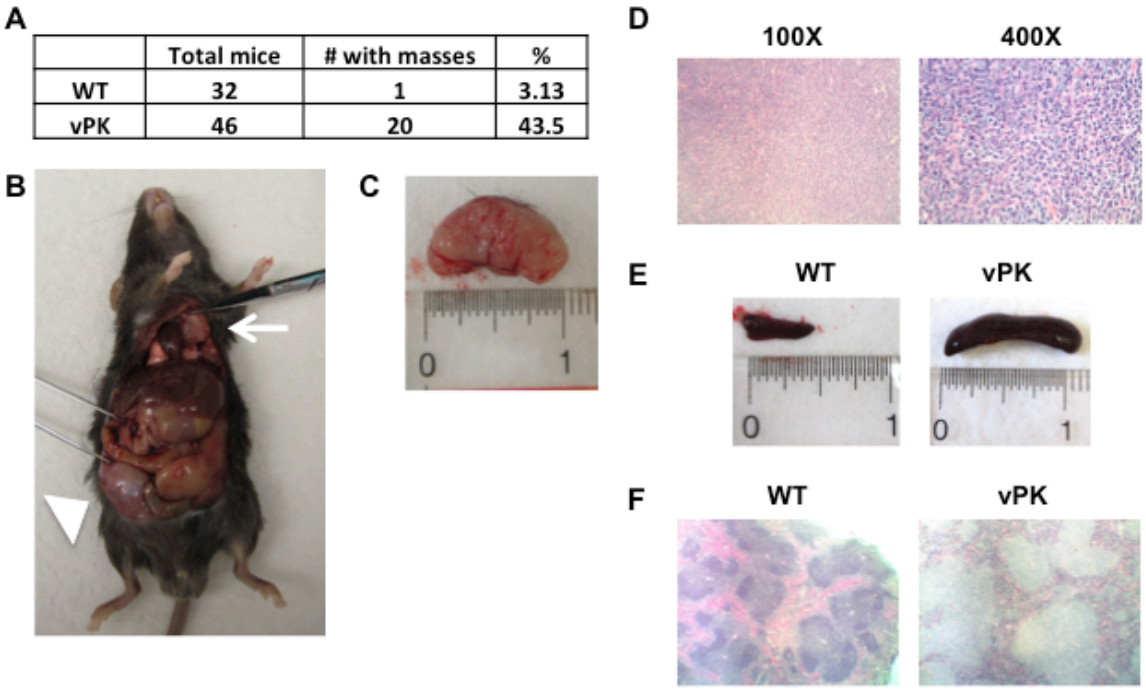

Figure 4.11. Aged-vPK transgenic mice are more prone to developing tumors than WT mice. (A) The total number of aged-WT and vPK transgenic mice sacrificed over time, the number of mice with observed masses, and the percentage of mice with masses for each group. (B) vPK transgenic mouse with 2 masses: one mass is located on the left side of the heart (arrow), and the other mass is on the lower right of the mouse's abdomen (arrow head). (C) Mass extracted from vPK transgenic mouse. (D) Hematoxylin and eosin (H&E) staining of a tumor section from a vPK transgenic mouse. (E) Spleens from WT and vPK transgenic mice. (F) H&E staining of spleens from WT and vPK mice (40X).

The tumors in vPK transgenic mice could be found located throughout the body (Fig. 4.11B) and most were large and pale (Fig. 4.11C). Hematoxylin and eosin (H&E) staining of tumor sections revealed a homogenous tissue composed of lymphocytes (Fig. 4.11D). Tumor-bearing vPK transgenic mice often had larger

spleens compared to WT spleens, suggesting robust lymphoproliferation (Fig. 4.11E). By H&E staining, the spleens from tumor-bearing vPK transgenic mice had distorted splenic architecture compared to WT (Fig. 4.11F).

Following an initial review of some of the H&E stained lungs, liver, kidney, spleen and tumor sections by blinded pathologists, about 60% of the vPK transgenic mice had overt lymphomas (lymph) compared to WT mice (Table 4.4). Both vPK lines 1 and 2 developed lymphomas.

Table 4.4 : Viral PK transgenic mice have increased incidence of lymphoma.

	WT	vPK	LINE 1	LINE 2
normal	6	5	4	1
LP	1	4	4	0
lymphoma	0	16	8	8
% LP	14	16	25	0
% lymphoma	0	64	50	89

LP = lymphoproliferation

Overt lymphoma was determined as an effacement of normal tissue architecture by atypical cells. Atypical cells have features of enlarged nuclear size, irregular contours, prominent nucleoli and increased mitotic figures. Some WT and vPK transgenic mice also had lymphoproliferation (LP) (Table 4.4).

DISCUSSION

Our preliminary findings suggest that naïve vPK transgenic mice have an activated immune system that is comparable to NP-KLH-immunized WT mice, at least as indicated by our evaluation of splenic B and T cell subsets and activation status by flow cytometry. After aging, vPK transgenic mice develop tumors that

appear to be filled with lymphocytes. We are currently completing experiments to identify the tumor cells by flow cytometry and immunohistochemical staining. Based on the preliminary evaluation by pathologists who have blindly evaluated H&E stained tissues from WT and vPK mice, the masses appear to be lymphomas. To determine the subtype of lymphoma, we will evaluate the vPK and WT tissues by immunohistochemical and flow cytometry staining using a comprehensive panel of markers.

During development and in response to antigen and the cytokine milieu, B cells undergo several genetic rearrangements that diversify the B cell receptor and fine-tune it for antigen recognition. It is during these processes that mutations can be introduced and contribute to lymphomagenesis. Such alterations are prevalent in B-cell non-Hodgkin lymphomas [179]. We observed that vPK expression in mice promotes low-grade immune system activation, and we see increased numbers of class switched B cells and germinal center B cells, which indicate an active B cell response. We may speculate that vPK-induced B cell activation promotes the various genetic rearrangements of the BCR, and facilitates the acquisition of mutations that contribute to lymphomagenesis.

Viral PK has been reported to be an S6KB1 mimic, and it phosphorylates S6 protein. Although vPK does not phosphorylate all of the S6K substrates involved in translation such as eIF4B (S422), it appears to phosphorylate other substrates not activated by S6KB1 such as eIF4E (S209) [62]. Phosphorylation of eIF4E (S209) is strongly associated with cancer by its involvement in cell survival, proliferation and anchorage independence [180].

The cytokines interleukin-6 (IL-6) and interleukin-10 (IL-10) are survival factors for KSHV PEL, and PEL cells produce high levels of IL-6 and IL-10. [81, 181]. The production of IL-6 and IL-10 is dependent on translation since treatment of PEL cells with rapamycin, an mTORC1 inhibitor, results in eIF4E/eIF4B complex formation, inhibition of translation, and a reduction in the levels of IL-6 and IL-10 [81]. We may speculate that the phosphorylation of ribosomal protein S6 and eIF4E by vPK promotes translation and the production of IL-6 and IL-10. These cytokines may then promote the survival of pathogenic B cells leading to lymphoma. Since vPK is expressed ubiquitously, we may expect that vPK promotes the development of lymphomas by multiple contributory mechanisms.

MATERIALS AND METHODS

Transgenic Mice. The sequence for KSHV ORF 36 was optimized for translation and expression by GenScript. The optimized sequence containing the FLAG sequence at the N-terminus [62] was then cloned into the backbone pBS.Ub.hGH, a plasmid previously modified from pBluescript to include an ubiquitin promoter (Ub) and a stabilization sequence (hGH). The plasmid was linearized with restriction enzymes PvuI-HF (high fidelity) and SapI from New England BioLabs. The transgene fragment was microinjected into fertilized embryos of C57BL/6 mice and subsequently implanted into pseudopregnant female mice by UNC Animal Models Core Facility at the University of North Carolina at Chapel Hill. Viral protein kinase-expressing mice were identified by isolating mouse genomic DNA from foot or tail biopsies and by completing polymerase chain reaction (PCR). The Institutional

Animal Care and Use Committees at The University of North Carolina at Chapel Hill approved all experiments.

Genotyping and PCR. To evaluate vPK expression in mouse foot, tail, or ear biopsies, each tissue sample was resuspended in 0.1mL of Solution A (25mM NaOH, 0.2mM EDTA (pH ~12) for 1 hour at 95°C. 0.1mL of Solution B (40mM Tris-HCL, pH ~5) was then added the samples are vortexed and centrifugated for 3 minutes at approximately 10,000 RCF. Two microliters of mouse genomic DNA is then added to a PCR master mix containing the primers vPKfor-5'-CAGAAGCAGTGTTACCTGTA-3' and vPKrev-5'-ACATGGCGATACTCACATTC-3'.

Immunoblots. Tissues that are to be used for the evaluation of protein expression are immediately flash frozen in an ethanol/dry ice bath following extraction. The frozen tissues are maintained at -80°C until processed. For processing, each tissue sample is homogenized in RIPA buffer containing protease and phosphatase inhibitors (Roche). To clarify, the samples are then centrifugated 16,000 RCF for 15 minutes at 4°C. Protein expression is evaluated using the Pierce BCA protein assay. To evaluate vPK protein expression, equal amounts of protein (100 µg) were loaded per lane and resolved by SDS-PAGE and then transferred to a nitrocellulose membrane. Blots are then probed using a monoclonal vPK antibody and anti-rabbit secondary from Cell Signaling.

Tissue preparation and flow cytometry. Mice were sacrificed by exposure to carbon dioxide and subsequent cervical dislocation. A single cell suspension was prepared from spleens by mashing the organ on ice with the top of a sterile syringe plunger in a 6-well dish containing cold DMEM. This suspension was then passed

through a 40-μm strainer. All procedures were carried out on ice. Cells were washed in cold PBS and incubated with ACK lysis buffer for 5 minutes at room temperature to lyse red blood cells. Cells were washed again with cold PBS to remove the lysis buffer. Cells were then resusupended in FACS buffer that contains PBS and 1% bovine serum albumin (BSA). Cells were counted and subsequently incubated with mouse Fc block (BD Biosciences, 553142) per the manufacturer's instructions. Cells were then stained with fluorochrome-conjugated antibodies in FACS buffer at 1e6/0.100 mL/reaction on ice for 30 minutes in the dark. After staining, cells were washed in FACS buffer 3X and resuspended in FACS buffer containing 1% formaldehyde. The fluorochrome-conjugated antibodies used for flow cytometry were purchased from eBioscience: CD8 PE (12-0081-83), CD4 FITC (11-0041-82), CD19 e450 (48-0193-80), CD3 APC (17-5993-80), CD21 PE (12-0211-81), CD23 FITC (11-0232-81), live/dead e780 (65-0865-14), IgM PE (12-5890-81), IgD APC (17-5993-80), B220 e450 (48-0452), GL-7 AF488 (53-5902-80), CD95 PE (12-0951-81), CD86 FITC (11-0862), CD69 FITC (11-0691), CD44 e450 (48-0441). CD138 PE was from Biolegend 142503. Samples were processed and data acquired on a MACSQuant VYB (Miltenyi Biotec,). Data was analyzed using FlowJo software (Tree Star).

Preparation of tissues for H&E staining. Tissues were collected in 10% buffered formalin. After 3-7 days, the tissues were placed in cassettes, washed with water for 10 minutes and then placed in 70% ethanol. The tissues were then paraffin-embedded, cut into 4 μm sections and placed on slides. The sections were then visualized at magnifications of 100X and 200X using a Leica DMLS

microscope. Images were acquired using the Leica DFC480 camera and associated Leica Firecam software.

NP-KLH immunization. vPK heterozygous or WT littermate C57BL/6 mice 8-12 weeks old were injected interperitoneally with 100ug NP-KLH precipitated in alum (1:1) or PBS control. Mice were sacrificed 10 days following immunization.

Tissue extraction from old vPK transgenic and WT mice. Mice were sacrificed by exposure to carbon dioxide and subsequent cervical dislocation. Blood was collected in serum gel z1.1 tubes (Sarstedt). An ear biopsy was also collected for genotype confirmation. Lungs, liver, spleen, kidney, and mass were collected. Each tissue was divided into 3 pieces for snap freeze, RNAlater (Qiagen) and 10% buffered formalin preservation.

Statistical analysis. All statistical analysis was completed using GraphPad Prism.

CHAPTER 5. SUMMARY, CONCLUSIONS AND FUTURE DIRECTIONS

GENERAL SUMMARY

The overarching objective of my dissertation was to determine how KSHV and its viral proteins alter host cellular proteins and signaling pathways that contribute to oncogenesis.

Over the course of completing the research for this dissertation, I had the opportunity to work on a translational research project that involved testing the efficacy of two drugs *in vitro* and *in vivo*. The outcome of this project has clinical value to the medical and scientific community. In our experiments, we found that dual inhibition of two major cell survival pathways, PI3K and MAPK was no more effective at killing tumor cells than inhibition of the PI3K pathway alone. This is in contrast to solid tumors such as in breast cancer where dual PI3K and MAPK inhibitors were shown to be more effective [117]. Although ours is a negative result, our data informs practitioners and scientists and guides them on the development of future NHL therapies.

The main objective for my second project was to provide additional insight into how the KSHV K1 protein promotes oncogenesis. Our lab had already reported that K1 activates the PI3K pathway, resulting in the inhibition of apoptosis [51]. We thought that there might be additional mechanisms by which K1 promotes cell

survival. My work confirmed mass spectrometry results indicating that K1 associates with AMPKγ1, and that this association is important for K1's survival advantage following exposure to metabolic stress. This project not only added to our knowledge about K1, it also began to explore the role of AMPKγ1 as a pro-survival factor during KSHV infection. Some very interesting future research projects should involve understanding AMPK biology during KSHV latent and lytic infection.

My third project objective was to evaluate vPK expression *in vivo*. During the generation of the vPK mouse lines, our lab was trying to understand the impact of vPK *in vitro*. At that time, we had begun to realize that vPK was an S6KB1 mimic in that it phosphorylates some of the same proteins as S6KB1 such as ribosomal protein S6 and have since published that data [62]. We found that naïve vPK mice have a mildly activated immune system that resembles the immune response of immunized WT mice. We also observed for the first time in the herpesvirus field that vPK expression *in vivo* promotes the development of lymphomas in aged-vPK mice. This finding may also have relevance in our understanding of cellular S6KB1 biology.

Although the projects that compose my dissertation appear fairly diverse in terms of the techniques and models employed; the overall objective, which ties these projects together, is to understand how KSHV and its viral proteins alter host cellular proteins and signaling pathways that then contribute to oncogenesis.

DUAL INHIBITION OF THE PI3K/MTOR AND MAPK PATHWAYS IN NON-HODGKIN LYMPHOMA

The objective of my first project was to evaluate the effectiveness of dual inhibition of the PI3K and MAPK pathways in NHL, which includes latently KSHV-infected PEL. Because both the PI3K and MAPK pathways are active in PEL and other non-Hodgkin lymphomas and dual inhibition of these pathways has been shown to be effective at reducing tumor burden in solid tumor models [117], we sought to evaluate the effectiveness at dual inhibition in NHL. The PI3K pathway inhibitor, NVP-BEZ235, inhibits two nodes of this pathway, PI3K and mTOR, making it a very effective PI3K pathway inhibitor. Our lab had already shown that NVP-BEZ235 could reduce PEL cell proliferation and tumor burden in a PEL xenograft model [80] indicating that the PI3K pathway is important for PEL survival.

Thus, we proceeded to evaluate dual inhibition of the PI3K and MAPK pathways by treating NHL cell lines with a constant concentration of NVP-BEZ235 and a titration of the MAPK pathway inhibitor, AZD6244. By inhibiting MEK1/2 and downstream ERK1/2, AZD6244 targets only one arm of the MAPK pathway. We evaluated cell proliferation by MTS assay. In all of the cell lines that we evaluated, AZD6244 was simply not very effective at killing these cells. We also evaluated dual inhibition of these pathways *in vivo* by treating with both inhibitors and determining tumor size over time in a xenograft model of follicular lymphoma, an NHL. As we had observed *in vitro,* dual inhibition of these pathways was not as effective as PI3K pathway inhibition alone. The conclusion of this project is that NHL cells are more reliant on the PI3K pathway for survival than the MAPK pathway.

Because AZD6244 inhibits MEK1/2, which is only one arm of the MAPK pathway, future efforts may involve the inhibition of one of the other arms of the MAPK pathway such as the p38 or JNK arms, depending on the activity levels in NHL. We may also have to pursue a more individualized approach since there appear to be differences in response among the various NHL cell lines suggesting that these pathways may be differentially active in each NHL line.

THE KSHV K1 PROTEIN MODULATES AMPK FUNCTION TO ENHANCE CELL SURVIVAL

For my second project, we wanted to understand whether K1 modulated cellular proteins in addition to the PI3K pathway to promote oncogenesis. We completed a tandem affinity purification of K1 or EV, and identified K1-associating proteins by mass spectrometry. In addition to HSP90, which we had already identified as a K1-associating protein and thus supported our current mass spectrometry result [145], we found that K1 associates with AMPKγ1.

We initially investigated the impact of AMPK activity on the PI3K pathway in the context of K1 expression. In replete conditions, the PI3K/mTOR pathway is active, and when cells are starved, the pathway is inhibited by active AMPK [86]. When we serum starve cells for about 8 hours and then evaluate phosphorylated S6K in EV and K1-expressing cells, we find that phosphorylated S6K levels are reduced in both EV and K1-expresssing cells compared to cells in replete conditions but the level of phosphorylated S6K is on average higher in K1 cells than EV. At the same time, we observe a slight increase in phosphorylated AMPK following serum starvation, in K1

expressing cells compared to EV. With longer periods of serum starvation such as around 24 hours, phosphorylated S6K can be remarkably reduced in both EV and K1-expressing cells. Overall, this data suggests that under certain circumstances, K1 maintains the activation of the PI3K pathway despite AMPK activation (Fig. 5.1). This may be beneficial for the virus since it allows infected cells to generate ATP, yet simultaneously activate protein synthesis to support viral protein production.

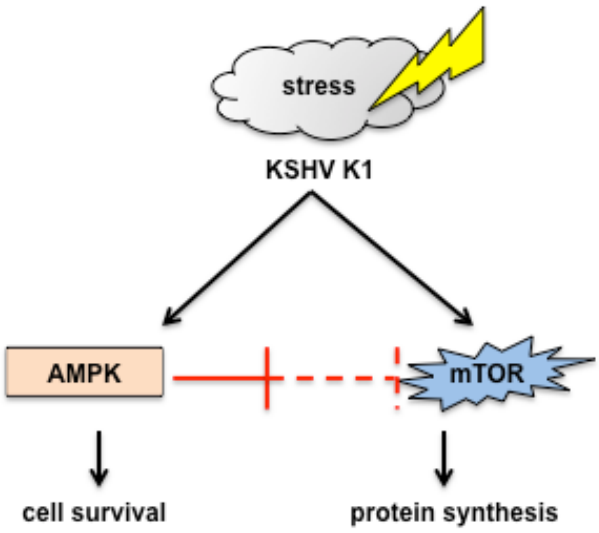

Figure 5.1. K1 maintains PI3K pathway activation despite AMPK activation.

Next, we used cells infected with WT K1 containing virus and K1 mutant recombinant viruses [182]. We observed that upon serum starvation, particularly after 48 and 72 hours, the KSHV- K1 WT infected cells had a survival advantage compared to KSHV-K1 mutants (Fig. 3.1). Knowing that AMPK is a major metabolic regulator in the cell and it becomes activated in response to various cellular stresses, we suspected that AMPK has a role in K1-mediated cell survival.

We next found that K1 expression rendered cells less sensitive to cell death following AMPK inhibition and that the association between K1 and AMPKγ1 appears important for K1's survival advantage following exposure to metabolic stress. We also observed increased AMPK activity in K1-expressing cells compared to EV when starved of serum and growth factors and treated with an AMPK inhibitor. Thus, we suggest that K1 mediates cell survival following exposure to nutrient deprivation via its association with AMPK.

However, we do not suggest that the increase in AMPK activity in K1-expressing cells translates fully to the survival advantage observed in KSHV K1 WT cells (Fig. 3.1). AMPK has previously been reported to have kinase-independent functions [183, 184]. Therefore, in addition to facilitating AMPK activity under specific cellular conditions, K1 could modulate kinase-independent activity of AMPK. Others have suggested that when AMPK is in an active conformation, it inhibits factors such as PPARα and PPARγ [183]. The inhibition of these factors appears to be independent of kinase activity. Thus, binding of K1 to AMPKγ1 could facilitate AMPK independent activity. We observed that K1-expressing cells are less sensitive to compound C treatment as observed by improved cell viability compared to EV (Fig. 3.3A). Association of K1 and AMPKγ1 may promote AMPK stability thereby facilitating kinase dependent and independent activity.

Although AMPK has historically been thought of as a tumor suppressor, there is accumulating evidence to suggest that AMPK promotes metabolic adaptation in tumor cells and in this way, promotes tumor cell survival. Several mechanisms for how AMPK promotes tumor cell survival have been proposed. Jeon et al. found that

nicotinamide adenine dinucleotide phosphate (NADPH) production was impaired when cells were deprived of glucose, and that by activating AMPK, homeostatic levels of NADPH could be maintained and prevent cell death [185]. Activated AMPK inhibited acetyl-CoA carboxylases ACC-1 and ACC-2. Inhibition of ACC-1 and ACC-2 resulted in inhibition of fatty acid synthesis, which consumes NADPH and increased fatty acid oxidation, which results in the production of NADPH [185]. Through the control of these processes, AMPK maintains NADPH levels and prevents H_2O_2-induced cell death [185].

Somewhat in support of this idea, Buzzai et al. found that Akt expressing cells where susceptible to cell death when deprived of glucose [151]. They found that cells could be rescued from death by activating AMPK, which promoted fatty acid oxidation and inhibited cell death. Cell survival was not dependent on translation or lipid synthesis [151].

To explore the possibility that K1 may mediate cell survival following exposure to stress via AMPK's regulation of fatty acid oxidation, future experiments could involve the evaluation of fatty acid oxidation in EV and K1-expressing cells under normal and various conditions of stress as well as with and without AMPK activators and inhibitors.

Many questions related to this project still remain. AMPK has multiple subunits and isoforms as previously mentioned, and we still lack a clear understanding of the specific functions of AMPK when composed of different combinations of isoforms. Because AMPK does respond to various types of cellular stress and is a major

metabolic regulator of energy homeostasis, we suspect that AMPK will have different roles throughout the life cycle of KSHV.

Future efforts to evaluate K1-mediated cell survival may involve the investigation of some of the other K1-associating proteins that were identified by mass spectrometry.

THE KSHV ORF36 PROTEIN KINASE AUGMENTS TUMORIGENESIS IN A MOUSE MODEL SYSTEM

My third project involved the evaluation of ubiquitous expression of vPK or ORF36 *in vivo*. We started the initial characterization by simply evaluating the basic immune cell subsets in the spleen. Because the phenotype was somewhat subtle, we had to complete additional experiments, in which spleens from more mice of each line were evaluated. The flow cytometry panel was fine-tuned each time based on the results from previous experiments.

Because the vPK mice had mildly activated immune systems, we sought to exacerbate the immune response in naïve vPK mice by administering a primary immunization of NP-KLH. NP-KLH administration did not exacerbate the immune response in vPK transgenic mice. We observed approximately equal numbers of B and T cell subsets in vPK mice that had been immunized with NP-KLH compared to vPK mice that had been administered PBS. The salient finding of this experiment is that the vPK immune response following PBS injection was similar to the immune response of immunized WT mice.

As we characterized the immune response using 8-12 weeks of age mice, we allowed a cohort of vPK and littermate controls to age. We sacrificed these mice in

small numbers as they reached about 18-24 months of age or as necessitated due to health issues or an observed mass. We observed that there was greater tumor prevalence in vPK mice compared to age-matched controls. The tumors are composed of lymphocytes, and appear to be lymphomas based on the preliminary review of H&E stained tumor sections by pathologists. We are currently determining clonality by determining VDJ recombination and the ratio of kappa:lambda light chain in tumors.

Some of the vPK mice exhibited lymphoproliferation in various organs such as the lung, spleen, liver and kidney; and yet were not classified as having overt morphologic lymphoma. Thus, the vPK transgenic mice may have a spectrum of progressive stages that lead from lymphoproliferation to neoplasia. To understand the progression to lymphoma, future work should involve harvesting cohorts of vPK and control mice at different time-points as they age for the classification of lymphoproliferation, pre-malignant lesions and malignant lesions.

The paradigm of KSHV pathology has been that the episodic reactivation of KSHV results in the production of angiogenic and inflammatory factors that promote the survival of the KSHV latently infected cell, which then spurs oncogenesis. This paradigm is supported by some of the *in vivo* studies. The expression of latent genes *in vivo* can directly result in the development of tumors such as those observed in mice expressing v-FLIP in stage-specific B cells [42]; whereas *in vivo* expression of the lytic gene ORF74, which is a constitutively active G-protein coupled receptor (GPCR) develop tumors that most likely arise from paracrine mechanisms since only some of the tumor cells express GPCR, and there is the

presence of inflammatory cytokines and angiogenic factors in these models [186-188].

Viral PK, which is a lytic protein, may promote oncogenesis via direct and indirect mechanisms. As a kinase, vPK expression *in vivo* may simultaneously directly and indirectly instigate lymphogenesis by activating substrates that are involved in cell growth, proliferation and cell cycle [57, 62], and by modulating substrates resulting in the production of cytokines that support malignant B cell survival. Future efforts will involve exploration into the mechanisms by which vPK facilitates lymphogenesis.

Because the vPK mouse expresses vPK ubiquitously, our mouse model system explores the extreme of vPK expression. In a KSHV infected individual, KSHV infects a subset of cells out of the total number of cells in the body and then only a subset of those cells would express vPK. Thus, our model does not recapitulate human KSHV infection, but for the first time, we are able to evaluate the pathology of *in vivo* vPK expression and the changes in cell signaling pathways that lead to the pathology.

In conclusion, the PI3K pathway is important for KSHV-infected cell survival. The viral proteins K1 and vPK promote the activation of this pathway by different mechanisms. K1 activates the PI3K by activating PI3K via its ITAM. At the same time, we found that K1 associates with AMPK in the perinculear area of the cell, promotes cell survival following long periods of metabolic stress, and maintains activation of the PI3K pathway despite AMPK activity. Viral PK phosphorylates

proteins downstream in the PI3K pathway such as S6 protein and eIF4E. By maintaining the activity of this pathway, KSHV promotes protein synthesis and cell survival; on the other hand, aberrant activation of this pathway contributes to KSHV oncogenesis (Fig. 5.2).

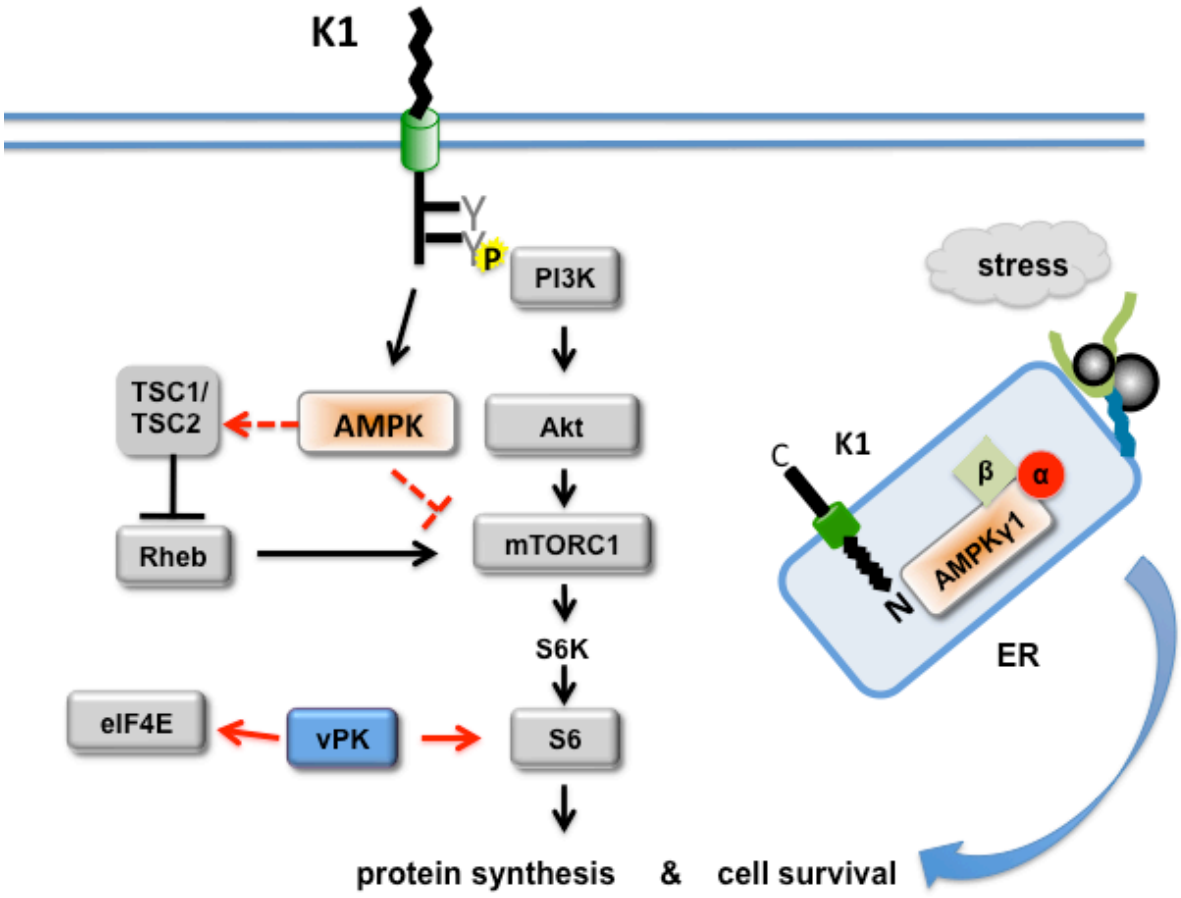

Figure 5.2. The KSHV viral proteins K1 and vPK modulate the PI3K pathway.

REFERENCES

1. Chang Y, Cesarman E, Pessin MS, Lee F, Culpepper J, Knowles DM, et al. Identification of herpesvirus-like DNA sequences in AIDS-associated Kaposi's sarcoma. Science. 1994;266(5192):1865-9.

2. Cesarman E, Chang Y, Moore PS, Said JW, Knowles DM. Kaposi's sarcoma-associated herpesvirus-like DNA sequences in AIDS-related body-cavity-based lymphomas. The New England journal of medicine. 1995;332(18):1186-91.

3. Soulier J, Grollet L, Oksenhendler E, Cacoub P, Cazals-Hatem D, Babinet P, et al. Kaposi's sarcoma-associated herpesvirus-like DNA sequences in multicentric Castleman's disease. Blood. 1995;86(4):1276-80.

4. Parkin DM. The global health burden of infection-associated cancers in the year 2002. International journal of cancer Journal international du cancer. 2006;118(12):3030-44.

5. Ferlay J, Shin HR, Bray F, Forman D, Mathers C, Parkin DM. Estimates of worldwide burden of cancer in 2008: GLOBOCAN 2008. International journal of cancer Journal international du cancer. 2010;127(12):2893-917.

6. Boulanger E, Gerard L, Gabarre J, Molina JM, Rapp C, Abino JF, et al. Prognostic factors and outcome of human herpesvirus 8-associated primary effusion lymphoma in patients with AIDS. Journal of clinical oncology : official journal of the American Society of Clinical Oncology. 2005;23(19):4372-80.

7. Fields virology [electronic resource]. Fields BN, Howley PM, Knipe DM, editors. Philadelphia: Wolters Kluwer Health/Lippincott Williams & Wilkins; 2013.

8. Ioachim HL, Adsay V, Giancotti FR, Dorsett B, Melamed J. Kaposi's sarcoma of internal organs. A multiparameter study of 86 cases. Cancer. 1995;75(6):1376-85.

9. Ganem D. KSHV infection and the pathogenesis of Kaposi's sarcoma. Annu Rev Pathol. 2006;1:273-96.

10. Dupin N, Fisher C, Kellam P, Ariad S, Tulliez M, Franck N, et al. Distribution of human herpesvirus-8 latently infected cells in Kaposi's sarcoma, multicentric Castleman's disease, and primary effusion lymphoma. Proceedings of the National Academy of Sciences of the United States of America. 1999;96(8):4546-51.

11. Hussein MR. Immunohistological evaluation of immune cell infiltrate in cutaneous Kaposi's sarcoma. Cell biology international. 2008;32(1):157-62.

12. Ensoli B, Sturzl M. Kaposi's sarcoma: a result of the interplay among inflammatory cytokines, angiogenic factors and viral agents. Cytokine Growth Factor Rev. 1998;9(1):63-83.

13. Sirianni MC, Vincenzi L, Fiorelli V, Topino S, Scala E, Uccini S, et al. gamma-Interferon production in peripheral blood mononuclear cells and tumor infiltrating lymphocytes from Kaposi's sarcoma patients: correlation with the presence of human herpesvirus-8 in peripheral blood mononuclear cells and lesional macrophages. Blood. 1998;91(3):968-76.

14. Ensoli B, Sturzl M, Monini P. Reactivation and role of HHV-8 in Kaposi's sarcoma initiation. Adv Cancer Res. 2001;81:161-200.

15. Yarchoan R, Davis DA. Development of Kaposi's sarcoma at the site of a biopsy. The New England journal of medicine. 2002;347(10):763-4; author reply -4.

16. Maral T. The Koebner phenomenon in immunosuppression-related Kaposi's sarcoma. Ann Plast Surg. 2000;44(6):646-8.

17. Stallone G, Schena A, Infante B, Di Paolo S, Loverre A, Maggio G, et al. Sirolimus for Kaposi's sarcoma in renal-transplant recipients. The New England journal of medicine. 2005;352(13):1317-23.

18. Jacobson LP, Yamashita TE, Detels R, Margolick JB, Chmiel JS, Kingsley LA, et al. Impact of potent antiretroviral therapy on the incidence of Kaposi's sarcoma and non-Hodgkin's lymphomas among HIV-1-infected individuals. Multicenter AIDS Cohort Study. J Acquir Immune Defic Syndr. 1999;21 Suppl 1:S34-41.

19. Boulanger E, Duprez R, Delabesse E, Gabarre J, Macintyre E, Gessain A. Mono/oligoclonal pattern of Kaposi Sarcoma-associated herpesvirus (KSHV/HHV-8) episomes in primary effusion lymphoma cells. International journal of cancer Journal international du cancer. 2005;115(4):511-8.

20. Cesarman E, Moore PS, Rao PH, Inghirami G, Knowles DM, Chang Y. In vitro establishment and characterization of two acquired immunodeficiency syndrome-related lymphoma cell lines (BC-1 and BC-2) containing Kaposi's sarcoma-associated herpesvirus-like (KSHV) DNA sequences. Blood. 1995;86(7):2708-14.

21. Renne R, Lagunoff M, Zhong W, Ganem D. The size and conformation of Kaposi's sarcoma-associated herpesvirus (human herpesvirus 8) DNA in infected cells and virions. Journal of virology. 1996;70(11):8151-4.

22. Radaszkiewicz T, Hansmann ML, Lennert K. Monoclonality and polyclonality of plasma cells in Castleman's disease of the plasma cell variant. Histopathology. 1989;14(1):11-24.

23. Du MQ, Liu H, Diss TC, Ye H, Hamoudi RA, Dupin N, et al. Kaposi sarcoma-associated herpesvirus infects monotypic (IgM lambda) but polyclonal naive B cells in Castleman disease and associated lymphoproliferative disorders. Blood. 2001;97(7):2130-6.

24. Arias C, Weisburd B, Stern-Ginossar N, Mercier A, Madrid AS, Bellare P, et al. KSHV 2.0: a comprehensive annotation of the Kaposi's sarcoma-associated herpesvirus genome using next-generation sequencing reveals novel genomic and functional features. PLoS pathogens. 2014;10(1):e1003847.

25. Umbach JL, Cullen BR. In-depth analysis of Kaposi's sarcoma-associated herpesvirus microRNA expression provides insights into the mammalian microRNA-processing machinery. Journal of virology. 2010;84(2):695-703.

26. Samols MA, Hu J, Skalsky RL, Renne R. Cloning and identification of a microRNA cluster within the latency-associated region of Kaposi's sarcoma-associated herpesvirus. Journal of virology. 2005;79(14):9301-5.

27. Pfeffer S, Sewer A, Lagos-Quintana M, Sheridan R, Sander C, Grasser FA, et al. Identification of microRNAs of the herpesvirus family. Nature methods. 2005;2(4):269-76.

28. Lin YT, Kincaid RP, Arasappan D, Dowd SE, Hunicke-Smith SP, Sullivan CS. Small RNA profiling reveals antisense transcription throughout the KSHV genome and novel small RNAs. RNA. 2010;16(8):1540-58.

29. Grundhoff A, Sullivan CS, Ganem D. A combined computational and microarray-based approach identifies novel microRNAs encoded by human gamma-herpesviruses. RNA. 2006;12(5):733-50.

30. Cai X, Lu S, Zhang Z, Gonzalez CM, Damania B, Cullen BR. Kaposi's sarcoma-associated herpesvirus expresses an array of viral microRNAs in latently infected cells. Proceedings of the National Academy of Sciences of the United States of America. 2005;102(15):5570-5.

31. Pauk J, Huang ML, Brodie SJ, Wald A, Koelle DM, Schacker T, et al. Mucosal shedding of human herpesvirus 8 in men. The New England journal of medicine. 2000;343(19):1369-77.

32. Blasig C, Zietz C, Haar B, Neipel F, Esser S, Brockmeyer NH, et al. Monocytes in Kaposi's sarcoma lesions are productively infected by human herpesvirus 8. Journal of virology. 1997;71(10):7963-8.

33. Ambroziak JA, Blackbourn DJ, Herndier BG, Glogau RG, Gullett JH, McDonald AR, et al. Herpes-like sequences in HIV-infected and uninfected Kaposi's sarcoma patients. Science. 1995;268(5210):582-3.

34. Dittmer D, Lagunoff M, Renne R, Staskus K, Haase A, Ganem D. A cluster of latently expressed genes in Kaposi's sarcoma-associated herpesvirus. Journal of virology. 1998;72(10):8309-15.

35. Chandriani S, Ganem D. Array-based transcript profiling and limiting-dilution reverse transcription-PCR analysis identify additional latent genes in Kaposi's sarcoma-associated herpesvirus. Journal of virology. 2010;84(11):5565-73.

36. Gregory SM, West JA, Dillon PJ, Hilscher C, Dittmer DP, Damania B. Toll-like receptor signaling controls reactivation of KSHV from latency. Proceedings of the National Academy of Sciences of the United States of America. 2009;106(28):11725-30.

37. Sin SH, Dittmer DP. Viral latency locus augments B-cell response in vivo to induce chronic marginal zone enlargement, plasma cell hyperplasia, and lymphoma. Blood. 2013;121(15):2952-63.

38. Sin SH, Kim Y, Eason A, Dittmer DP. KSHV Latency Locus Cooperates with Myc to Drive Lymphoma in Mice. PLoS pathogens. 2015;11(9):e1005135.

39. Fakhari FD, Jeong JH, Kanan Y, Dittmer DP. The latency-associated nuclear antigen of Kaposi sarcoma-associated herpesvirus induces B cell hyperplasia and lymphoma. The Journal of clinical investigation. 2006;116(3):735-42.

40. Sun Q, Zachariah S, Chaudhary PM. The human herpes virus 8-encoded viral FLICE-inhibitory protein induces cellular transformation via NF-kappaB activation. The Journal of biological chemistry. 2003;278(52):52437-45.

41. Chugh P, Matta H, Schamus S, Zachariah S, Kumar A, Richardson JA, et al. Constitutive NF-kappaB activation, normal Fas-induced apoptosis, and increased incidence of lymphoma in human herpes virus 8 K13 transgenic mice. Proceedings of the National Academy of Sciences of the United States of America. 2005;102(36):12885-90.

42. Ballon G, Chen K, Perez R, Tam W, Cesarman E. Kaposi sarcoma herpesvirus (KSHV) vFLIP oncoprotein induces B cell transdifferentiation and tumorigenesis in mice. The Journal of clinical investigation. 2011;121(3):1141-53.

43. Sadler R, Wu L, Forghani B, Renne R, Zhong W, Herndier B, et al. A complex translational program generates multiple novel proteins from the latently expressed kaposin (K12) locus of Kaposi's sarcoma-associated herpesvirus. Journal of virology. 1999;73(7):5722-30.

44. Muralidhar S, Pumfery AM, Hassani M, Sadaie MR, Kishishita M, Brady JN, et al. Identification of kaposin (open reading frame K12) as a human herpesvirus 8 (Kaposi's sarcoma-associated herpesvirus) transforming gene. Journal of virology. 1998;72(6):4980-8.

45. Bowser BS, DeWire SM, Damania B. Transcriptional regulation of the K1 gene product of Kaposi's sarcoma-associated herpesvirus. Journal of virology. 2002;76(24):12574-83.

46. Lee BS, Alvarez X, Ishido S, Lackner AA, Jung JU. Inhibition of intracellular transport of B cell antigen receptor complexes by Kaposi's sarcoma-associated herpesvirus K1. The Journal of experimental medicine. 2000;192(1):11-21.

47. Lee H, Guo J, Li M, Choi JK, DeMaria M, Rosenzweig M, et al. Identification of an immunoreceptor tyrosine-based activation motif of K1 transforming protein of Kaposi's sarcoma-associated herpesvirus. Molecular and cellular biology. 1998;18(9):5219-28.

48. Reth M. Antigen receptor tail clue. Nature. 1989;338(6214):383-4.

49. Lagunoff M, Majeti R, Weiss A, Ganem D. Deregulated signal transduction by the K1 gene product of Kaposi's sarcoma-associated herpesvirus. Proceedings of the National Academy of Sciences of the United States of America. 1999;96(10):5704-9.

50. Lee BS, Lee SH, Feng P, Chang H, Cho NH, Jung JU. Characterization of the Kaposi's sarcoma-associated herpesvirus K1 signalosome. Journal of virology. 2005;79(19):12173-84.

51. Tomlinson CC, Damania B. The K1 protein of Kaposi's sarcoma-associated herpesvirus activates the Akt signaling pathway. Journal of virology. 2004;78(4):1918-27.

52. Wang S, Wang S, Maeng H, Young DP, Prakash O, Fayad LE, et al. K1 protein of human herpesvirus 8 suppresses lymphoma cell Fas-mediated apoptosis. Blood. 2007;109(5):2174-82.

53. Berkova Z, Wang S, Wise JF, Maeng H, Ji Y, Samaniego F. Mechanism of Fas signaling regulation by human herpesvirus 8 K1 oncoprotein. Journal of the National Cancer Institute. 2009;101(6):399-411.

54. Lee H, Veazey R, Williams K, Li M, Guo J, Neipel F, et al. Deregulation of cell growth by the K1 gene of Kaposi's sarcoma-associated herpesvirus. Nature medicine. 1998;4(4):435-40.

55. Wang L, Dittmer DP, Tomlinson CC, Fakhari FD, Damania B. Immortalization of primary endothelial cells by the K1 protein of Kaposi's sarcoma-associated herpesvirus. Cancer research. 2006;66(7):3658-66.

56. Prakash O, Tang ZY, Peng X, Coleman R, Gill J, Farr G, et al. Tumorigenesis and aberrant signaling in transgenic mice expressing the human herpesvirus-8 K1 gene. Journal of the National Cancer Institute. 2002;94(12):926-35.

57. Kuny CV, Chinchilla K, Culbertson MR, Kalejta RF. Cyclin-dependent kinase-like function is shared by the beta- and gamma- subset of the conserved herpesvirus protein kinases. PLoS pathogens. 2010;6(9):e1001092.

58. Jacob T, Van den Broeke C, Favoreel HW. Viral serine/threonine protein kinases. Journal of virology. 2011;85(3):1158-73.

59. Hamza MS, Reyes RA, Izumiya Y, Wisdom R, Kung HJ, Luciw PA. ORF36 protein kinase of Kaposi's sarcoma herpesvirus activates the c-Jun N-terminal kinase signaling pathway. The Journal of biological chemistry. 2004;279(37):38325-30.

60. Izumiya Y, Izumiya C, Van Geelen A, Wang DH, Lam KS, Luciw PA, et al. Kaposi's sarcoma-associated herpesvirus-encoded protein kinase and its interaction with K-bZIP. Journal of virology. 2007;81(3):1072-82.

61. Hwang S, Kim KS, Flano E, Wu TT, Tong LM, Park AN, et al. Conserved herpesviral kinase promotes viral persistence by inhibiting the IRF-3-mediated type I interferon response. Cell host & microbe. 2009;5(2):166-78.

62. Bhatt AP, Wong JP, Weinberg MS, Host KM, Giffin LC, Buijnink J, et al. A viral kinase mimics S6 kinase to enhance cell proliferation. Proceedings of the National Academy of Sciences of the United States of America. 2016;113(28):7876-81.

63. Ma XM, Blenis J. Molecular mechanisms of mTOR-mediated translational control. Nat Rev Mol Cell Biol. 2009;10(5):307-18.

64. Davis DA, Rinderknecht AS, Zoeteweij JP, Aoki Y, Read-Connole EL, Tosato G, et al. Hypoxia induces lytic replication of Kaposi sarcoma-associated herpesvirus. Blood. 2001;97(10):3244-50.

65. Davis DA, Singer KE, Reynolds IP, Haque M, Yarchoan R. Hypoxia enhances the phosphorylation and cytotoxicity of ganciclovir and zidovudine in Kaposi's sarcoma-associated herpesvirus infected cells. Cancer research. 2007;67(14):7003-10.

66. Roberts PJ, Der CJ. Targeting the Raf-MEK-ERK mitogen-activated protein kinase cascade for the treatment of cancer. Oncogene. 2007;26(22):3291-310.

67. Fruman DA, Rommel C. PI3K and cancer: lessons, challenges and opportunities. Nat Rev Drug Discov. 2014;13(2):140-56.

68. Sarbassov DD, Guertin DA, Ali SM, Sabatini DM. Phosphorylation and regulation of Akt/PKB by the rictor-mTOR complex. Science. 2005;307(5712):1098-101.

69. Mundi PS, Sachdev J, McCourt C, Kalinsky K. AKT in cancer: new molecular insights and advances in drug development. British journal of clinical pharmacology. 2016.

70. Inoki K, Li Y, Zhu T, Wu J, Guan KL. TSC2 is phosphorylated and inhibited by Akt and suppresses mTOR signalling. Nature cell biology. 2002;4(9):648-57.

71. Dan HC, Sun M, Yang L, Feldman RI, Sui XM, Ou CC, et al. Phosphatidylinositol 3-kinase/Akt pathway regulates tuberous sclerosis tumor suppressor complex by phosphorylation of tuberin. The Journal of biological chemistry. 2002;277(38):35364-70.

72. Manning BD, Tee AR, Logsdon MN, Blenis J, Cantley LC. Identification of the tuberous sclerosis complex-2 tumor suppressor gene product tuberin as a target of the phosphoinositide 3-kinase/akt pathway. Molecular cell. 2002;10(1):151-62.

73. Potter CJ, Pedraza LG, Xu T. Akt regulates growth by directly phosphorylating Tsc2. Nature cell biology. 2002;4(9):658-65.

74. Laplante M, Sabatini DM. mTOR signaling in growth control and disease. Cell. 2012;149(2):274-93.

75. Xu K, Liu P, Wei W. mTOR signaling in tumorigenesis. Biochimica et biophysica acta. 2014;1846(2):638-54.

76. Sharma-Walia N, Naranatt PP, Krishnan HH, Zeng L, Chandran B. Kaposi's sarcoma-associated herpesvirus/human herpesvirus 8 envelope glycoprotein gB induces the integrin-dependent focal adhesion kinase-Src-phosphatidylinositol 3-kinase-rho GTPase signal pathways and cytoskeletal rearrangements. Journal of virology. 2004;78(8):4207-23.

77. Veettil MV, Sharma-Walia N, Sadagopan S, Raghu H, Sivakumar R, Naranatt PP, et al. RhoA-GTPase facilitates entry of Kaposi's sarcoma-associated herpesvirus into adherent target cells in a Src-dependent manner. Journal of virology. 2006;80(23):11432-46.

78. Naranatt PP, Akula SM, Zien CA, Krishnan HH, Chandran B. Kaposi's sarcoma-associated herpesvirus induces the phosphatidylinositol 3-kinase-PKC-zeta-MEK-ERK signaling pathway in target cells early during infection: implications for infectivity. Journal of virology. 2003;77(2):1524-39.

79. Sharma-Walia N, Krishnan HH, Naranatt PP, Zeng L, Smith MS, Chandran B. ERK1/2 and MEK1/2 induced by Kaposi's sarcoma-associated herpesvirus (human herpesvirus 8) early during infection of target cells are essential for expression of viral genes and for establishment of infection. Journal of virology. 2005;79(16):10308-29.

80. Bhatt AP, Bhende PM, Sin SH, Roy D, Dittmer DP, Damania B. Dual inhibition of PI3K and mTOR inhibits autocrine and paracrine proliferative loops in PI3K/Akt/mTOR-addicted lymphomas. Blood. 2010;115(22):4455-63.

81. Sin SH, Roy D, Wang L, Staudt MR, Fakhari FD, Patel DD, et al. Rapamycin is efficacious against primary effusion lymphoma (PEL) cell lines in vivo by inhibiting autocrine signaling. Blood. 2007;109(5):2165-73.

82. Xie J, Ajibade AO, Ye F, Kuhne K, Gao SJ. Reactivation of Kaposi's sarcoma-associated herpesvirus from latency requires MEK/ERK, JNK and p38 multiple mitogen-activated protein kinase pathways. Virology. 2008;371(1):139-54.

83. Roy D, Sin SH, Lucas A, Venkataramanan R, Wang L, Eason A, et al. mTOR inhibitors block Kaposi sarcoma growth by inhibiting essential autocrine growth factors and tumor angiogenesis. Cancer research. 2013;73(7):2235-46.

84. Cohen A, Brodie C, Sarid R. An essential role of ERK signalling in TPA-induced reactivation of Kaposi's sarcoma-associated herpesvirus. The Journal of general virology. 2006;87(Pt 4):795-802.

85. Hardie DG. AMP-activated/SNF1 protein kinases: conserved guardians of cellular energy. Nat Rev Mol Cell Biol. 2007;8(10):774-85.

86. Hardie DG, Ross FA, Hawley SA. AMPK: a nutrient and energy sensor that maintains energy homeostasis. Nat Rev Mol Cell Biol. 2012;13(4):251-62.

87. Steinberg GR, Kemp BE. AMPK in Health and Disease. Physiological reviews. 2009;89(3):1025-78.

88. Gowans GJ, Hardie DG. AMPK: a cellular energy sensor primarily regulated by AMP. Biochemical Society transactions. 2014;42(1):71-5.

89. Hong SP, Leiper FC, Woods A, Carling D, Carlson M. Activation of yeast Snf1 and mammalian AMP-activated protein kinase by upstream kinases. Proceedings of the National Academy of Sciences of the United States of America. 2003;100(15):8839-43.

90. Woods A, Johnstone SR, Dickerson K, Leiper FC, Fryer LG, Neumann D, et al. LKB1 is the upstream kinase in the AMP-activated protein kinase cascade. Current biology : CB. 2003;13(22):2004-8.

91. Gowans GJ, Hawley SA, Ross FA, Hardie DG. AMP is a true physiological regulator of AMP-activated protein kinase by both allosteric activation and enhancing net phosphorylation. Cell metabolism. 2013;18(4):556-66.

92. Hawley SA, Selbert MA, Goldstein EG, Edelman AM, Carling D, Hardie DG. 5'-AMP activates the AMP-activated protein kinase cascade, and Ca2+/calmodulin activates the calmodulin-dependent protein kinase I cascade, via three independent mechanisms. The Journal of biological chemistry. 1995;270(45):27186-91.

93. Momcilovic M, Hong SP, Carlson M. Mammalian TAK1 activates Snf1 protein kinase in yeast and phosphorylates AMP-activated protein kinase in vitro. The Journal of biological chemistry. 2006;281(35):25336-43.

94. Hurley RL, Anderson KA, Franzone JM, Kemp BE, Means AR, Witters LA. The Ca2+/calmodulin-dependent protein kinase kinases are AMP-activated protein kinase kinases. The Journal of biological chemistry. 2005;280(32):29060-6.

95. Woods A, Dickerson K, Heath R, Hong SP, Momcilovic M, Johnstone SR, et al. Ca2+/calmodulin-dependent protein kinase kinase-beta acts upstream of AMP-activated protein kinase in mammalian cells. Cell metabolism. 2005;2(1):21-33.

96. Minokoshi Y, Kim YB, Peroni OD, Fryer LG, Muller C, Carling D, et al. Leptin stimulates fatty-acid oxidation by activating AMP-activated protein kinase. Nature. 2002;415(6869):339-43.

97. Zhou L, Deepa SS, Etzler JC, Ryu J, Mao X, Fang Q, et al. Adiponectin activates AMP-activated protein kinase in muscle cells via APPL1/LKB1-dependent and phospholipase C/Ca2+/Ca2+/calmodulin-dependent protein kinase kinase-dependent pathways. The Journal of biological chemistry. 2009;284(33):22426-35.

98. Hattori A, Mawatari K, Tsuzuki S, Yoshioka E, Toda S, Yoshida M, et al. Beta-adrenergic-AMPK pathway phosphorylates acetyl-CoA carboxylase in a high-epinephrine rat model, SPORTS. Obesity (Silver Spring). 2010;18(1):48-54.

99. Koh HJ, Hirshman MF, He H, Li Y, Manabe Y, Balschi JA, et al. Adrenaline is a critical mediator of acute exercise-induced AMP-activated protein kinase activation in adipocytes. The Biochemical journal. 2007;403(3):473-81.

100. Kelly M, Keller C, Avilucea PR, Keller P, Luo Z, Xiang X, et al. AMPK activity is diminished in tissues of IL-6 knockout mice: the effect of exercise. Biochemical and biophysical research communications. 2004;320(2):449-54.

101. Ruderman NB, Keller C, Richard AM, Saha AK, Luo Z, Xiang X, et al. Interleukin-6 regulation of AMP-activated protein kinase. Potential role in the systemic response to exercise and prevention of the metabolic syndrome. Diabetes. 2006;55 Suppl 2:S48-54.

102. Jeon SM, Hay N. The double-edged sword of AMPK signaling in cancer and its therapeutic implications. Arch Pharm Res. 2015;38(3):346-57.

103. Jeon SM, Hay N. The dark face of AMPK as an essential tumor promoter. Cell Logist. 2012;2(4):197-202.

104. Chhipa RR, Wu Y, Mohler JL, Ip C. Survival advantage of AMPK activation to androgen-independent prostate cancer cells during energy stress. Cellular signalling. 2010;22(10):1554-61.

105. Park HU, Suy S, Danner M, Dailey V, Zhang Y, Li H, et al. AMP-activated protein kinase promotes human prostate cancer cell growth and survival. Molecular cancer therapeutics. 2009;8(4):733-41.

106. Jin J, Mullen TD, Hou Q, Bielawski J, Bielawska A, Zhang X, et al. AMPK inhibitor Compound C stimulates ceramide production and promotes Bax redistribution and apoptosis in MCF7 breast carcinoma cells. Journal of lipid research. 2009;50(12):2389-97.

107. Yang WL, Perillo W, Liou D, Marambaud P, Wang P. AMPK inhibitor compound C suppresses cell proliferation by induction of apoptosis and autophagy in human colorectal cancer cells. J Surg Oncol. 2012;106(6):680-8.

108. Vucicevic L, Misirkic M, Janjetovic K, Harhaji-Trajkovic L, Prica M, Stevanovic D, et al. AMP-activated protein kinase-dependent and -independent mechanisms underlying in vitro antiglioma action of compound C. Biochemical pharmacology. 2009;77(11):1684-93.

109. Baumann P, Mandl-Weber S, Emmerich B, Straka C, Schmidmaier R. Inhibition of adenosine monophosphate-activated protein kinase induces apoptosis in multiple myeloma cells. Anticancer Drugs. 2007;18(4):405-10.

110. Jang T, Calaoagan JM, Kwon E, Samuelsson S, Recht L, Laderoute KR. 5'-AMP-activated protein kinase activity is elevated early during primary brain tumor development in the rat. International journal of cancer Journal international du cancer. 2011;128(9):2230-9.

111. Laderoute KR, Amin K, Calaoagan JM, Knapp M, Le T, Orduna J, et al. 5'-AMP-activated protein kinase (AMPK) is induced by low-oxygen and glucose deprivation conditions found in solid-tumor microenvironments. Molecular and cellular biology. 2006;26(14):5336-47.

112. Bardeesy N, Sinha M, Hezel AF, Signoretti S, Hathaway NA, Sharpless NE, et al. Loss of the Lkb1 tumour suppressor provokes intestinal polyposis but resistance to transformation. Nature. 2002;419(6903):162-7.

113. Bhende PM, Park SI, Lim MS, Dittmer DP, Damania B. The dual PI3K/mTOR inhibitor, NVP-BEZ235, is efficacious against follicular lymphoma. Leukemia. 2010;24(10):1781-4.

114. Elenitoba-Johnson KS, Jenson SD, Abbott RT, Palais RA, Bohling SD, Lin Z, et al. Involvement of multiple signaling pathways in follicular lymphoma transformation: p38-mitogen-activated protein kinase as a target for therapy. Proceedings of the National Academy of Sciences of the United States of America. 2003;100(12):7259-64.

115. Ogasawara T, Yasuyama M, Kawauchi K. Constitutive activation of extracellular signal-regulated kinase and p38 mitogen-activated protein kinase in B-

cell lymphoproliferative disorders. International journal of hematology. 2003;77(4):364-70.

116. Ding H, Gabali AM, Jenson SD, Lim MS, Elenitoba-Johnson KS. P38 mitogen activated protein kinase expression and regulation by interleukin-4 in human B cell non-Hodgkin lymphomas. Journal of hematopathology. 2009;2(4):195-204.

117. Roberts PJ, Usary JE, Darr DB, Dillon PM, Pfefferle AD, Whittle MC, et al. Combined PI3K/mTOR and MEK inhibition provides broad antitumor activity in faithful murine cancer models. Clinical cancer research : an official journal of the American Association for Cancer Research. 2012;18(19):5290-303.

118. She QB, Halilovic E, Ye Q, Zhen W, Shirasawa S, Sasazuki T, et al. 4E-BP1 is a key effector of the oncogenic activation of the AKT and ERK signaling pathways that integrates their function in tumors. Cancer cell. 2010;18(1):39-51.

119. Maira SM, Stauffer F, Brueggen J, Furet P, Schnell C, Fritsch C, et al. Identification and characterization of NVP-BEZ235, a new orally available dual phosphatidylinositol 3-kinase/mammalian target of rapamycin inhibitor with potent in vivo antitumor activity. Molecular cancer therapeutics. 2008;7(7):1851-63.

120. Serra V, Markman B, Scaltriti M, Eichhorn PJ, Valero V, Guzman M, et al. NVP-BEZ235, a dual PI3K/mTOR inhibitor, prevents PI3K signaling and inhibits the growth of cancer cells with activating PI3K mutations. Cancer research. 2008;68(19):8022-30.

121. Yeh TC, Marsh V, Bernat BA, Ballard J, Colwell H, Evans RJ, et al. Biological characterization of ARRY-142886 (AZD6244), a potent, highly selective mitogen-activated protein kinase kinase 1/2 inhibitor. Clinical cancer research : an official journal of the American Association for Cancer Research. 2007;13(5):1576-83.

122. Davies BR, Logie A, McKay JS, Martin P, Steele S, Jenkins R, et al. AZD6244 (ARRY-142886), a potent inhibitor of mitogen-activated protein kinase/extracellular signal-regulated kinase kinase 1/2 kinases: mechanism of action in vivo, pharmacokinetic/pharmacodynamic relationship, and potential for combination in preclinical models. Molecular cancer therapeutics. 2007;6(8):2209-19.

123. Nguyen TK, Jordan N, Friedberg J, Fisher RI, Dent P, Grant S. Inhibition of MEK/ERK1/2 sensitizes lymphoma cells to sorafenib-induced apoptosis. Leukemia research. 2010;34(3):379-86.

124. Lannutti BJ, Meadows SA, Herman SE, Kashishian A, Steiner B, Johnson AJ, et al. CAL-101, a p110delta selective phosphatidylinositol-3-kinase inhibitor for the treatment of B-cell malignancies, inhibits PI3K signaling and cellular viability. Blood. 2011;117(2):591-4.

125. Gopal AK, Kahl BS, de Vos S, Wagner-Johnston ND, Schuster SJ, Jurczak WJ, et al. PI3Kdelta inhibition by idelalisib in patients with relapsed indolent lymphoma. The New England journal of medicine. 2014;370(11):1008-18.

126. Ahuja HG, Foti A, Bar-Eli M, Cline MJ. The pattern of mutational involvement of RAS genes in human hematologic malignancies determined by DNA amplification and direct sequencing. Blood. 1990;75(8):1684-90.

127. Lam KP, Kuhn R, Rajewsky K. In vivo ablation of surface immunoglobulin on mature B cells by inducible gene targeting results in rapid cell death. Cell. 1997;90(6):1073-83.

128. Oh JK, Weiderpass E. Infection and Cancer: Global Distribution and Burden of Diseases. Annals of global health. 2014;80(5):384-92.

129. Russo JJ, Bohenzky RA, Chien MC, Chen J, Yan M, Maddalena D, et al. Nucleotide sequence of the Kaposi sarcoma-associated herpesvirus (HHV8). Proceedings of the National Academy of Sciences of the United States of America. 1996;93(25):14862-7.

130. Stapleton D, Mitchelhill KI, Gao G, Widmer J, Michell BJ, Teh T, et al. Mammalian AMP-activated protein kinase subfamily. The Journal of biological chemistry. 1996;271(2):611-4.

131. Gao G, Fernandez CS, Stapleton D, Auster AS, Widmer J, Dyck JR, et al. Non-catalytic beta- and gamma-subunit isoforms of the 5'-AMP-activated protein kinase. The Journal of biological chemistry. 1996;271(15):8675-81.

132. Thornton C, Snowden MA, Carling D. Identification of a novel AMP-activated protein kinase beta subunit isoform that is highly expressed in skeletal muscle. The Journal of biological chemistry. 1998;273(20):12443-50.

133. Cheung PC, Salt IP, Davies SP, Hardie DG, Carling D. Characterization of AMP-activated protein kinase gamma-subunit isoforms and their role in AMP binding. The Biochemical journal. 2000;346 Pt 3:659-69.

134. Salt I, Celler JW, Hawley SA, Prescott A, Woods A, Carling D, et al. AMP-activated protein kinase: greater AMP dependence, and preferential nuclear localization, of complexes containing the alpha2 isoform. The Biochemical journal. 1998;334 (Pt 1):177-87.

135. Warden SM, Richardson C, O'Donnell J, Jr., Stapleton D, Kemp BE, Witters LA. Post-translational modifications of the beta-1 subunit of AMP-activated protein kinase affect enzyme activity and cellular localization. The Biochemical journal. 2001;354(Pt 2):275-83.

136. Turnley AM, Stapleton D, Mann RJ, Witters LA, Kemp BE, Bartlett PF. Cellular distribution and developmental expression of AMP-activated protein kinase

isoforms in mouse central nervous system. Journal of neurochemistry. 1999;72(4):1707-16.

137. Crute BE, Seefeld K, Gamble J, Kemp BE, Witters LA. Functional domains of the alpha1 catalytic subunit of the AMP-activated protein kinase. The Journal of biological chemistry. 1998;273(52):35347-54.

138. Peralta C, Bartrons R, Serafin A, Blazquez C, Guzman M, Prats N, et al. Adenosine monophosphate-activated protein kinase mediates the protective effects of ischemic preconditioning on hepatic ischemia-reperfusion injury in the rat. Hepatology. 2001;34(6):1164-73.

139. Marsin AS, Bouzin C, Bertrand L, Hue L. The stimulation of glycolysis by hypoxia in activated monocytes is mediated by AMP-activated protein kinase and inducible 6-phosphofructo-2-kinase. The Journal of biological chemistry. 2002;277(34):30778-83.

140. Lee M, Hwang JT, Lee HJ, Jung SN, Kang I, Chi SG, et al. AMP-activated protein kinase activity is critical for hypoxia-inducible factor-1 transcriptional activity and its target gene expression under hypoxic conditions in DU145 cells. The Journal of biological chemistry. 2003;278(41):39653-61.

141. Zhang Z, Chen W., Sanders M., Brulois K., Dittmer D., Damania B. Journal of virology. 2016.

142. Hardie DG. AMP-activated protein kinase: an energy sensor that regulates all aspects of cell function. Genes & development. 2011;25(18):1895-908.

143. Zhou G, Myers R, Li Y, Chen Y, Shen X, Fenyk-Melody J, et al. Role of AMP-activated protein kinase in mechanism of metformin action. The Journal of clinical investigation. 2001;108(8):1167-74.

144. Accordi B, Galla L, Milani G, Curtarello M, Serafin V, Lissandron V, et al. AMPK inhibition enhances apoptosis in MLL-rearranged pediatric B-acute lymphoblastic leukemia cells. Leukemia. 2013;27(5):1019-27.

145. Wen KW, Damania B. Hsp90 and Hsp40/Erdj3 are required for the expression and anti-apoptotic function of KSHV K1. Oncogene. 2010;29(24):3532-44.

146. Tomlinson CC, Damania B. Critical role for endocytosis in the regulation of signaling by the Kaposi's sarcoma-associated herpesvirus K1 protein. Journal of virology. 2008;82(13):6514-23.

147. Davies SP, Carling D, Hardie DG. Tissue distribution of the AMP-activated protein kinase, and lack of activation by cyclic-AMP-dependent protein kinase, studied using a specific and sensitive peptide assay. Eur J Biochem. 1989;186(1-2):123-8.

148. Inoki K, Zhu T, Guan KL. TSC2 mediates cellular energy response to control cell growth and survival. Cell. 2003;115(5):577-90.

149. Gwinn DM, Shackelford DB, Egan DF, Mihaylova MM, Mery A, Vasquez DS, et al. AMPK phosphorylation of raptor mediates a metabolic checkpoint. Molecular cell. 2008;30(2):214-26.

150. Giffin L, Anders P, Damania B. Kaposi's Sarcoma-Associated Herpesvirus:

Pathogenesis and Host Immune Response. In: Hudnall SD, editor. Viruses and Human Cancer. New York: Springer Science; 2014. p. 289-322.

151. Buzzai M, Bauer DE, Jones RG, Deberardinis RJ, Hatzivassiliou G, Elstrom RL, et al. The glucose dependence of Akt-transformed cells can be reversed by pharmacologic activation of fatty acid beta-oxidation. Oncogene. 2005;24(26):4165-73.

152. Bhatt AP, Jacobs SR, Freemerman AJ, Makowski L, Rathmell JC, Dittmer DP, et al. Dysregulation of fatty acid synthesis and glycolysis in non-Hodgkin lymphoma. Proceedings of the National Academy of Sciences of the United States of America. 2012;109(29):11818-23.

153. Delgado T, Carroll PA, Punjabi AS, Margineantu D, Hockenbery DM, Lagunoff M. Induction of the Warburg effect by Kaposi's sarcoma herpesvirus is required for the maintenance of latently infected endothelial cells. Proceedings of the National Academy of Sciences of the United States of America. 2010;107(23):10696-701.

154. Murata Y, Uehara Y, Hosoi Y. Activation of mTORC1 under nutrient starvation conditions increases cellular radiosensitivity in human liver cancer cell lines, HepG2 and HuH6. Biochemical and biophysical research communications. 2015;468(4):684-90.

155. Bittremieux M, Parys JB, Pinton P, Bultynck G. ER functions of oncogenes and tumor suppressors: Modulators of intracellular Ca(2+) signaling. Biochimica et biophysica acta. 2016;1863(6 Pt B):1364-78.

156. Vandecaetsbeek I, Vangheluwe P, Raeymaekers L, Wuytack F, Vanoevelen J. The Ca2+ pumps of the endoplasmic reticulum and Golgi apparatus. Cold Spring Harb Perspect Biol. 2011;3(5).

157. Dong Y, Zhang M, Liang B, Xie Z, Zhao Z, Asfa S, et al. Reduction of AMP-activated protein kinase alpha2 increases endoplasmic reticulum stress and atherosclerosis in vivo. Circulation. 2010;121(6):792-803.

158. Hetz C. The unfolded protein response: controlling cell fate decisions under ER stress and beyond. Nat Rev Mol Cell Biol. 2012;13(2):89-102.

159. Terry LJ, Vastag L, Rabinowitz JD, Shenk T. Human kinome profiling identifies a requirement for AMP-activated protein kinase during human cytomegalovirus infection. Proceedings of the National Academy of Sciences of the United States of America. 2012;109(8):3071-6.

160. McArdle J, Moorman NJ, Munger J. HCMV targets the metabolic stress response through activation of AMPK whose activity is important for viral replication. PLoS pathogens. 2012;8(1):e1002502.

161. Kudchodkar SB, Del Prete GQ, Maguire TG, Alwine JC. AMPK-mediated inhibition of mTOR kinase is circumvented during immediate-early times of human cytomegalovirus infection. Journal of virology. 2007;81(7):3649-51.

162. Leyton L, Hott M, Acuna F, Caroca J, Nunez M, Martin C, et al. Nutraceutical activators of AMPK/Sirt1 axis inhibit viral production and protect neurons from neurodegenerative events triggered during HSV-1 infection. Virus research. 2015;205:63-72.

163. Cheng F, He M, Jung JU, Lu C, Gao SJ. Suppression of Kaposi's sarcoma-associated herpesvirus infection and replication by 5' AMP-activated protein kinase. Journal of virology. 2016.

164. Wang L, Wakisaka N, Tomlinson CC, DeWire SM, Krall S, Pagano JS, et al. The Kaposi's sarcoma-associated herpesvirus (KSHV/HHV-8) K1 protein induces expression of angiogenic and invasion factors. Cancer research. 2004;64(8):2774-81.

165. Park J, Lee D, Seo T, Chung J, Choe J. Kaposi's sarcoma-associated herpesvirus (human herpesvirus-8) open reading frame 36 protein is a serine protein kinase. The Journal of general virology. 2000;81(Pt 4):1067-71.

166. Stavnezer J, Schrader CE. IgH chain class switch recombination: mechanism and regulation. J Immunol. 2014;193(11):5370-8.

167. Mboko WP, Olteanu H, Ray A, Xin G, Darrah EJ, Kumar SN, et al. Tumor Suppressor Interferon-Regulatory Factor 1 Counteracts the Germinal Center Reaction Driven by a Cancer-Associated Gammaherpesvirus. Journal of virology. 2016;90(6):2818-29.

168. Wolniak KL, Noelle RJ, Waldschmidt TJ. Characterization of (4-hydroxy-3-nitrophenyl)acetyl (NP)-specific germinal center B cells and antigen-binding B220- cells after primary NP challenge in mice. J Immunol. 2006;177(4):2072-9.

169. DeGrendele HC, Kosfiszer M, Estess P, Siegelman MH. CD44 activation and associated primary adhesion is inducible via T cell receptor stimulation. J Immunol. 1997;159(6):2549-53.

170. Paine A, Kirchner H, Immenschuh S, Oelke M, Blasczyk R, Eiz-Vesper B. IL-2 upregulates CD86 expression on human CD4(+) and CD8(+) T cells. J Immunol. 2012;188(4):1620-9.

171. Jeannin P, Herbault N, Delneste Y, Magistrelli G, Lecoanet-Henchoz S, Caron G, et al. Human effector memory T cells express CD86: a functional role in naive T cell priming. J Immunol. 1999;162(4):2044-8.

172. Barnaba V, Watts C, de Boer M, Lane P, Lanzavecchia A. Professional presentation of antigen by activated human T cells. Eur J Immunol. 1994;24(1):71-5.

173. Azuma M, Yssel H, Phillips JH, Spits H, Lanier LL. Functional expression of B7/BB1 on activated T lymphocytes. The Journal of experimental medicine. 1993;177(3):845-50.

174. Lal G, Shaila MS, Nayak R. Activated mouse T-cells synthesize MHC class II, process, and present morbillivirus nucleocapsid protein to primed T-cells. Cell Immunol. 2005;234(2):133-45.

175. Prabhu Das MR, Zamvil SS, Borriello F, Weiner HL, Sharpe AH, Kuchroo VK. Reciprocal expression of co-stimulatory molecules, B7-1 and B7-2, on murine T cells following activation. Eur J Immunol. 1995;25(1):207-11.

176. Kochli C, Wendland T, Frutig K, Grunow R, Merlin S, Pichler WJ. CD80 and CD86 costimulatory molecules on circulating T cells of HIV infected individuals. Immunol Lett. 1999;65(3):197-201.

177. Nakada M, Nishizaki K, Yoshino T, Okano M, Yamamoto T, Masuda Y, et al. CD80 (B7-1) and CD86 (B7-2) antigens on house dust mite-specific T cells in atopic disease function through T-T cell interactions. The Journal of allergy and clinical immunology. 1999;104(1):222-7.

178. Melichar B, Nash MA, Lenzi R, Platsoucas CD, Freedman RS. Expression of costimulatory molecules CD80 and CD86 and their receptors CD28, CTLA-4 on malignant ascites CD3+ tumour-infiltrating lymphocytes (TIL) from patients with ovarian and other types of peritoneal carcinomatosis. Clin Exp Immunol. 2000;119(1):19-27.

179. Blombery PA, Wall M, Seymour JF. The molecular pathogenesis of B-cell non-Hodgkin lymphoma. Eur J Haematol. 2015;95(4):280-93.

180. Proud CG. Mnks, eIF4E phosphorylation and cancer. Biochimica et biophysica acta. 2015;1849(7):766-73.

181. Jones KD, Aoki Y, Chang Y, Moore PS, Yarchoan R, Tosato G. Involvement of interleukin-10 (IL-10) and viral IL-6 in the spontaneous growth of Kaposi's sarcoma herpesvirus-associated infected primary effusion lymphoma cells. Blood. 1999;94(8):2871-9.

182. Zhang Z, Chen W, Sanders MK, Brulois KF, Dittmer DP, Damania B. The K1 Protein of Kaposi's Sarcoma-Associated Herpesvirus Augments Viral Lytic Replication. Journal of virology. 2016;90(17):7657-66.

183. Sozio MS, Lu C, Zeng Y, Liangpunsakul S, Crabb DW. Activated AMPK inhibits PPAR-{alpha} and PPAR-{gamma} transcriptional activity in hepatoma cells. American journal of physiology Gastrointestinal and liver physiology. 2011;301(4):G739-47.

184. Bronner M, Hertz R, Bar-Tana J. Kinase-independent transcriptional co-activation of peroxisome proliferator-activated receptor alpha by AMP-activated protein kinase. The Biochemical journal. 2004;384(Pt 2):295-305.

185. Jeon SM, Chandel NS, Hay N. AMPK regulates NADPH homeostasis to promote tumour cell survival during energy stress. Nature. 2012;485(7400):661-5.

186. Yang TY, Chen SC, Leach MW, Manfra D, Homey B, Wiekowski M, et al. Transgenic expression of the chemokine receptor encoded by human herpesvirus 8 induces an angioproliferative disease resembling Kaposi's sarcoma. The Journal of experimental medicine. 2000;191(3):445-54.

187. Guo HG, Sadowska M, Reid W, Tschachler E, Hayward G, Reitz M. Kaposi's sarcoma-like tumors in a human herpesvirus 8 ORF74 transgenic mouse. Journal of virology. 2003;77(4):2631-9.

188. Bais C, Santomasso B, Coso O, Arvanitakis L, Raaka EG, Gutkind JS, et al. G-protein-coupled receptor of Kaposi's sarcoma-associated herpesvirus is a viral oncogene and angiogenesis activator. Nature. 1998;391(6662):86-9.